FINITE ELEMENT ANALYSIS OF DYKE IN THE CONCEPT OF EUROCODE 7

ADDITIONAL THESIS PROJECT
GEO-ENGINEERING SECTION

Antonios Mavritsakis
(4503937)

Supervising Professor: C. Jommi

TU Delft Delft University of Technology

Table of contents

Table of figures

ABSTRACT

State of the art geotechnical engineering and project designare nowadays rigidly connected to the mindful adaption of the Eurocode. However, questions can be raised on the critical selection of the characteristic values for parameters such as the soil compressibility and permeability. The experiment conducted at Leendert de Boerspolder, where a dyke was controllably brought to failure, poses as an excellent circumstance for investigating this issue. After setting up an FEM model in PLAXIS 2D, as well as orchestrating multiple ULS schemes and comparing the available soil constitutive models, the effects of these characteristic values on the response of the system are explored. Displacement profiles are collated, but more importantly, the safety factors and possible failure mechanisms of every analysis are put under comparison. The outcome is the evaluation of the characteristic value pick on a quantitative and qualitative level. Thus, certain concepts regarding the application of the Eurocode in geotechnical engineering can be tackled or validated, allowing for a critical implementation of the norms.

1 INTRODUCTION

In 2015 a dyke at Leendert de Boerspolder was deliberately brought to controlled failure by a team of Geo-engineers, focusing on monitoring and capturing the soil behavior up to failure. Having acquired a set of data, including displacements and pore pressures, efforts are being made in order to approach numerically the response of the dyke, but also simulate some scenarios of interest. The main focus of this project is to investigate the application of the Eurocode 7 concept of characteristic values on soil compressibility and permeability, analyze its impacts on construction safety and elaborate soil response through the use of a realistic model.

The first step is to set up the numerical model. In order to do so, the geometry and construction phases are defined. Then, possible constitutive models (Mohr-Coulomb, Soft Soil, Hardening Soil, Modified Cam Clay) have to be assessed, so that the most valid ones can be distinguished. Following, the soil parameters have to be calibrated, and so, statistical processing of the data gathered by the soil tests is necessary in order to estimate the characteristic values according to Eurocode 7. The model is simulated in PLAXIS.

Once an efficient model is set up, the analyses can begin.

- Firstly, the safety factor schemes available in the Eurocode 7 are introduced and tested into the model, for two constitutive models. This analysis aims at identifying the model fittest to describe soil response in this project by comparing combinations of safety schemes and constitutive models, pointing out their advantages and drawbacks. Thus, the analysis that suits best such construction cases can be made clear, as well as the conditions of its further application.

- Following, an issue to be addressed was raised by the Dutch Water Board authority; whether the maximum or minimum characteristic values of the compressibility are critical in the design. The response of the soil is simulated and multiple cases are put under comparison. The product of this realization answers in two aspects: both displacement-wise but also by assessing the safety factor of each case.

- Finally, a sensitivity analysis on the permeability of the peat layer is being executed, which is highly uncertain, in order to assess its importance on calculated safety factor and mode of failure. A range of permeabilities is attributed, as well as two possible ratios of vertical to horizontal permeability in the safety schemes of the Eurocode 7. While some realizations may be unrealistic, they surely raise awareness on soil behavior. This approach is an effort towards understanding how the permeability impacts this case, but also alarming about the importance of accurate estimation of the permeability and the necessity for proper and precise in situ measurements.

Thorough investigation and analysis has already been made on the case of Leendert de Boerspolder. The goal of this Additional Thesis Project is, by employing advanced constitutive models, to tackle or verify engineering concepts and "rules of thumb" upon applying the Eurocode, and thus promote engineering and critical thinking against habitual use of codes of practice.

2 SETTING THE FINITE ELEMENT MODEL

2.1 Basics of the model

The project involves a sequence of excavating, water pumping and impounding at the toe of a dyke in Leendert de Boerspolder.

It should be noted that the dyke failed during the third pumping phase. In the context of this project, failure is assumed to happen during phase Pumping II (explained in this chapter), as the value of the safety factor suggests failure. Also, in reality, 3D phenomena have assisted in avoiding an early failure, but these effects cannot be included in such a PLAXIS model.

The model geometry reproduces a cross section of the actual case. The dike has a slope of 1:3 and the excavation slopes are 1:1 and 1:2respectively for each stage. The boundary conditions are set as fixations for the bottom boundary and horizontal displacement restriction for the vertical ones. The top surface is free, so that gravity loads are properly applied and settlements can be normally produced. Considering hydraulic boundary conditions, a head of -0.61mis set behind the dyke, while -2.4m is set in front of it. The pumping conditions inside the excavation vary for the pumping phases, while the areas adjacent to the excavation and along the dyke are set to be defined by calculating the hydraulic state.

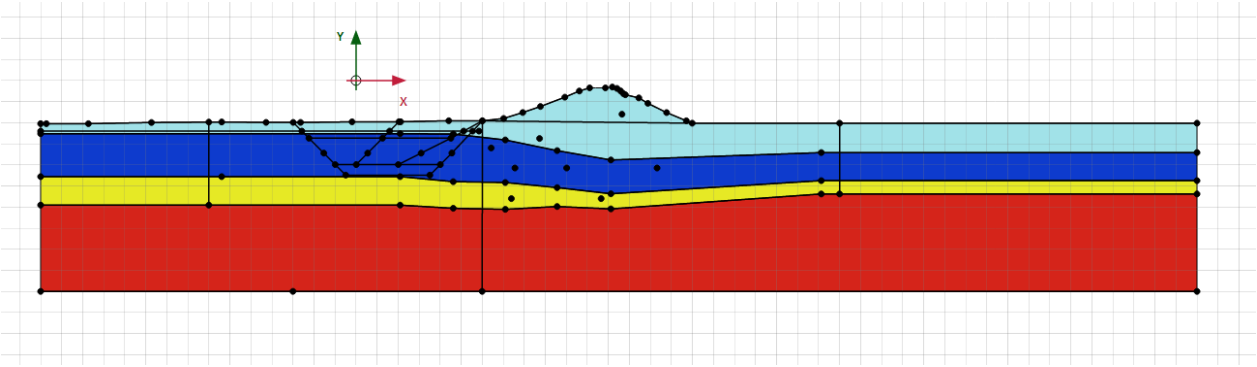

Figure 1: Geometry of the model

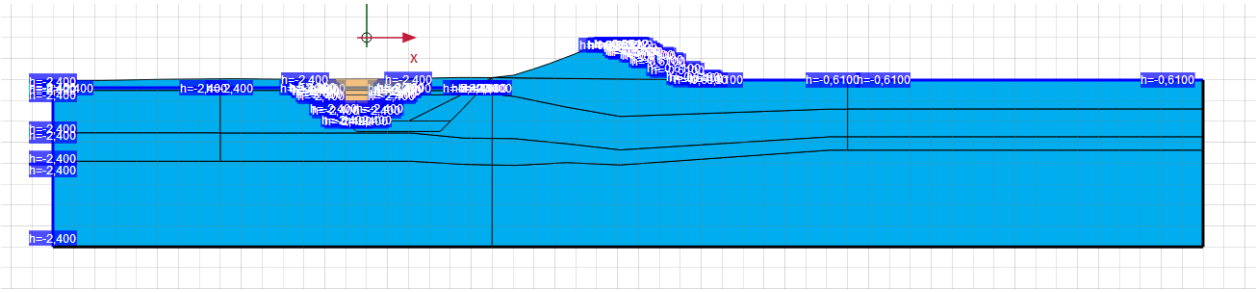

Figure 2: Hydraulic boundary conditions at Excavation I

A point of interest is the shape of the layers below the dyke. In this area, stresses induced by the dyke accelerate the creep effect, leading to deformations greater than those expected by an “instant loading”. This considerable settlement (almost 1m) below the dyke can be taken into account in the model, applying two methods:

- Employ a Creep model (such as Soft Soil Creep) and account for passing of time of the magnitude of centuries. For this approach, the soil starting should have horizontal layers.
- Use models that do not simulate creep. Then , the layer geometry should follow the current geometry. The creep effect in the course of the problem is minor (the experiment takes place in 9 days). This was the method chosen.

The model is set to calculate each phase using a "Fully coupled" analysis. This means that deformations and total pore water pressure are connected in a “two-way” manner, signifying that the hydraulic and deformational calculations are executed in parallel. Thus, a quite realistic approach to the actual problem behavior is provided. Alternatives were:

- "Consolidation" analysis, which only took into account the excess pre water pressures. This analysis employs an “one-way” coupling, meaning that the hydraulic state is calculated, and then the produced pressure is taken into account in the displacement calculation.
- "Plastic", where deformation calculation is not coupled to hydraulic calculation.

(Brinkgreve, Vermeer, 1998)

Finally, the mesh size is 10.0m x 55.0m with triangular 15-noded elements in plane strain conditions.

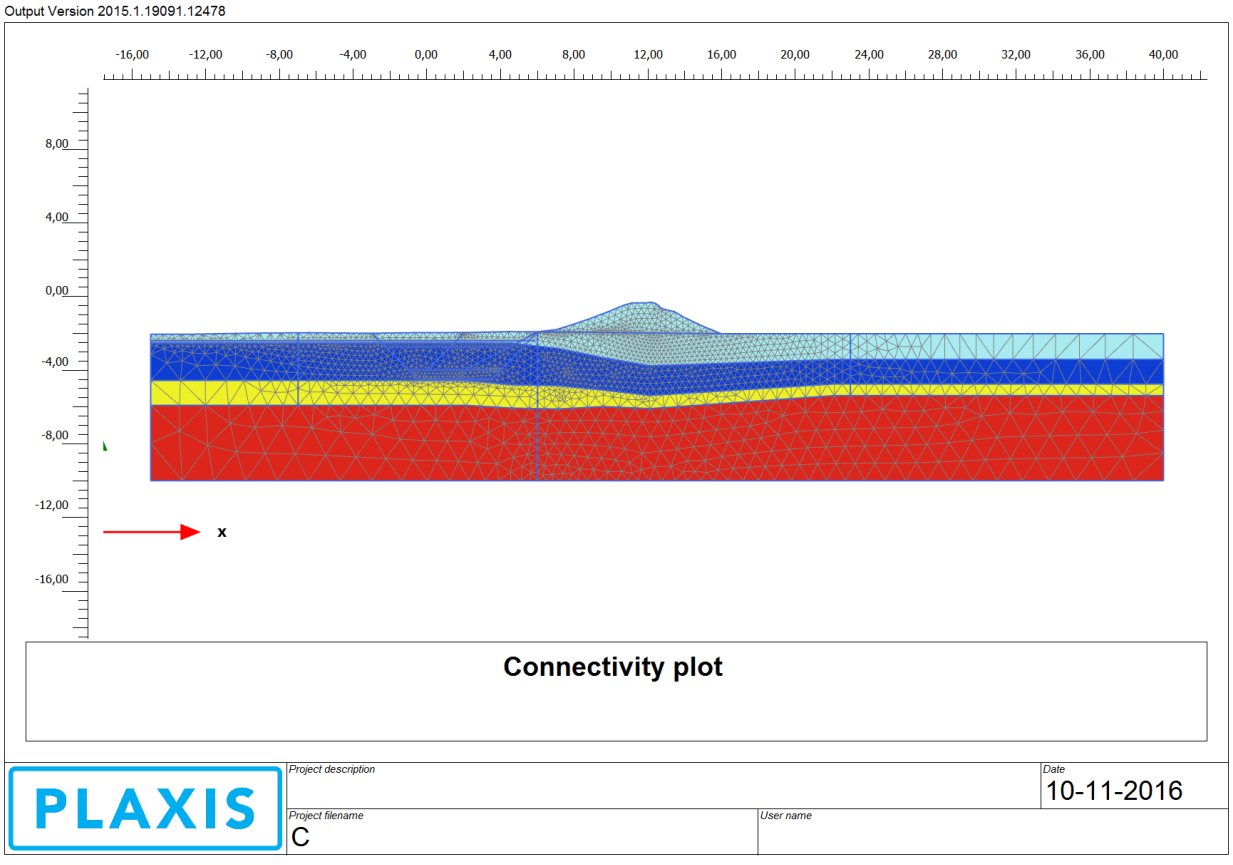

Figure 3: Project mesh

Table 1: Geotechnical layers according to the boreholes from the dyke crest and the excavation site (toe)

Borehole at dyke crest		
Layer	Upper boundary depth NAP (m)	Lower boundary depth NAP (m)
Dyke Material	-0,5	-3,8
Peat	-3,8	-5,3
Soft Clay	-5,3	-6,0
Silty Clay	-6,0	

Borehole at excavation site		
Layer	Upper boundary depth (m)	Lower boundary depth (m)
Dyke Material	-2,0	-2,5
Peat	-2,5	-4,5
Soft Clay	-4,5	-6,0
Silty Clay	-6,0	

A major point of the simulation is listing the construction phases:

- Excavation I: The soil in the polder in front of the dyke is excavated according the first phase plan. (Duration:0.29 day)
- Consolidation I: The pore water overpressures or underpressures produced at the previous stage are dissipated. (Duration: 1.71 day)
- Pumping I: The Water Level inside the excavation is lowered by 1.00m. (Duration:0.11 day)
- Consolidation II: the overpressures are dissipated. (Duration:1.03 day)
- Infill I: The water level inside the excavation is recovered. (Duration:0.05 day)
- Consolidation III: The underpressures are dissipated. (Duration:3.75 days)
- Excavation II: The excavation advances. (Duration:0.39 day)
- Consolidation IV: : The pore water overpressures or underpressures produced at the previous stage are dissipated. (Duration:1.65 day)
- Pumping II: The Water Level inside the excavation is lowered by 1.00m. (Duration:0.17)

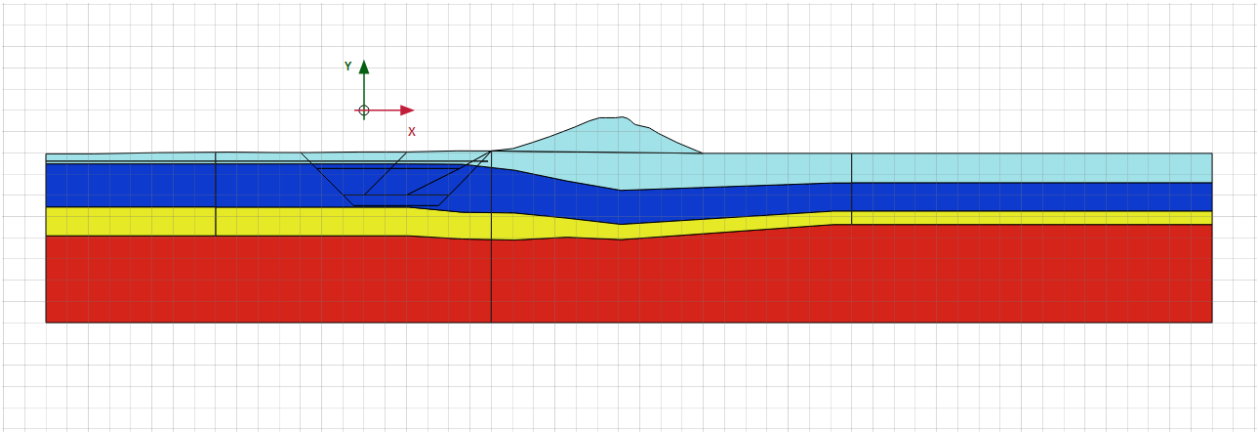

Figure 4: Initial project geometry

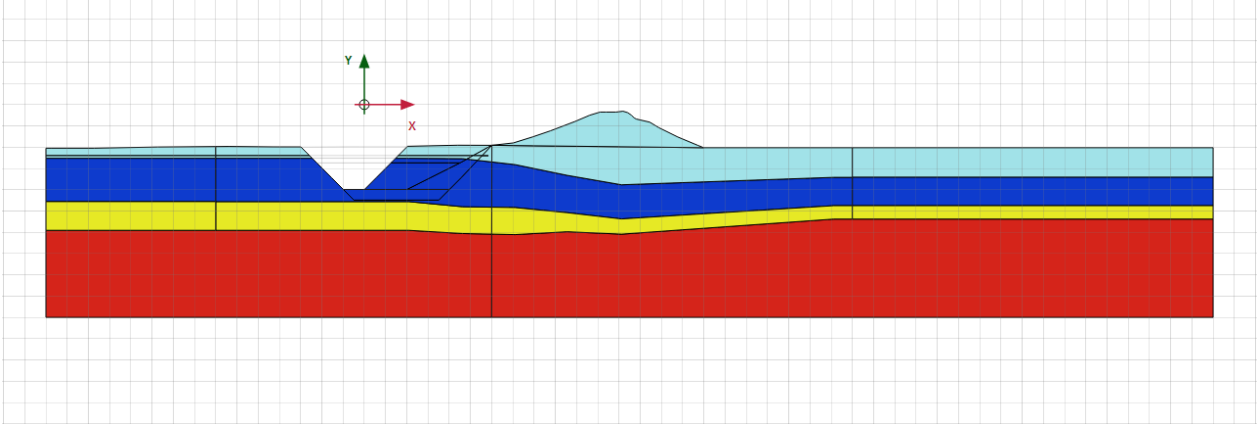

Figure 5:Project geometry at Excavation I

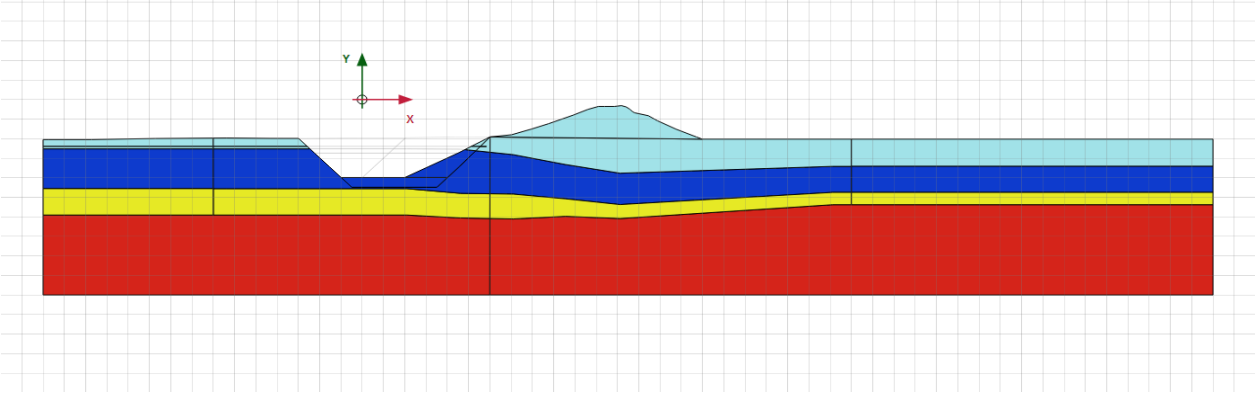

Figure 6:Project geometry at Excavation II

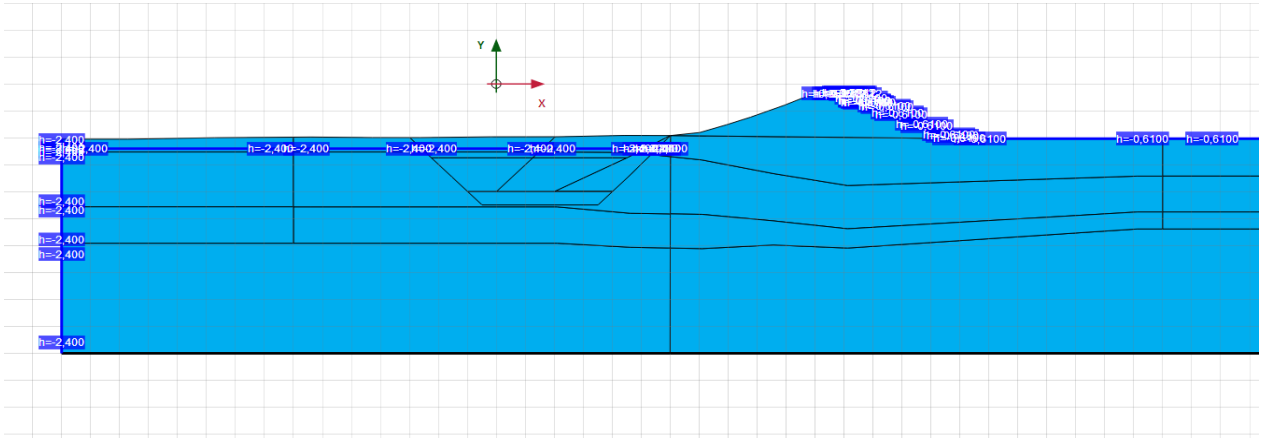

Figure 7: Initial hydraulic conditions

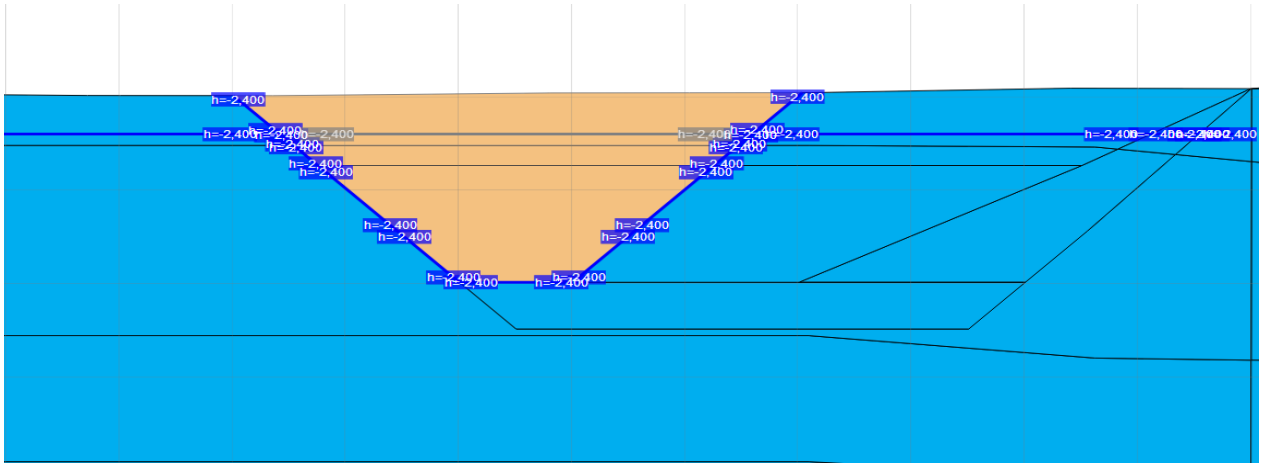

Figure 8:Hydraulic conditions at Excavation I (zoomed in)

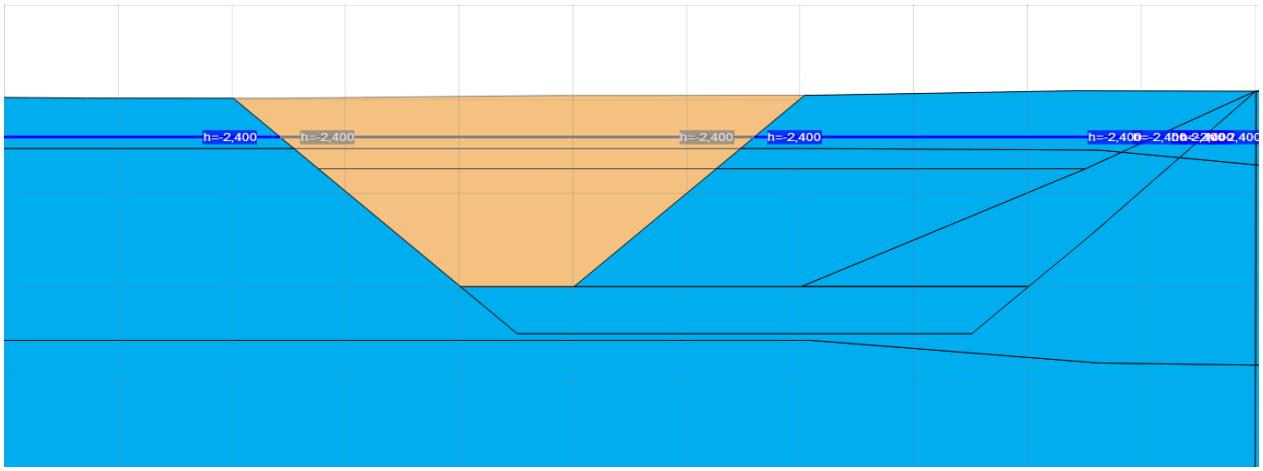

Figure 9:Hydraulic conditions at Consolidation I (zoomed in)

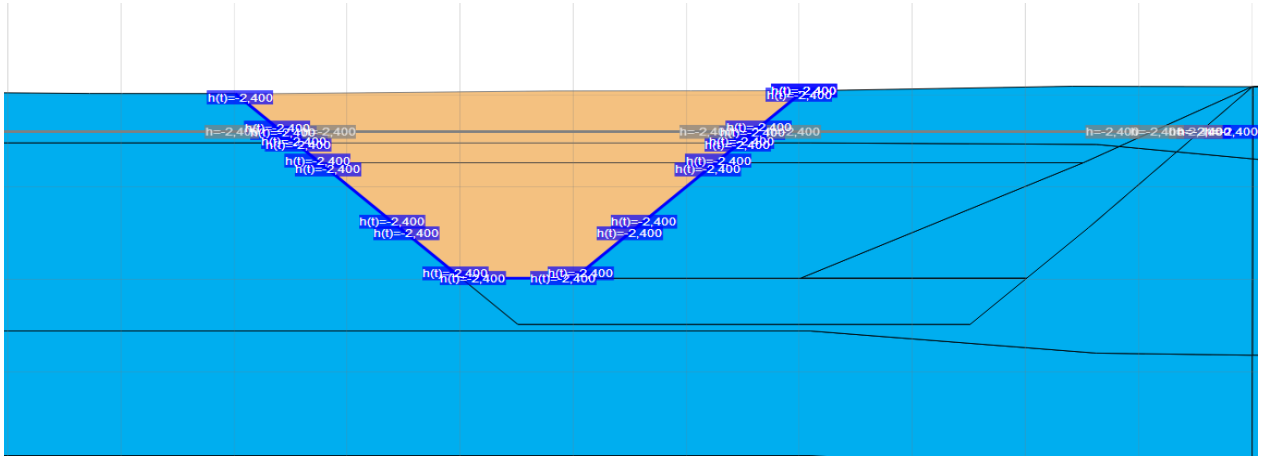

Figure 10:Hydraulic conditions at Pumping I (zoomed in)

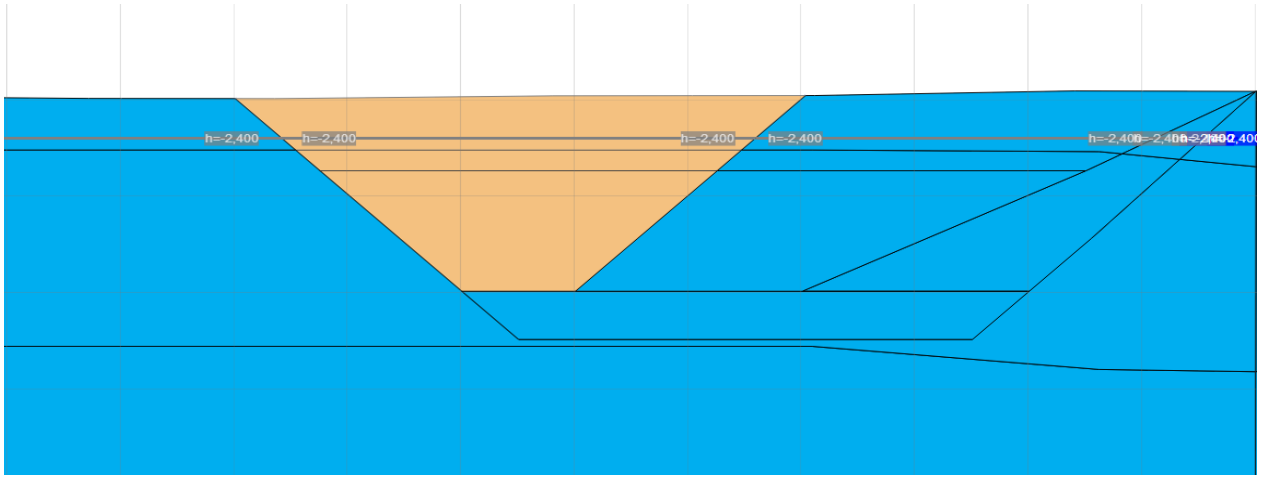

Figure 11:Hydraulic conditions at Consolidation II (zoomed in)

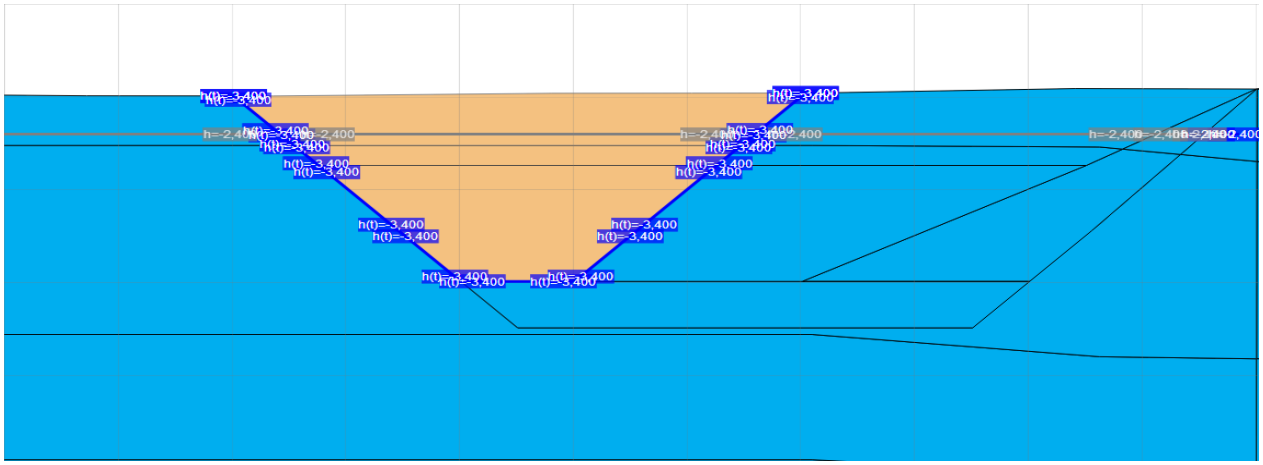

Figure 12:Hydraulic conditions at Infill I (zoomed in)

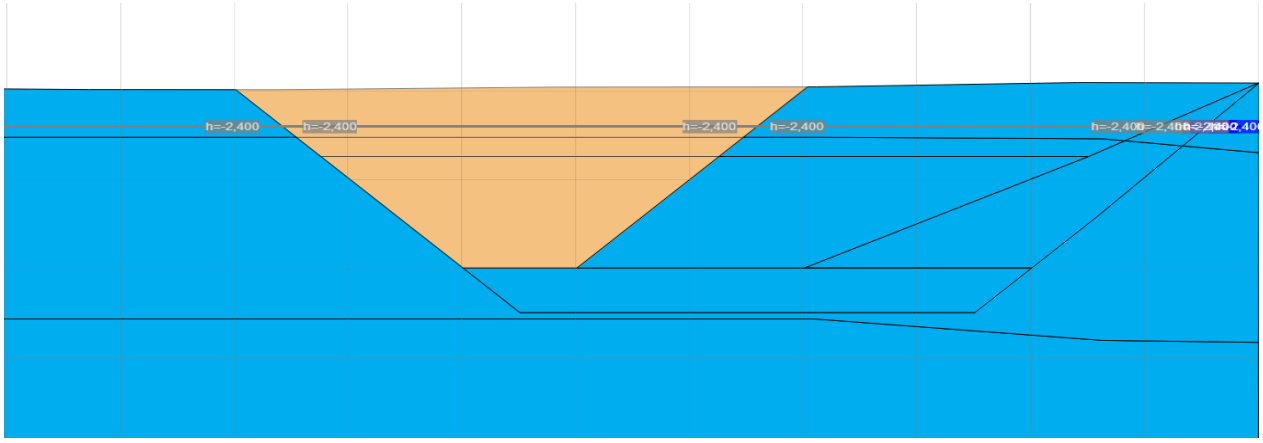

Figure 13:Hydraulic conditions at Consolidation III (zoomed in)

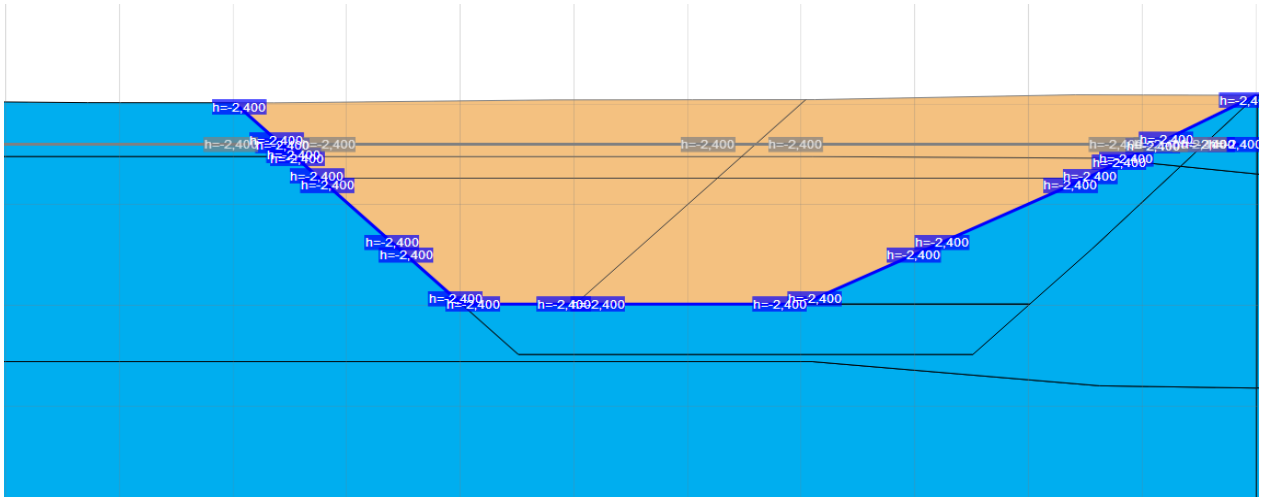

Figure 14:Hydraulic conditions at Excavation II (zoomed in)

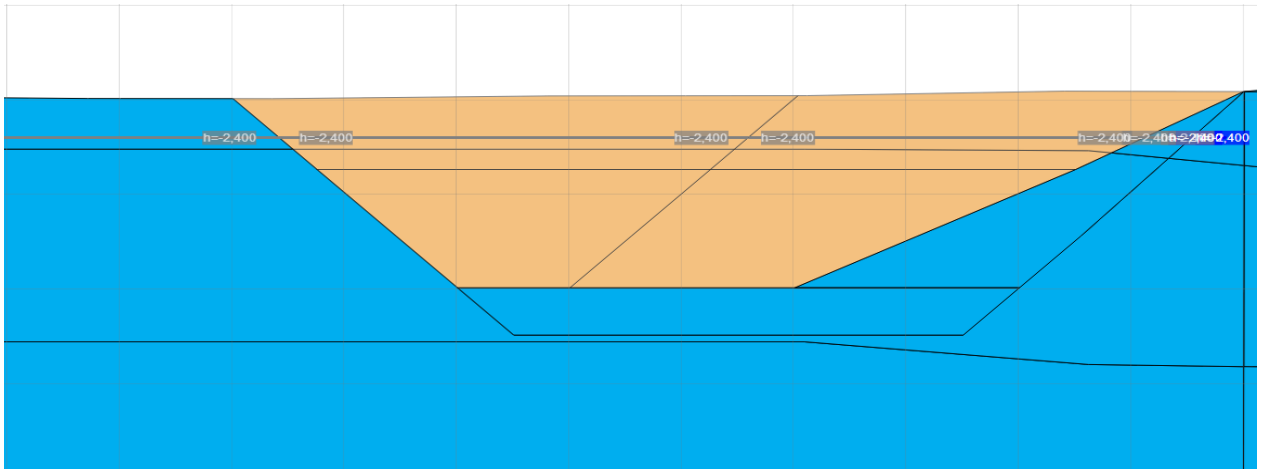

Figure 15:Hydraulic conditions at Consolidation IV (zoomed in)

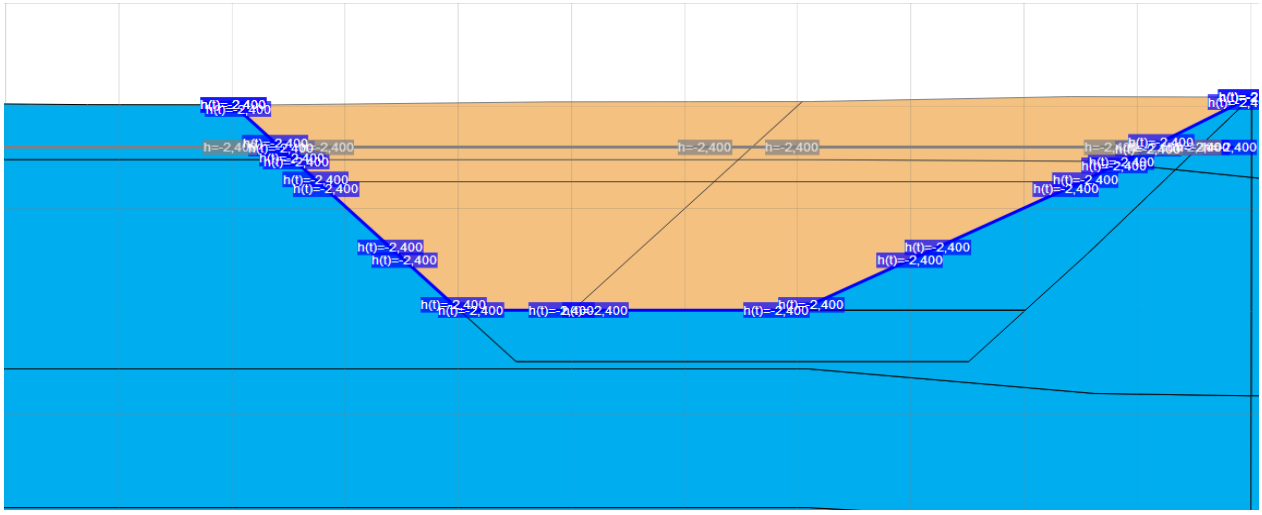

Figure 16:Hydraulic conditions at Pumping II (zoomed in)

2.2 Constitutive models

Advanced models were employed in order to capture the actual behavior of the problem. The Soft Soil model was selected to model the Peat and Soft Clay layers, while the Dyke Material and the Silty Clay layers are simulated with the Mohr-Coulomb model. Mohr-Coulomb enhances the solution time and provides a quite accurate view of failure. On the other hand, the Soft Soil model is used in order to better capture the deformations and pore water pressures development. It is used on these layers which seem critical to displacement evolution.

Shortly, the Soft Soil model includes a compressive yielding surface ("cap"), and is bounded by the Mohr-Coulomb failure criterion. It is based in the connection between volumetric strain and mean stress by the parameters λ*, κ*, which are a measure of the soil compressibility. Although it is mainly used for situations where compressive loading is greater than deviatoric loading (stress states far from the failure envelope), its application in this case is accepted.*(Brinkgreve, Vermeer, 1998)*

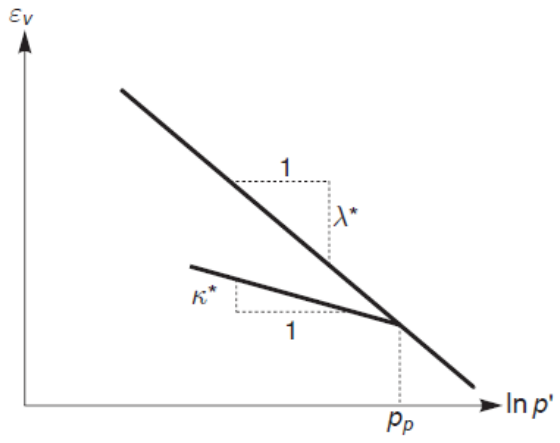

Figure 17: Relation between mean stress and volumetric strain in the Soft Soil model

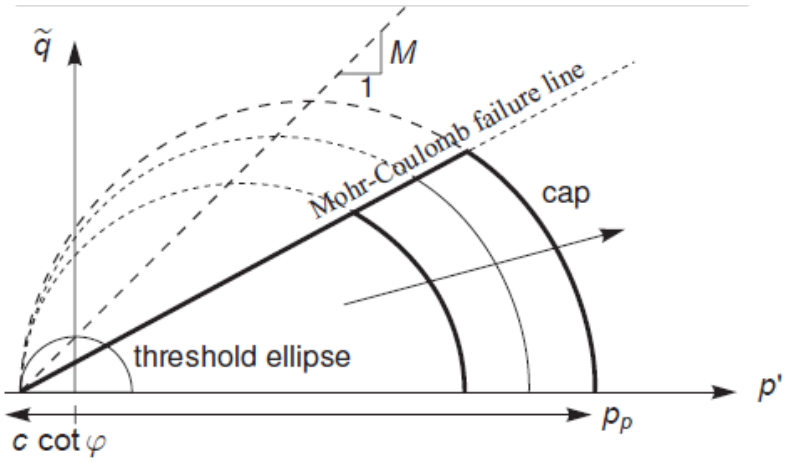

Figure 18: The Soft Soil model presented in a p', q plane

One more advantage of using the Soft Soil model is its ability to capture pre-consolidation. The peat layer is pre-consolidated to an OCR =3, because of the creep effect. The Soft Soil model is able to capture this behavior and attribute the proper horizontal to vertical initial stresses ratio. Moreover, the pre-consolidated state means that the peat layer behaves elastically up to a certain pre-consolidation equivalent stress. However, this pre-consolidation feature is not automatically taken into account in PLAXIS upon setting the OCR; an OCR profile is not translated into a different size of the yield locus, thus, leading to immediate elastoplastic deformation.

As this was not automatically taken into account in PLAXIS, the following alternatives were tested:

- Apply a suitable surface linear load and remove it at the start of the simulation.
- Increase the volumetric weight of Peat for a phase and then recover its original value.
- Lower the level of the groundwater, increasing the effective stresses, and then return it to the top.
- Apply a saturation ratio lower than unity. Then, suction is induced and the effective stresses increase, enhancing the current yield locus.

Comparing the alternatives, only the fourth method allows affecting the pre-consolidation locus of the Peat layer, while preserving the OCR of the Soft Clay layer. The problem of this methods is that the initial stress ratio may be altered, but without compromising the accuracy of the model[1].

2.3 Parameters

The parameters applied were a result of lab testing conducted by commercial laboratories and also TU Delft *(Zhao,Poutoni,2016)*.The performed analysis included mostly Triaxial, Oedometer and Direct Simple Shear tests.The6σ rule was applied in order to estimate the statistical properties of the stiffness and permeability distribution; the maximum and minimum of the data are supposed to be apart by 6 times the standard

[1] Changing the effective stress state leads to increase of horizontal stresses. After the stresses are returned to the original values, horizontal stresses are "locked" to the increased values, leading to a higher K_o. However, the impact of this initial stress state to the analysis is minor.

deviation*(Pohl, 2011)*. Thus, the standard deviation can be estimated and the normal distribution curve assumed.

The characteristic values are then derived according to Eurocode 7 *(European Committee of Standardization, 2004)*:

$$X_{char} = X_{mean} * (1 \pm k_n * V_x)$$

Where:

- X_{char} is the characteristic value of the parameter.
- X_{mean} is the mean of the parameter distribution.
- k_n is a factor based on number of tests performed but also the project type. When a large soil volume is affected, stress redistribution is possible and parameter fluctuation is averaged over strong and weak soil areas. Thus, the characteristic value will be closer to the mean, so k_n is lower.
- V_x is the coefficient of variation: $V_x = \frac{\sigma}{\mu}$

For the strength parameters, another approach was taken. As the angle of friction ϕ is negatively correlated with the cohesion c, a linear regression (least squares method) was used in the σ',τ plot. Then, the produced failure envelope was factorized according to the Eurocode partial safety factors, and its properties were used to calculate the characteristic strength of the soil.[2]*(Bond, Harris,2008)*

Table 2: Assumed characteristic and design values of strength parameters

Strength parameters (Characteristic and design values)				
Layer/Parameter	Reference		Design	
	ϕ (°)	c (kPa)	ϕ (°)	c (kPa)
Dyke Material	33,0	5,0	27,5	4,0
Peat	28,8	2,5	23,7	2,0
Soft Clay	29,5	4,5	24,4	3,6
Silty Clay	30,0	1,9	24,8	1,5

According to the philosophy of the Eurocode, the more test executed, the less the uncertainty of the subsoil. Thus, for a larger test number, a lower k_n factor is attributed to the statistical approach of the characteristic value*(Schneider et al, 2013)*. In the margins of this project, data from five tests was used to assess the statistics of the parameters, however, the k_n value corresponds to only one test. Hence, the spreads of the characteristic values of compressibility and permeability are greater and their impact on the FEM analysis results is more significant and easier to recognize.

[2]In the following, the analyses employ the mean values of soil strength as the characteristic ones, in order to enable a ULS reduction that would not bring the soil to failure, but would allow for discussion on the model's response.

Table 3: Statistical editing of compressibility for Peat and Soft Clay layers

Number of tests	5

PEAT LAYER

Statistical processing of compressibility distributions								
Parameter	Minimum	Mean	Maximum	St. deviation	V	$k_{n,mean}$	$X_{c,mean,low}$	$X_{c,mean,high}$
λ (-)	1,700	2,000	2,300	0,100	0,050	1,645	1,836	2,165
κ (-)	0,250	0,300	0,350	0,017	0,056	1,645	0,273	0,327

Compressibility mean and characteristic values			
Parameter	Minimum	Mean	Maximum
λ* (-)	0,167	0,182	0,197
κ* (-)	0,025	0,027	0,030

SOFT CLAY LAYER

Statistical processing of compressibility distributions								
Parameter	Minimum	Mean	Maximum	St. deviation	V	$k_{n,mean}$	$X_{c,mean,low}$	$X_{c,mean,high}$
λ (-)	0,200	0,275	0,350	0,025	0,091	1,645	0,234	0,316
κ (-)	0,035	0,038	0,040	0,001	0,022	1,645	0,036	0,039

Compressibility mean and characteristic values			
Parameter	Minimum	Mean	Maximum
λ* (-)	0,078	0,092	0,105
κ* (-)	0,012	0,013	0,013

3 Safety factor approaches

Two methods of applying the partial safety factor concept according to the Eurocode are orchestrated, as well as a third one according to traditional “overall safety factor” approach for comparison. The ULS checks are performed at the following selected stages: Excavation I, Pumping I, Consolidation III, Excavation II and Pumping II. The excavation and pumping stages are analyzed as the unloading induced increases the deviatoric stress while decreasing the mean. The consolidation phase chosen is the only one happening after an fill in stage, so the effect and amount of plastic, permanent strains can be studied.

3.1 Scheme 1a

Scheme 1a is the classical application of the Strength Reduction Factor method. The model is ran for the SLS with characteristic values and at selected phases, a SRF stage is introduced, so that the safety factor is estimated *(Brinkgreve, Bakker, 1991)*. The SRF method reduces by the same ratio both the cohesion and the (tangent of) the friction angle. Hence, it resembles and overall safety factor. The philosophy of applying a ULS stage along a SLS simulation resembles encountering a worst case scenario during construction, while no warning is given beforehand.

$$c_{SRF} = \frac{c}{SRF} \; and \; \varphi_{SRF} = arctan(\frac{\tan(\varphi)}{SRF})$$

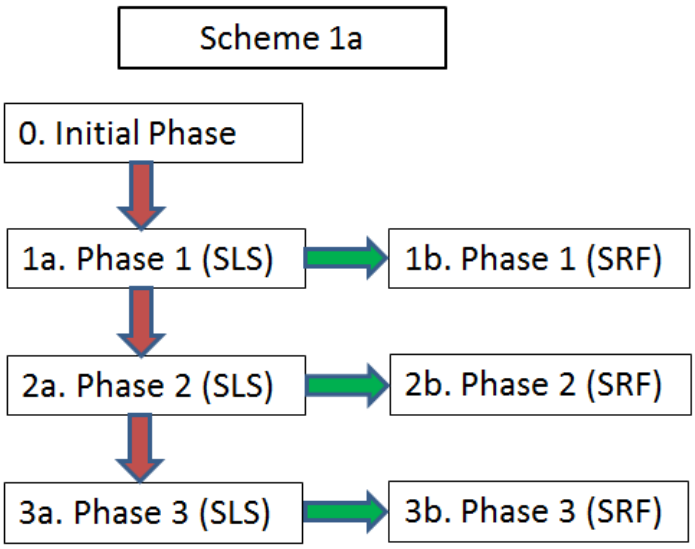

Figure 19: Illustration of Scheme 1a

3.2 Scheme 1b

This scheme employs the concept of partial safety factors, according to Eurocode 7. The model is ran in SLS as previously, but for the selected phases a ULS analysis takes place by applying a design approach of the Eurocode. The strength of the soil is reduced, and stability of the construction is tested for a worst case scenario. In this scheme, the logic of checking for ULS in parallel to the SLS is as the same as in Scheme 1a. *(Kavvadas 2008), (Brinkgreve et al, 2015), (Potts, Zdravkovic, 2012)*

Design Approach 3 was chosen, as it best fits for unsupported slope stability problems. DA3 applies the maximum decrease of material parameters, while loads, resistances and the support provided by any structure is not factorized. For this problem, this approach provides the greatest safety. Besides, in DA3, drained strength parameters are factorized by an equal 1.25 safety factor. It should be noted that the partial safety factor of the volumetric weight is unity, as it contributes both to the resistance and to the driving forces. *(Brinkgreve, Bakker, 1991)*.

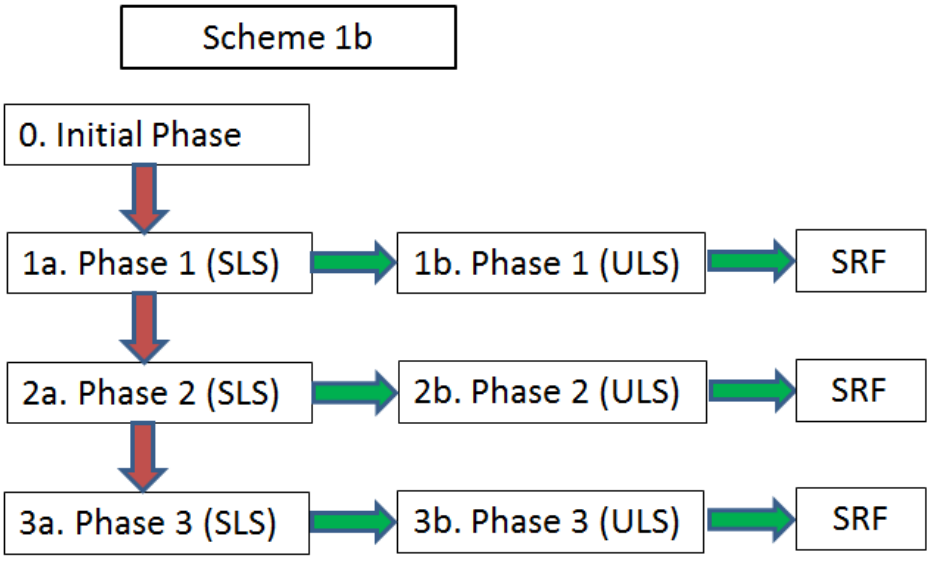

Figure 20: Illustration of Scheme 1b

The partial safety factor approach is a consistent check against failure, but does not offer a measure of stability. Hence, an SRF check is set after every ULS stage, so that the stability of the system at the different steps of the analysis can be quantified. As this SRF corresponds to reduced strength parameters, it should be multiplied by an SRF equivalent to the DA3, which can be roughly set to 1.25 as no loads, resistances or load effects are factorized, while both the angle of friction and the cohesion have the same factor *(Brinkgreve et al, 2013)*. In this way, Scheme 1b can be compared to Scheme 1a.

3.3 Scheme 2

The philosophy of Scheme 2 is the most straightforward; the analysis is conducted as if the worst case scenario is encountered from the beginning. This means that the partial safety factors of DA3 are effective from the first construction phase. This philosophy is more meaningful in an unsupported slope stability problem, as it reflects the permanent inadequate soil conditions that may be present. However, an SRF analysis is again executed in the designated phases, so as to quantify their measure of stability. As in Scheme 1b, the results of Scheme 2 have to be scaled up by 1.25 so that they are comparable to those of Scheme 1a and represent an overall safety factor. *(Brinkgreve et al, 2015), (Potts, Zdravkovic, 2012)*

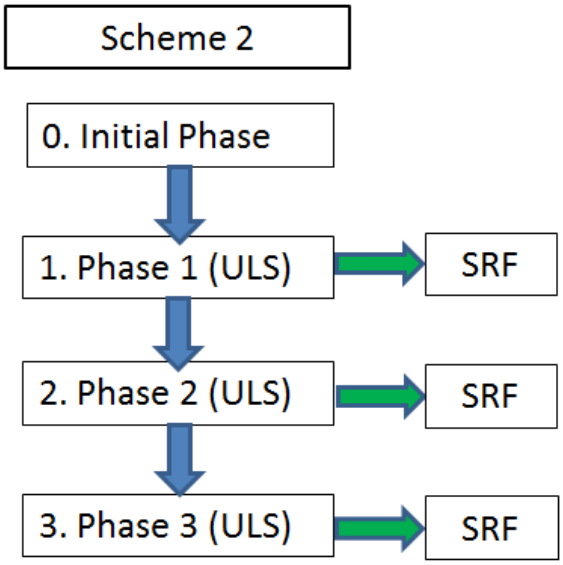

Figure 21: Illustration of Scheme 2

4 SERVICEABILITY ANALYSIS RESULTS

In the Serviceability Limit State (SLS), the analysis employs the characteristic values of soil properties and all partial safety factors are set to unity *(European Committee of Standardization, 2004)*. The deformational response of the construction is then evaluated.

In the context of this project, a question is raised on what the characteristic value should be. Such a parameter value should represent a case matching to a "worst case scenario", which after verification, will imply the verification of every other scenario *(Bond et al. 2013)*. For strength parameters, it is clear that the characteristic value should be the value that offers the designated reliability level (5% fractile or 95% confidence based on mobilized soil volume). However, this concept might not be entirely clear for deformation parameters.

In elastoplastic models, the stiffness is divided into two types: elastoplastic and elastic. The first one concerns the deformations happening during yielding, while the second is connected to the part of the deformations that are recoverable upon unloading, the elastic component. Typically in a SLS, the worst case scenario would be the case of maximum compressibility (equivalent to minimum stiffness). In the Soft Soil model, this is translated into the highest characteristic value of κ*, λ* (being the elastic and elastoplastic counterparts respectively). Thus, it is the compressibility value offering a 95% confidence level that larger deformations will not develop in situ (or that the compressibility value will not be surpassed if the 5% fractile were considered). However, another opinion offers a different view on this topic: the most severe case would be the boosting of the elastoplastic compressibility and the diminishing of the elastic one, meaning that the elastic compressibility will now subtract the fluctuation, not add it. The yielding deformation will be described by the same high value but the elastic deformations recovered during unloading would be considerably less, thus, maximizing the magnitude of the plastic, non-recoverable deformations. Then, this combination was equally evaluated as potentially critical in SLS.

Table 4: Compressibility parameter distribution for Peat layer

Compressibility mean and characteristic values for Peat			
Parameter	Minimum	Mean	Maximum
λ* (-)	0,175	0,182	0,189
κ* (-)	0,026	0,027	0,028

Table 5: Compressibility parameter distribution for Soft Clay layer

Compressibility mean and characteristic values for Soft Clay			
Parameter	Minimum	Mean	Maximum
λ* (-)	0,086	0,092	0,098
κ* (-)	0,012	0,013	0,013

The results of the analysis are presented below. The only varying parameters between two analyses are the κ* and λ* of the peat and soft clay layers.

However, in the examined case the two analyses show almost no difference at all. The major divergence expected in Consolidation III does not exist. The only variation between models is the final displacement of the Excavation II and Pumping II phases, which differs by some millimeters. Then this fact proves that the development of displacements is controlled by the elastoplastic compressibility, not the elastic one. However, this argument cannot be generalized, as the deformational history is heavily based on the type of problem and the succession and details of construction phases. In order to have the anticipated difference in this particular model, then maybe the elastic unloading should have been greater. On the other hand, the fluctuation between the marginal values of the elastic parameter may be to too low to produce considerable results (see Table 3: Statistical editing of compressibility for Peat and Soft Clay layers). A soil with different statistics could maybe fulfill the expectations of this analysis.

A final mention that should be made on these graphs is that the displacements seem to be diminished at the Peat-Soft Clay interface. This happens at all construction phases and points out the soil area that affects the behavior of the construction.

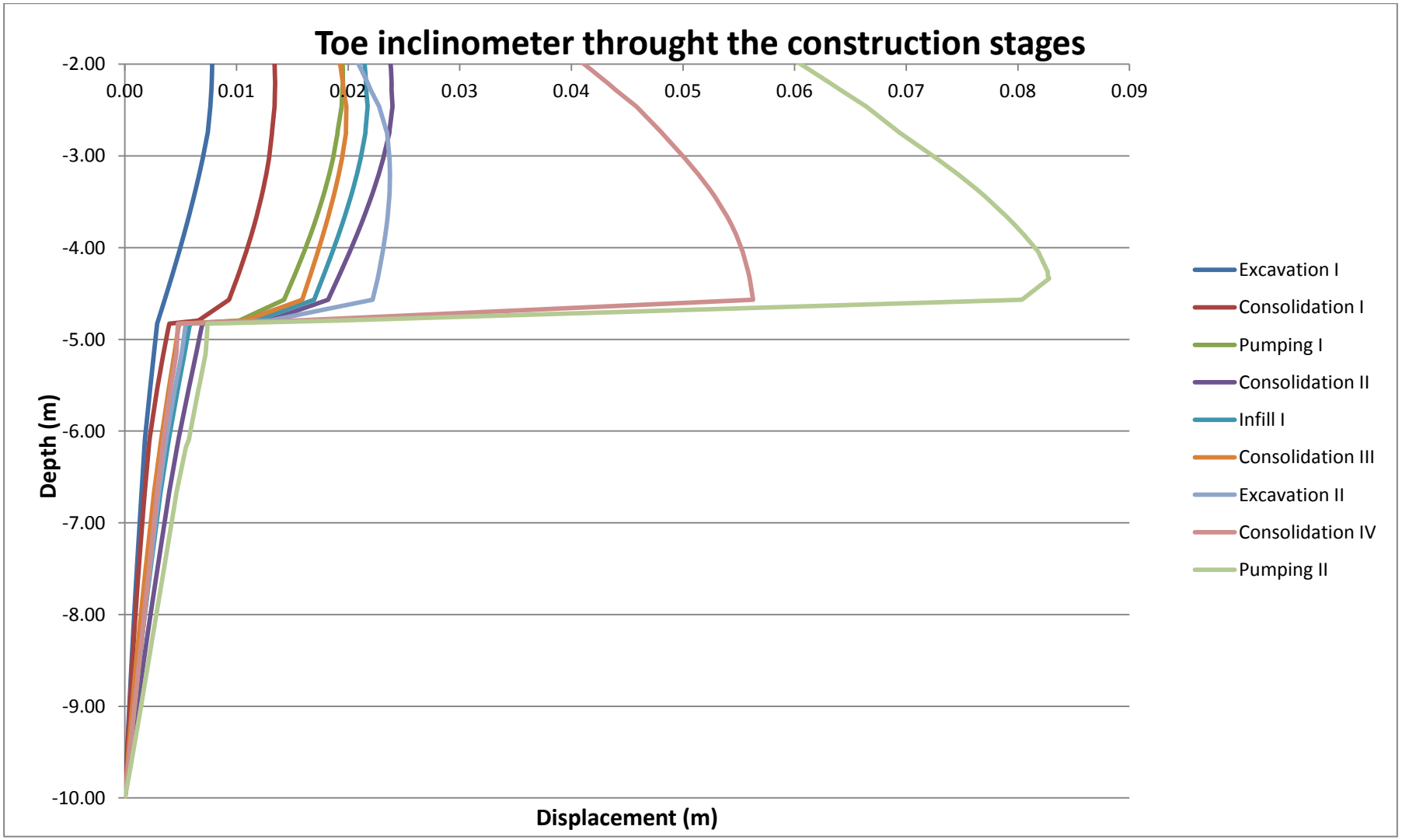

Figure 22: Displacement profiles at dyke toes for each construction phases (Maximum elastoplastic and elastic compressibilities)

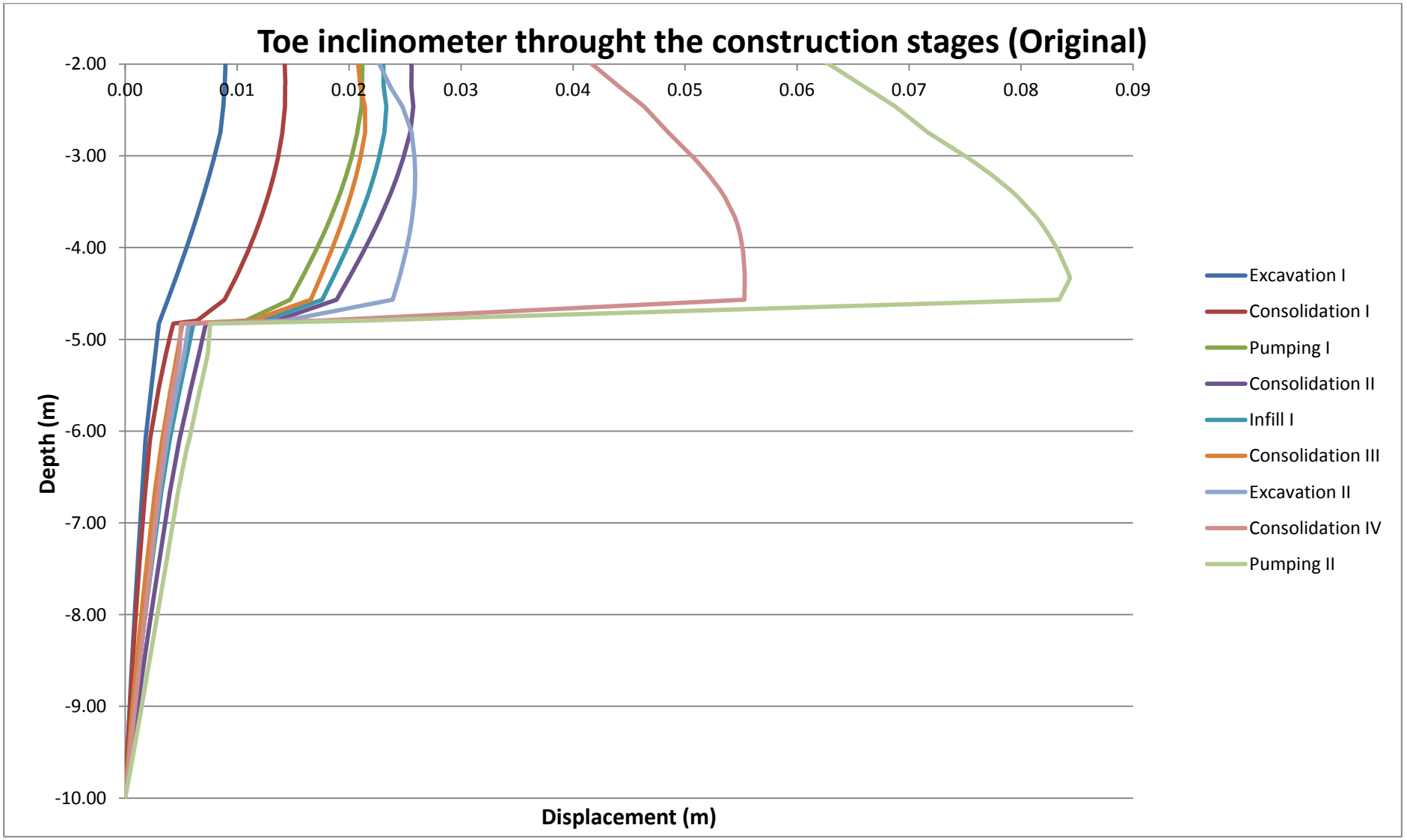

Figure 23: Displacement profiles at dyke toes for each construction phases (Maximum elastoplastic and minimum elastic compressibilities)

5 COMPARISON BETWEEN CONSTITUTIVE MODELS

Adopting the design schemes described in paragraph 3, the ULS response of the two employed constitutive models is compared. The labels of the different analyses are presented below:

Table 6: Analysis chart

Scheme/Model	Soft Soil	Mohr-Coulomb
1a - SRF	A	B
1b - DA3	C	D
2 - DA3	E	F

The resulting SRF for each analysis was recorded in the following chart. As already explained, the results of Scheme 1b and Scheme 2 are multiplied by an SRF of 1.25, equivalent to the partial safety factor decrease acting.

Table 7: Results of the analysis in terms of an overall safety factor

Overall Safety Factor of each analysis					
Analysis	Excavation I	Pumping I	Consolidation III	Excavation II	Pumping II
A	1,46	1,19	1,25	1,12	0,97
B	1,38	1,10	1,23	1,06	0,95
C	1,52	1,47	1,29	1,26	1,24
D	1,32	1,30	1,20	1,17	1,19
E	1,51	1,24	1,24	1,22	-FAILURE-
F	1,37	1,20	1,24	1,20	-FAILURE-

Both constitutive models approach failure in the same manner, and so, no SRF difference is expected. Both models employ a Mohr-Coulomb failure criterion, and this means that failure is expected to be achieved in the exact same state. However, in every scheme, the Soft Soil model produces a greater safety factor. There are mainly two reasons explaining this behavior.

Firstly, Soft Soil is an elastoplastic models, meaning that plastic yielding is possible before failure. Plastic deformations take place through the loading process, thus leading to pore water distributions different from that of a purely elastic model. Stress paths diverge from the linearly elastic pre-failure behavior of the Mohr-Coulomb, giving off a different Skempton's coefficient value. Secondly, one of the cornerstones of the Soft Soil model is that compressibility is stress-dependent. This means that deformability is not equal among elements, even for those which have not failed yet. Hence, stress states may vary from that of the Mohr-Coulomb and consequently the stress redistribution mechanisms that form failure surfaces.

An example of the pore water development divergence between models is presented:

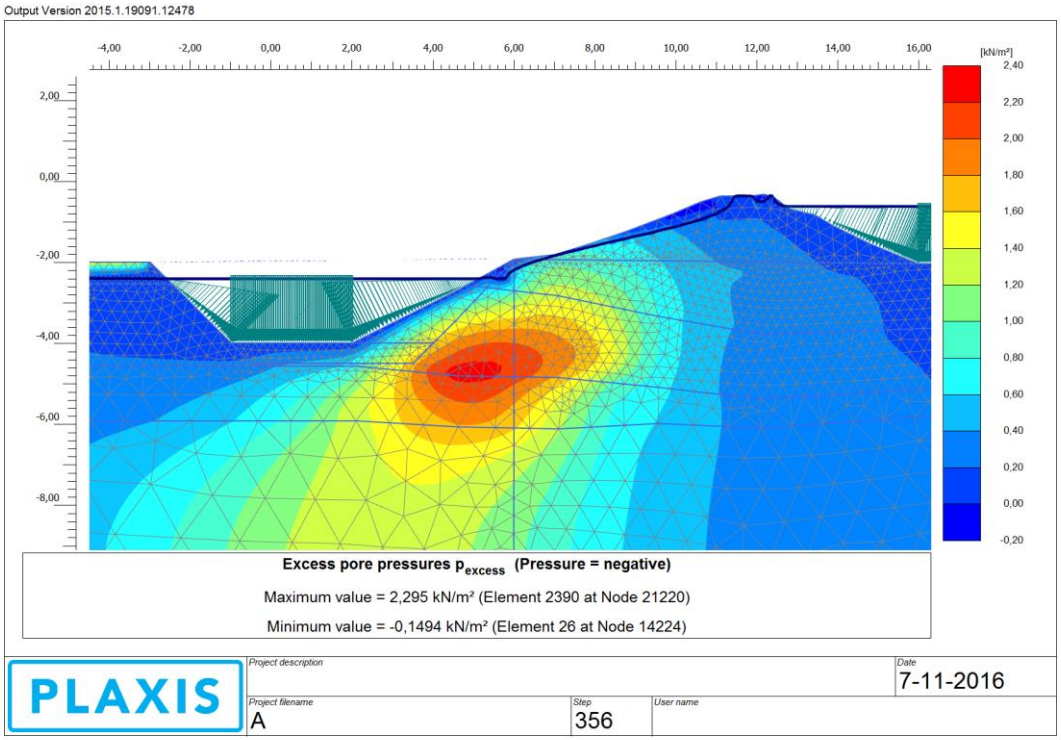

Figure 24: Excess pore water pressure (A, Excavation II)- (Underpressures in red)

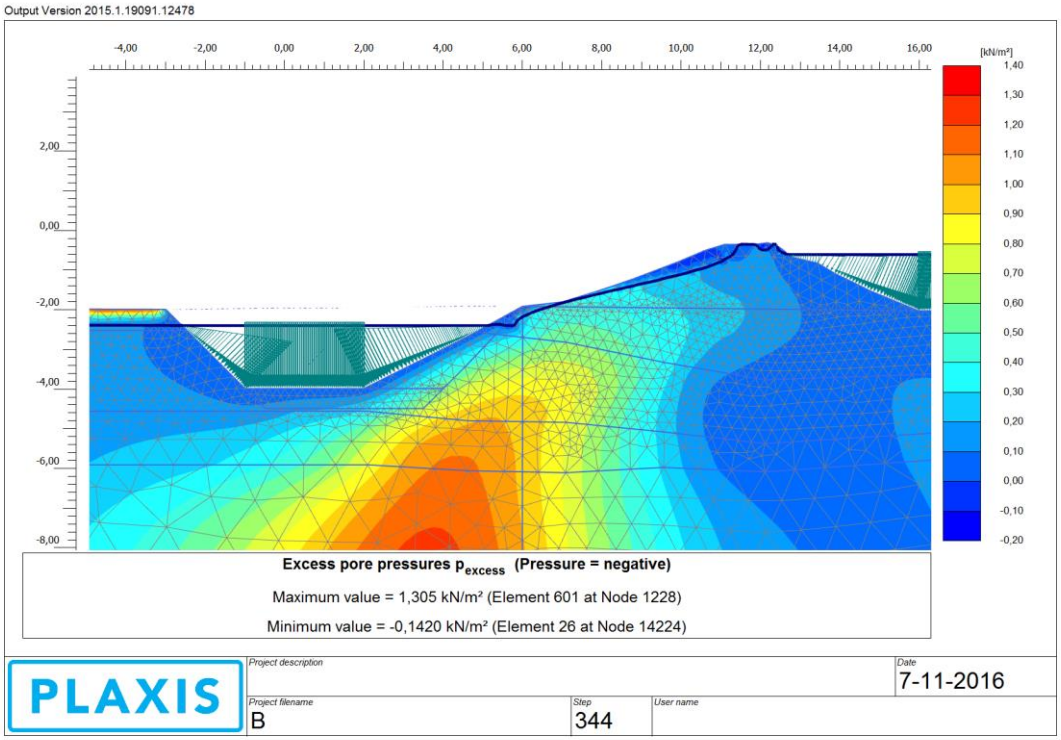

Figure 25: Excess pore water pressure (B, Excavation II)- (Underpressures in red)

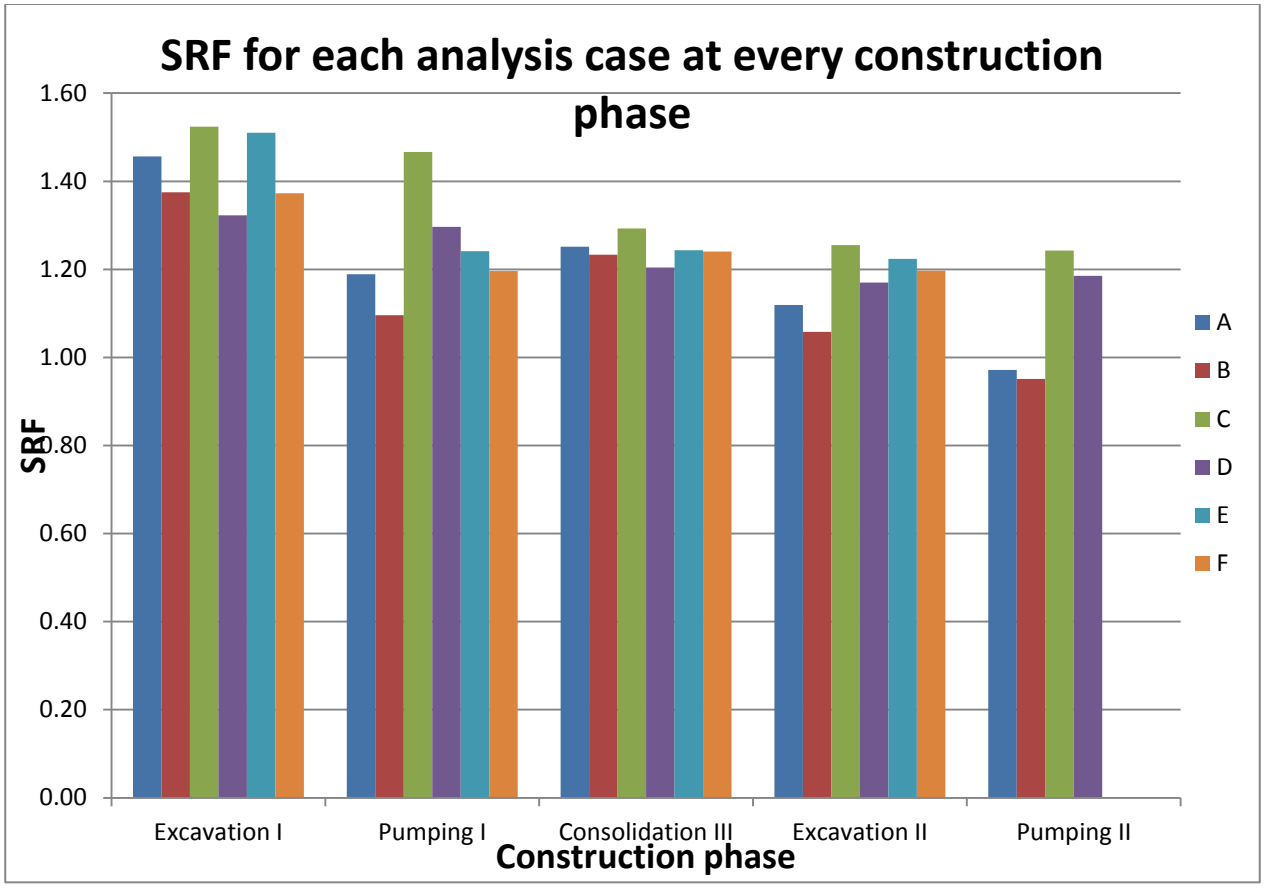

Figure 26: Overall SRF for each analysis case at each construction phase

These features lead to different SRF values, but the qualitative approach of the problem is the same; a uniform strength reduction leads to the creation of the similar failure mechanisms. Even more, in a slope stability case, the difference between schemes might not be enough to distinguish failure modes. As an example, the first construction phase is presented in every analysis. The failure takes the form of an overall slope slide. The shear strain band tends to be divided into two semi-continuous parts. This implies that there is a tendency for a retrogressive mechanism to be created, forming first an excavation slope slide, leading to a general failure. This phenomenon is more evident in later schemes. Some examples are presented below.

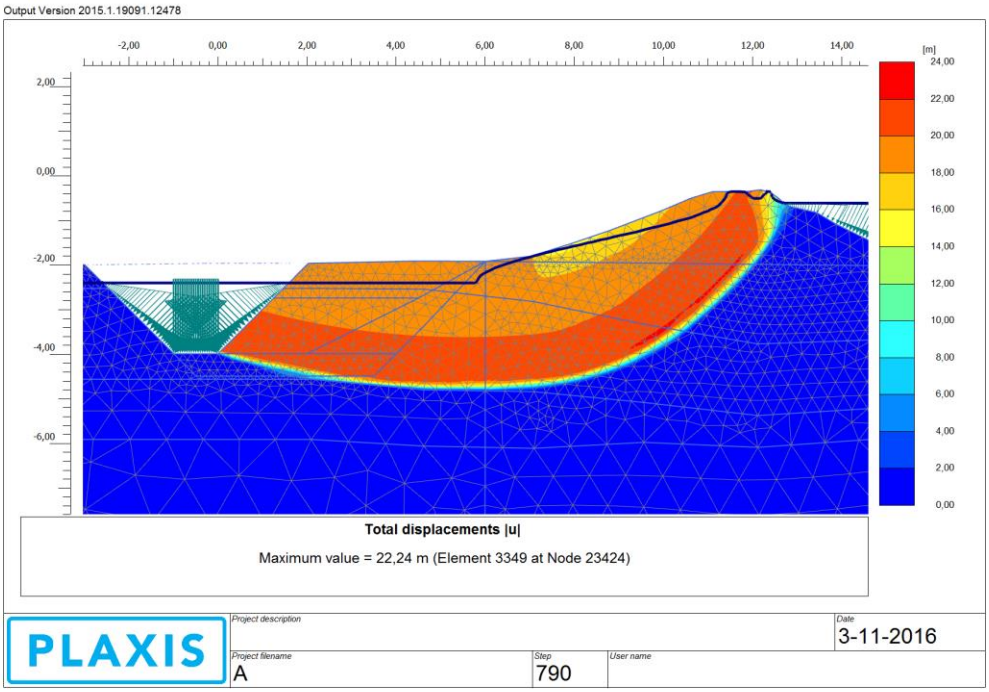

Figure 27: Displacement contour (A, Excavation I)

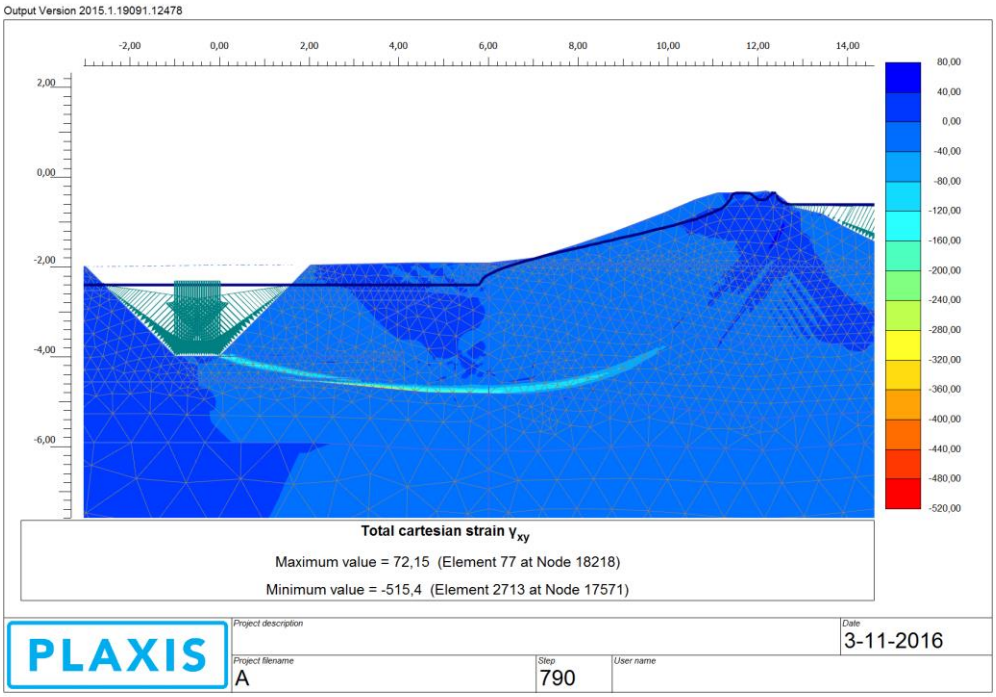

Figure 28: Shear strain contour (A, Excavation I)

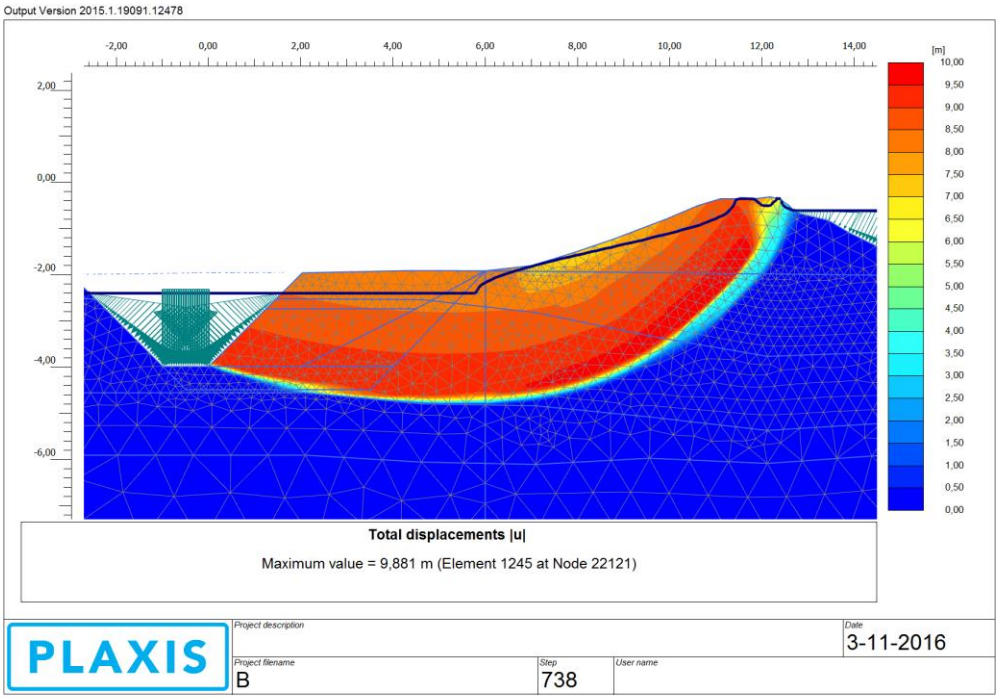

Figure 29: Displacement contour (B, Excavation I)

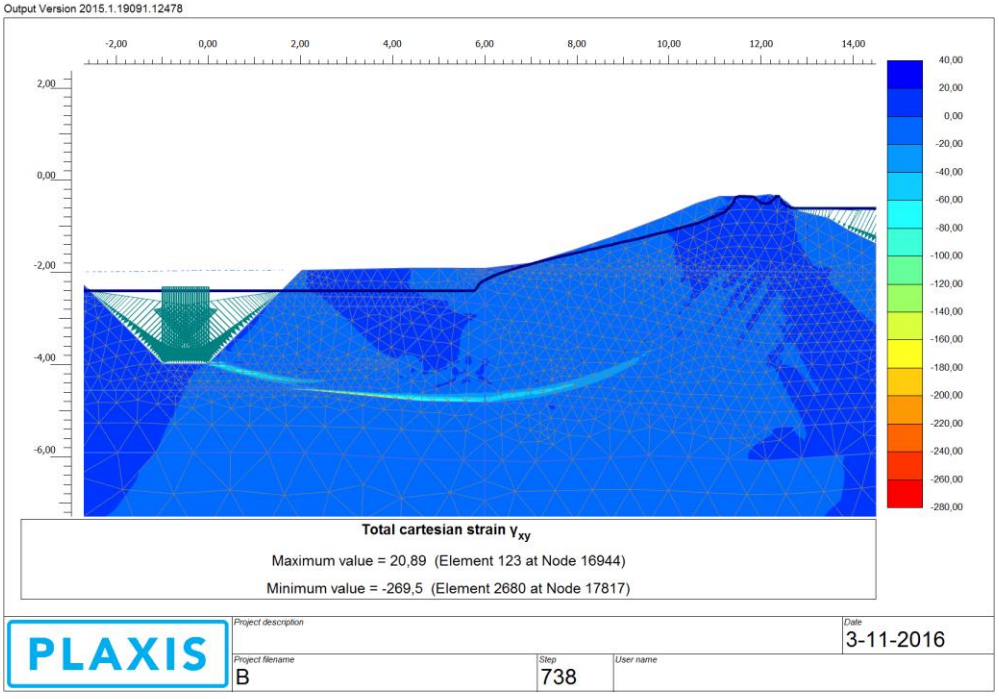

Figure 30: Shear strain contour (B, Excavation I)

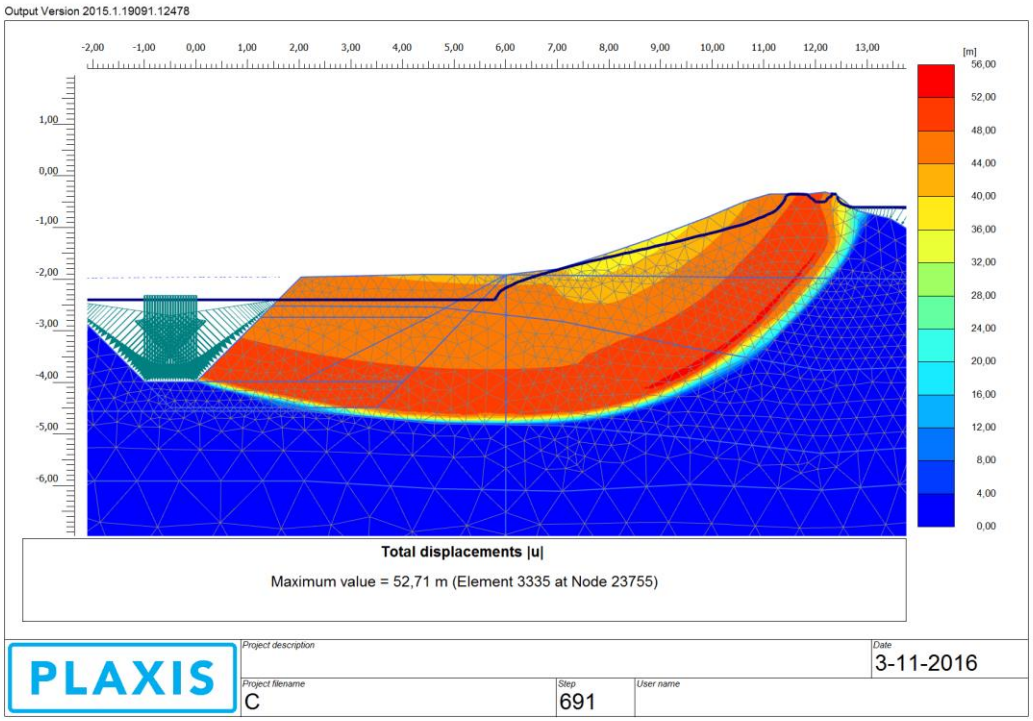

Figure 31: Displacement contour (C, Excavation I)

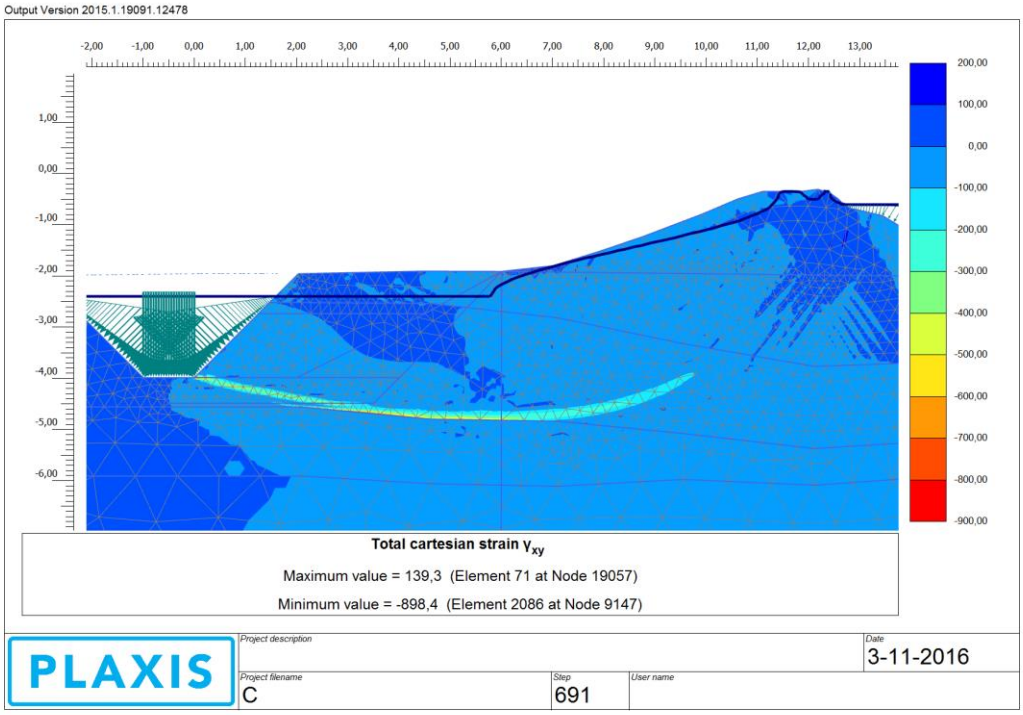

Figure 32: Shear strain contour (C, Excavation I)

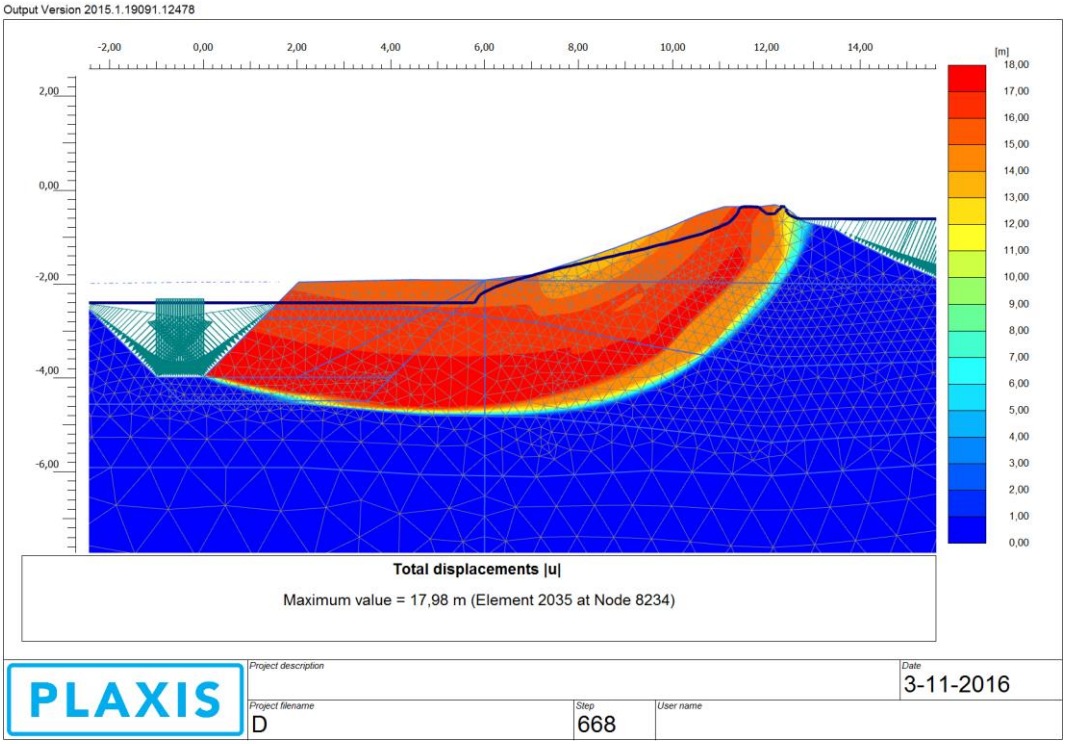

Figure 33: Displacement contour (D, Excavation I)

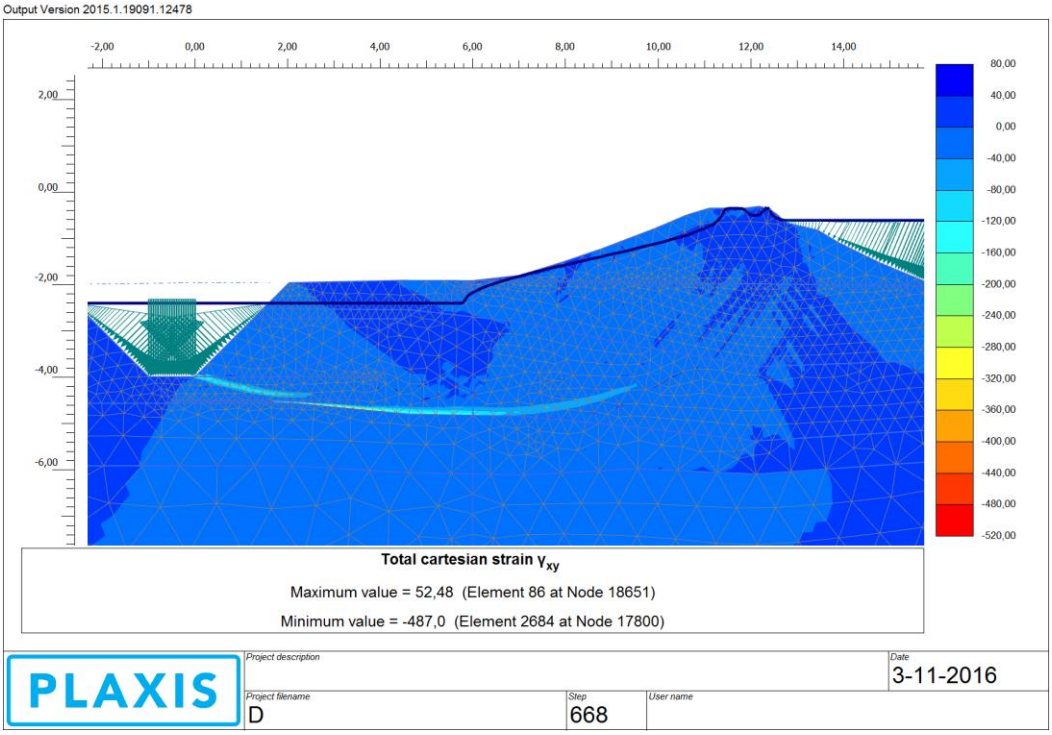

Figure 34: Shear strain contour (D, Excavation I)

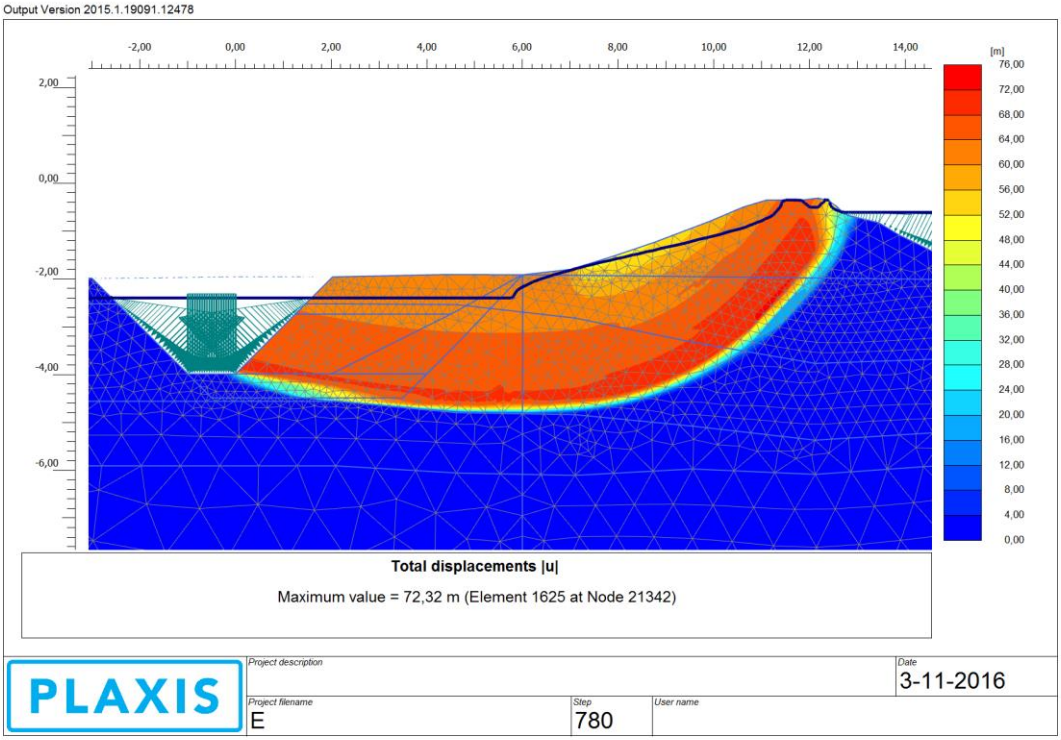

Figure 35: Displacement contour (E, Excavation I)

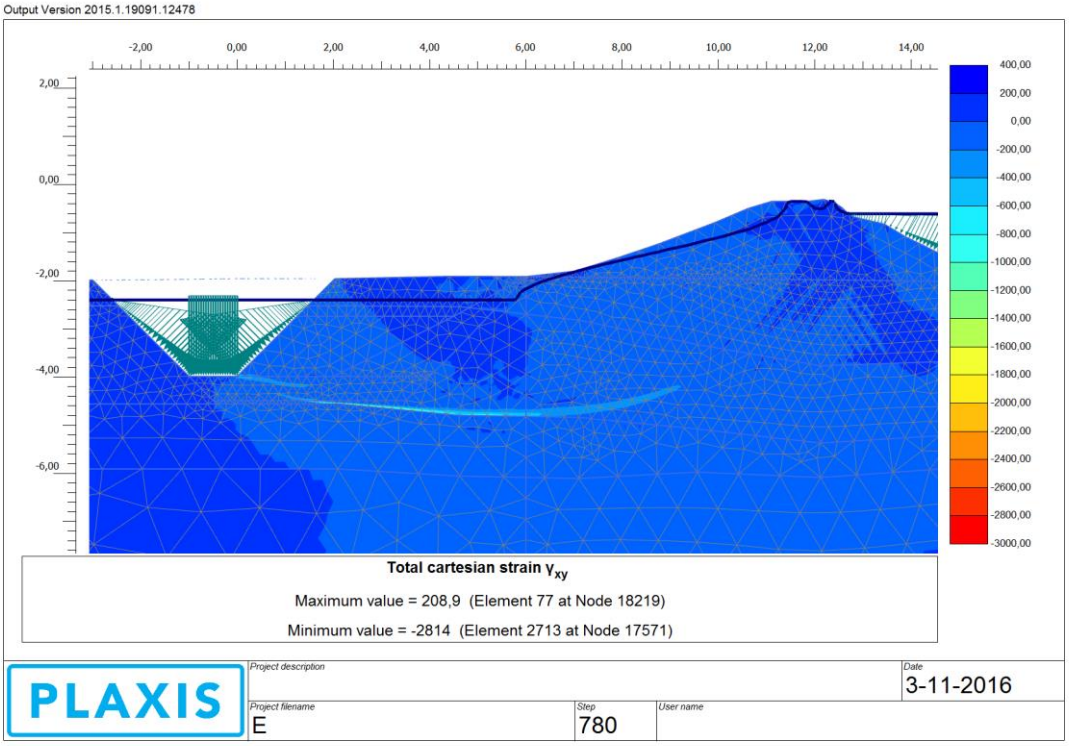

Figure 36: Shear strain contour (E, Excavation I)

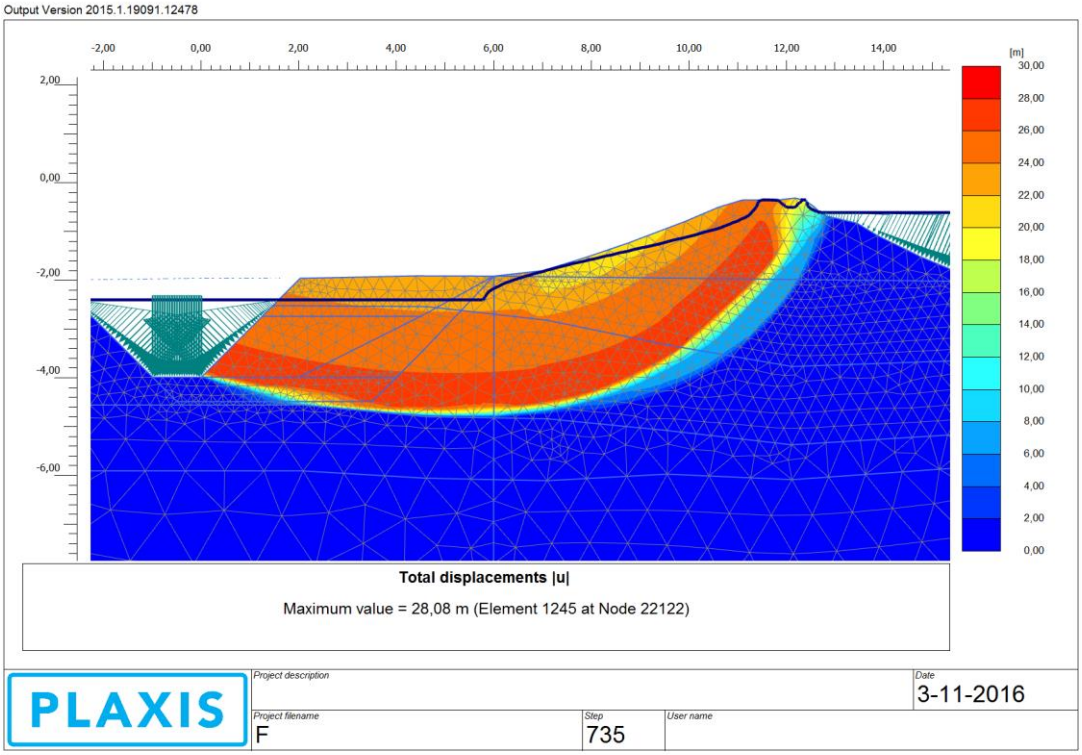

Figure 37: Displacement contour (F, Excavation I)

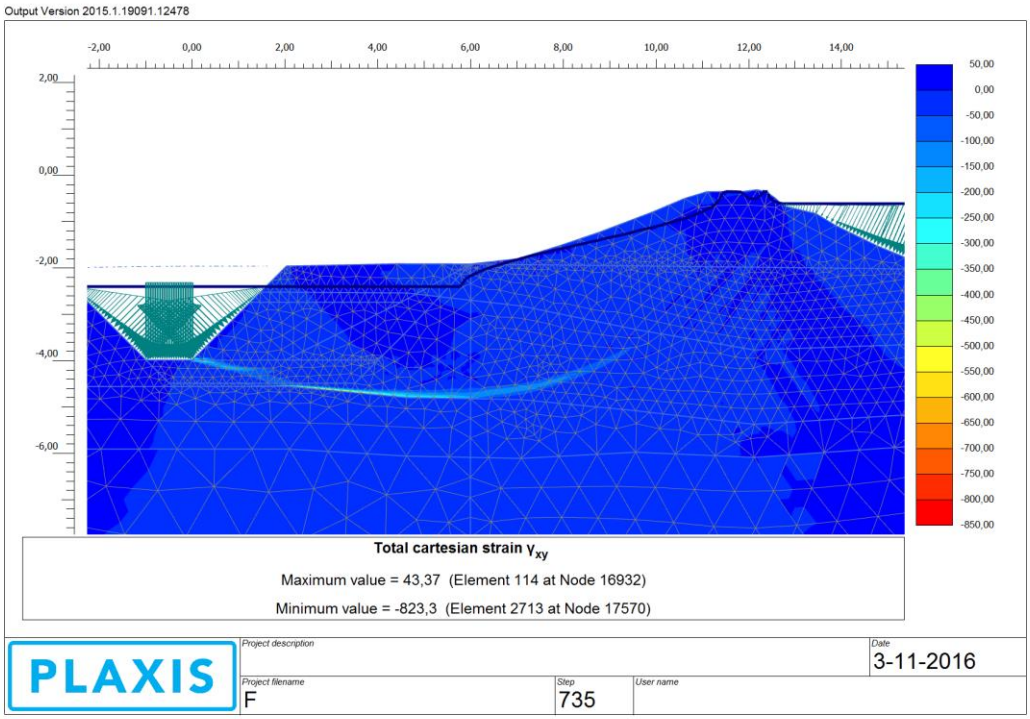

Figure 38: Shear strain contour (F, Excavation I)

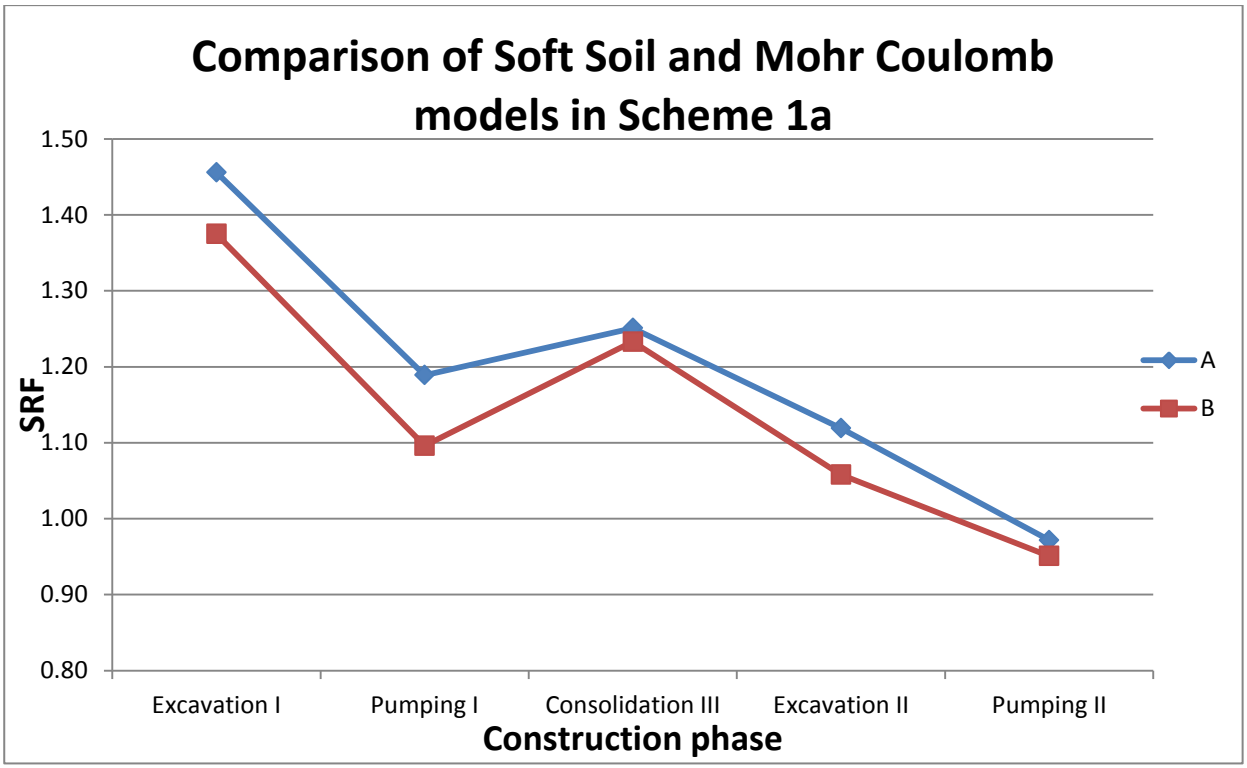

Figure 39: Comparison of Soft Soil and Mohr Coulomb models in Scheme 1a

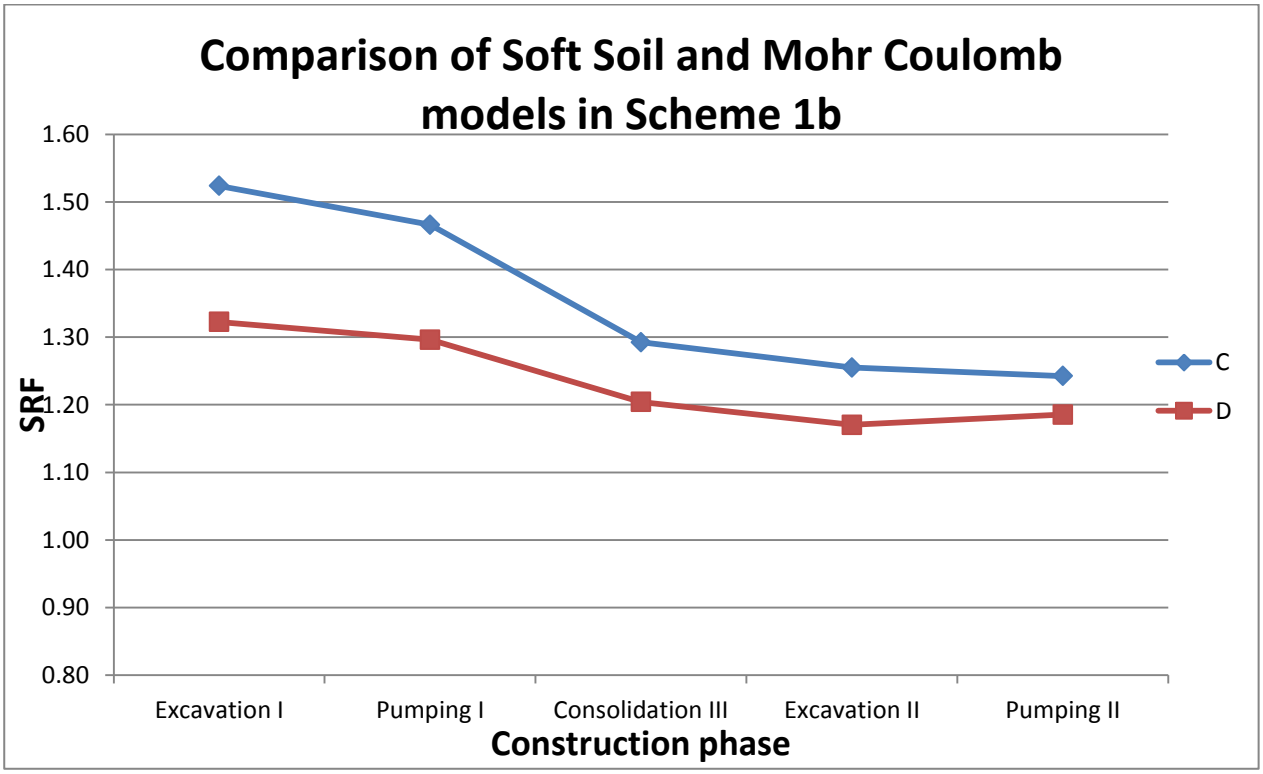

Figure 40: Comparison of Soft Soil and Mohr Coulomb models in Scheme 1b

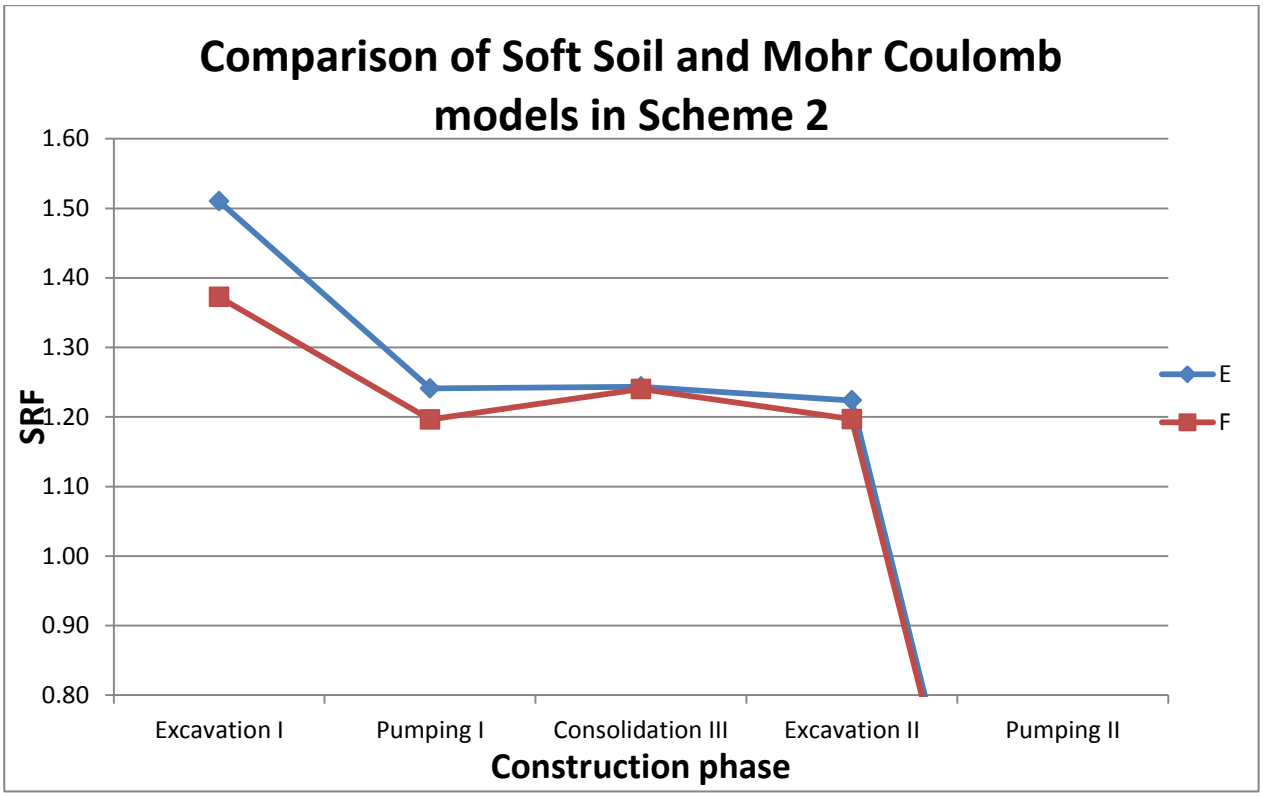

Figure 41: Comparison of Soft Soil and Mohr Coulomb models in Scheme 2

Each constitutive model exhibits a different pattern for the produced equivalent safety factors of each scheme. When applying Mohr-Coulomb, differences between schemes decline. In this linear elastic-perfectly plastic model, there are no elastoplastic effects and so pore water pressure dissipation and strain accumulation follow a similar history, but much different than the one of an advanced model. Notable differences between analyses B,D,F can be observed in stage “Pumping I”, which is happening due to the heavy plastic effects that take place. After yielding, larger strains occur and pore pressures are left to dissipate. Schemes 1b and 2 are better at handling these pressures, as the stage before the SRF calculation is employing a weaker soil (apply DA3 approach partial safety factors), and so, yielding takes place in a more conditioned manner. Differences in later stages are not that significant, as being closer to failure can disrupt FEM behavior.

Analyses applying the Soft Soil model exhibit higher SRF values. For the reasons mentioned above, Scheme 1a has considerably lower performance at all stages. Moreover, analysis C (Scheme 1a) surpasses analysis E (Scheme 2) in all stages, with the greatest difference being in “Pumping I”. Starting from a SLS basis, stress redistribution history is equivalent to that of a stronger soil. When DA3 factors are applied in Scheme 1b, plasticity is not yet as extensive as in Scheme 2, and so water dissipation (which is the critical issue of phase “Pumping I”) can easily occur in a larger soil volume than in other schemes, leading to different water flow paths and stress redistribution mechanisms. In the following stages, failure is near and so the differences among results are not to be taken into account (Scheme 2 even fails in an SRF check of the last stage).

The analysis that seems to be the fittest in describing the problem is C. It employs Scheme 1b, which is the safest as it provides the lowest safety factor, but also uses the Soft-Soil model, which seems to be the most

accurate in describing the phenomenon. The failure mechanisms in each stage of the chosen analysis are exhibited.

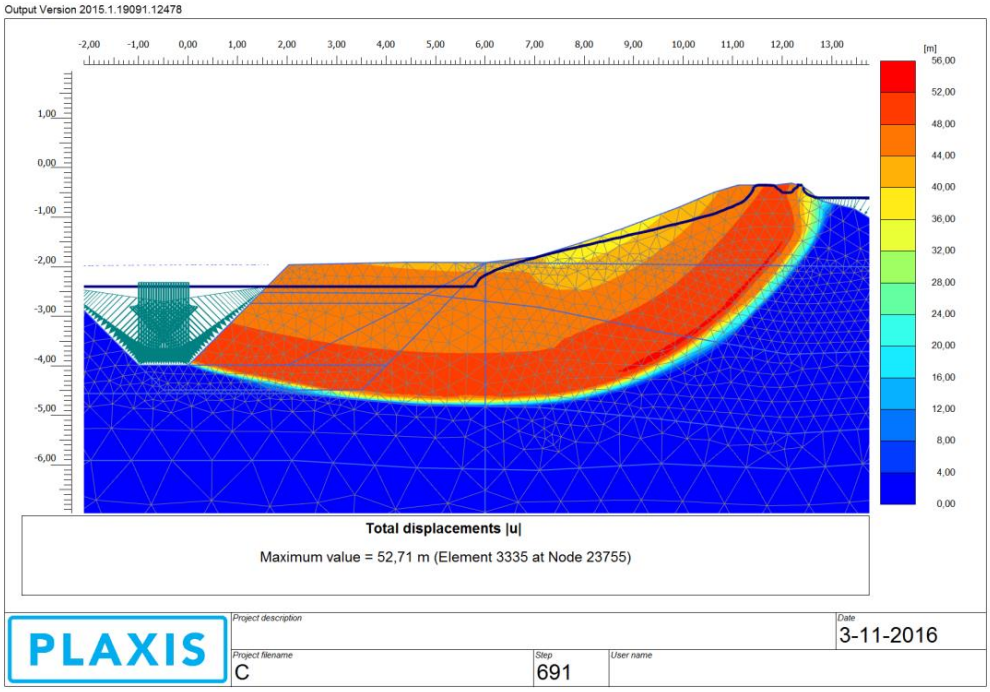

Figure 42: Displacement contour (C, Excavation I)

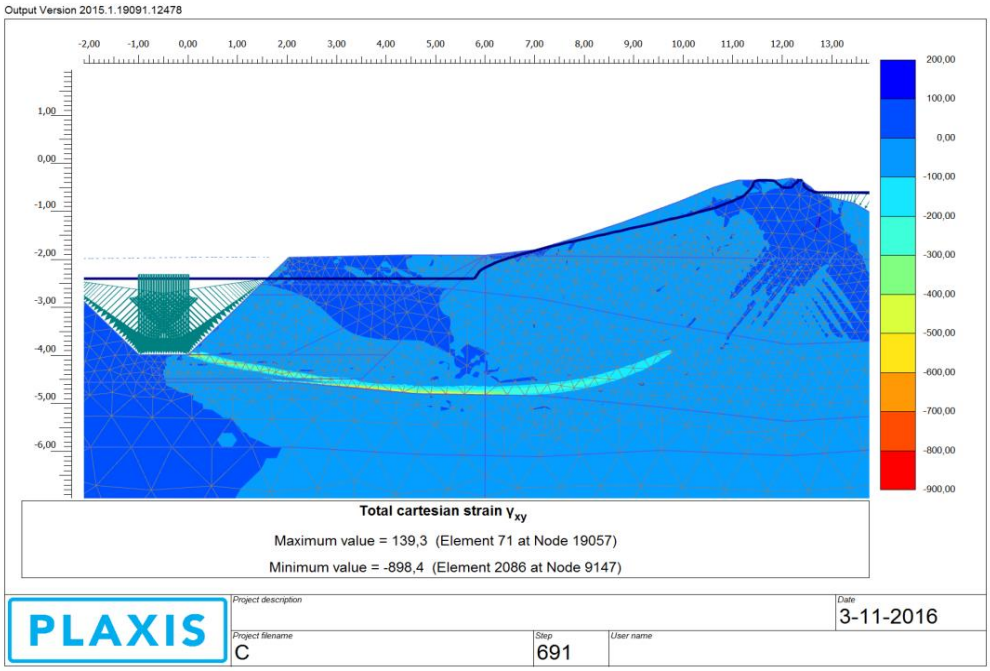

Figure 43: Shear strain contour (C, Excavation I)

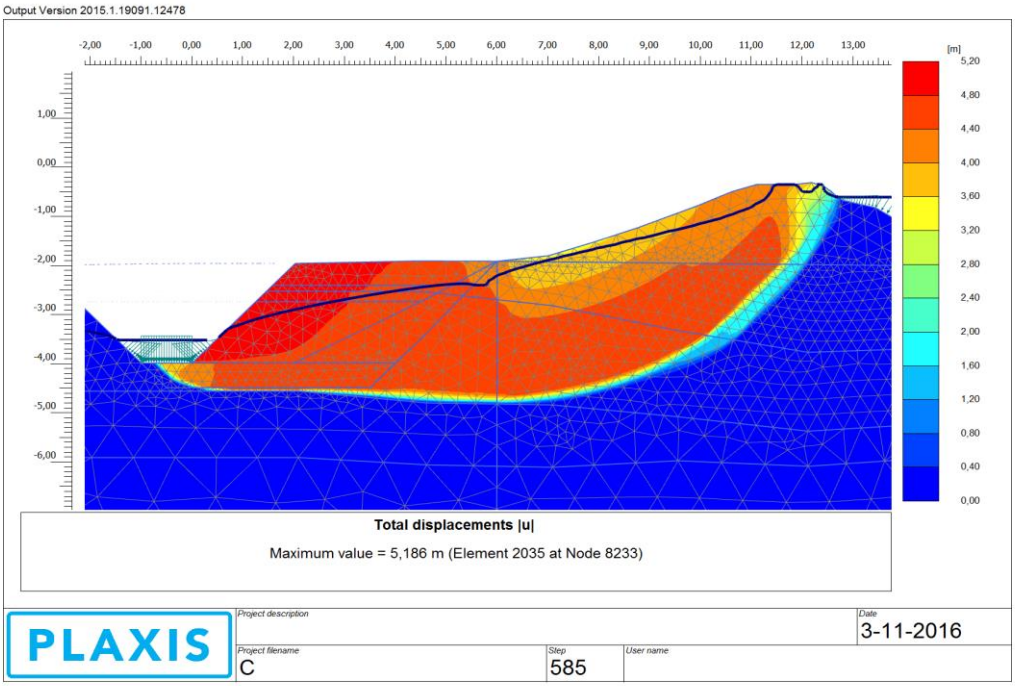

Figure 44: Displacement contour (C, Pumping I)

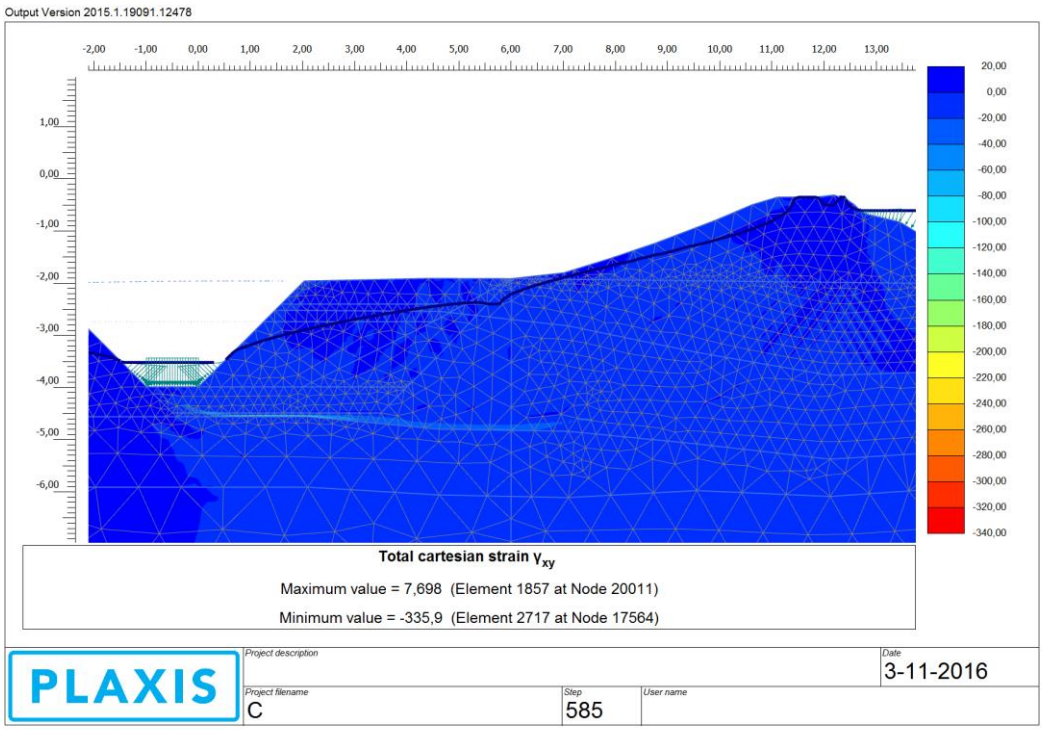

Figure 45: Shear strain contour (C, Pumping I)

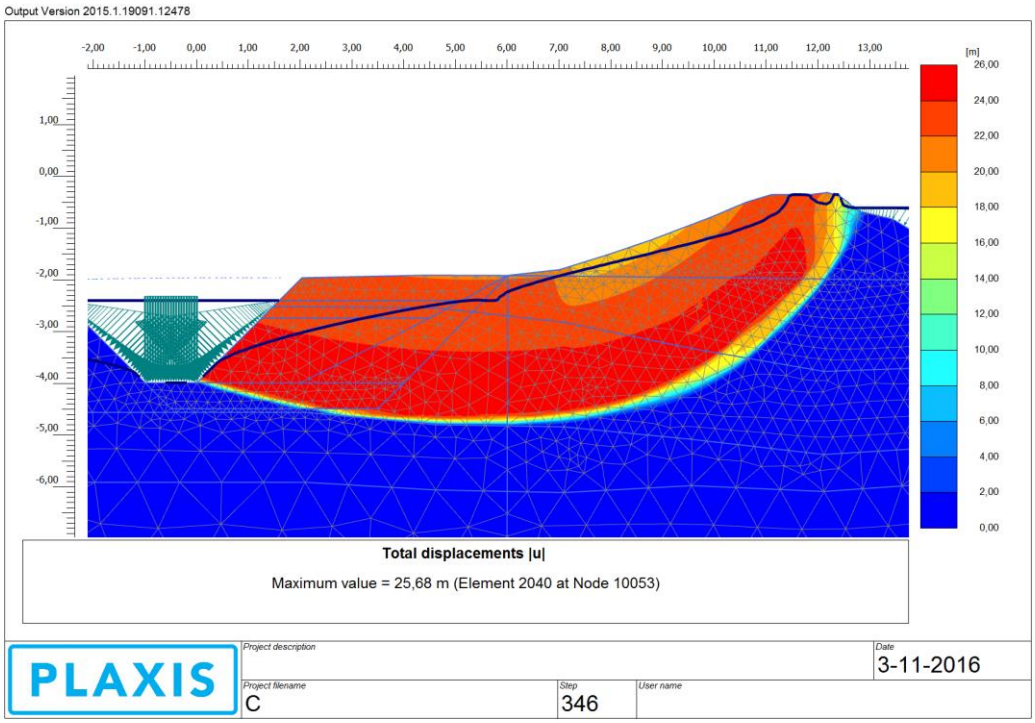

Figure 46: Displacement contour (C, Consolidation III)

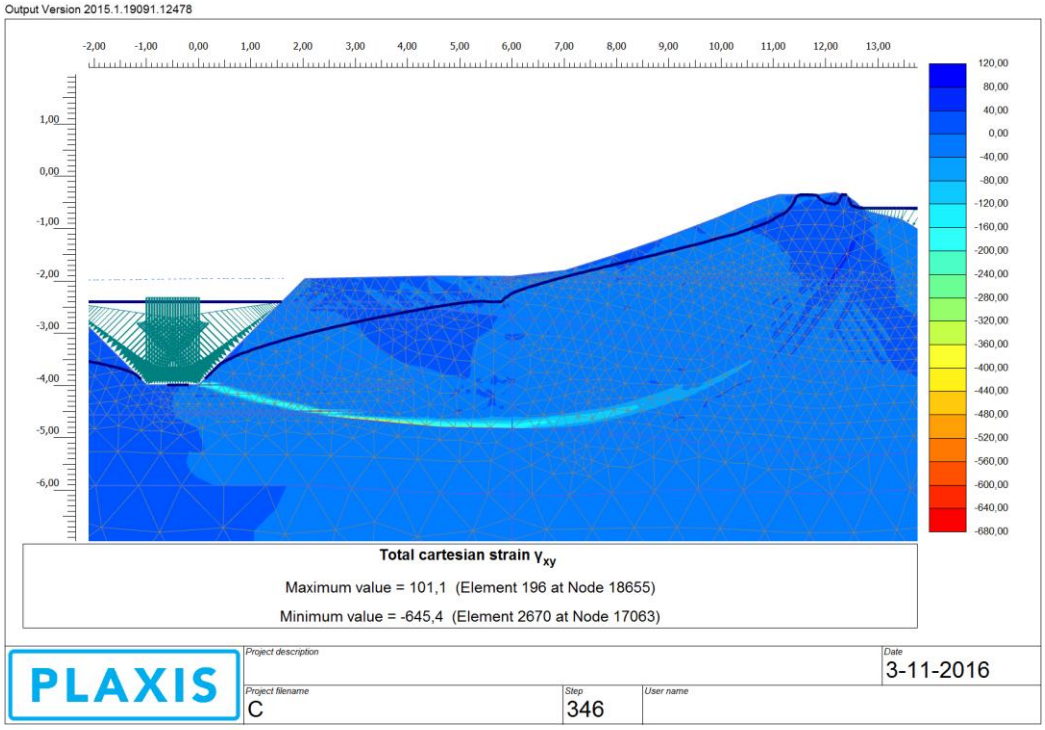

Figure 47: Shear strain contour (C, Consolidation III)

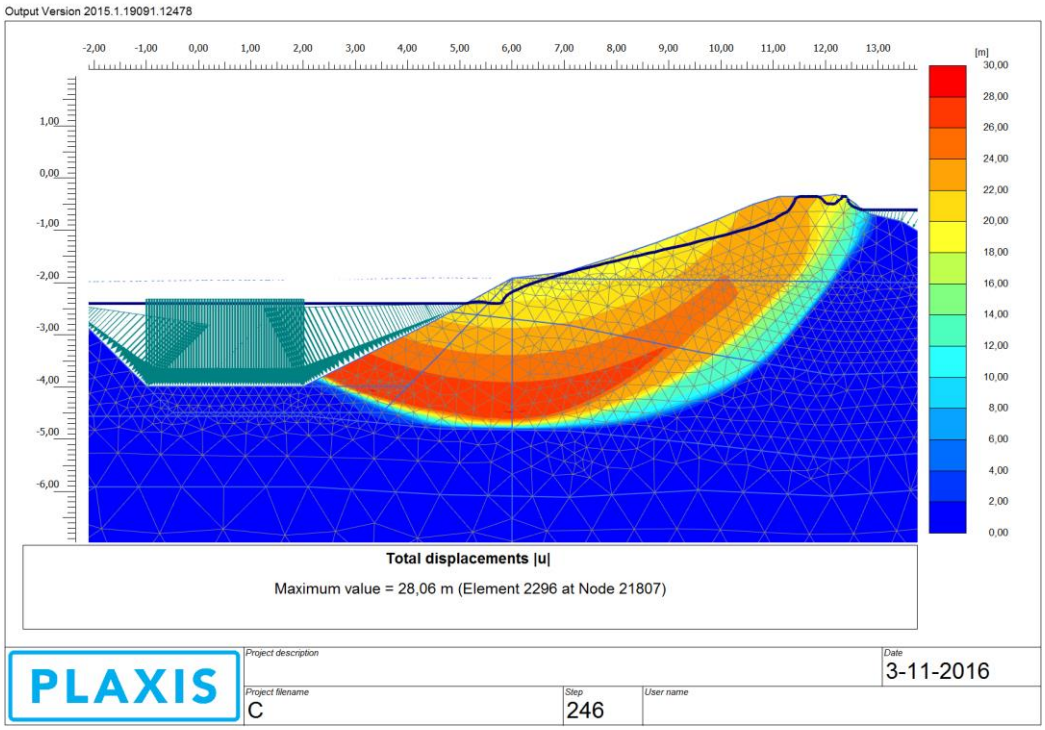

Figure 48: Displacement contour (C, Excavation II)

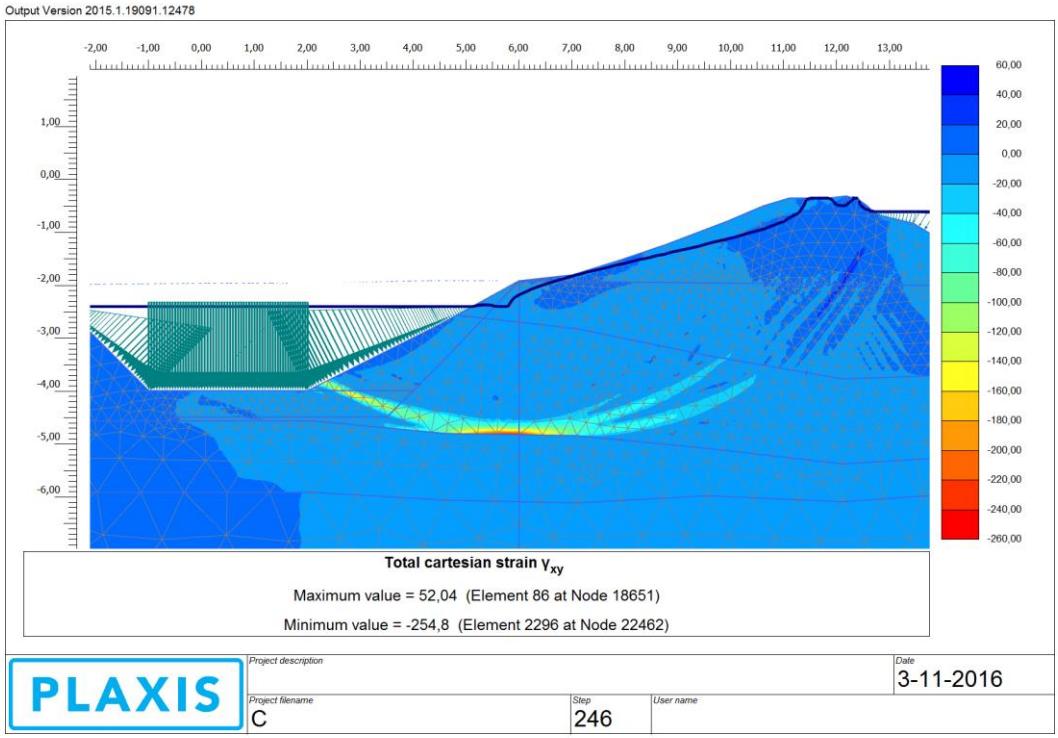

Figure 49: : Shear strain contour (C, Excavation II)

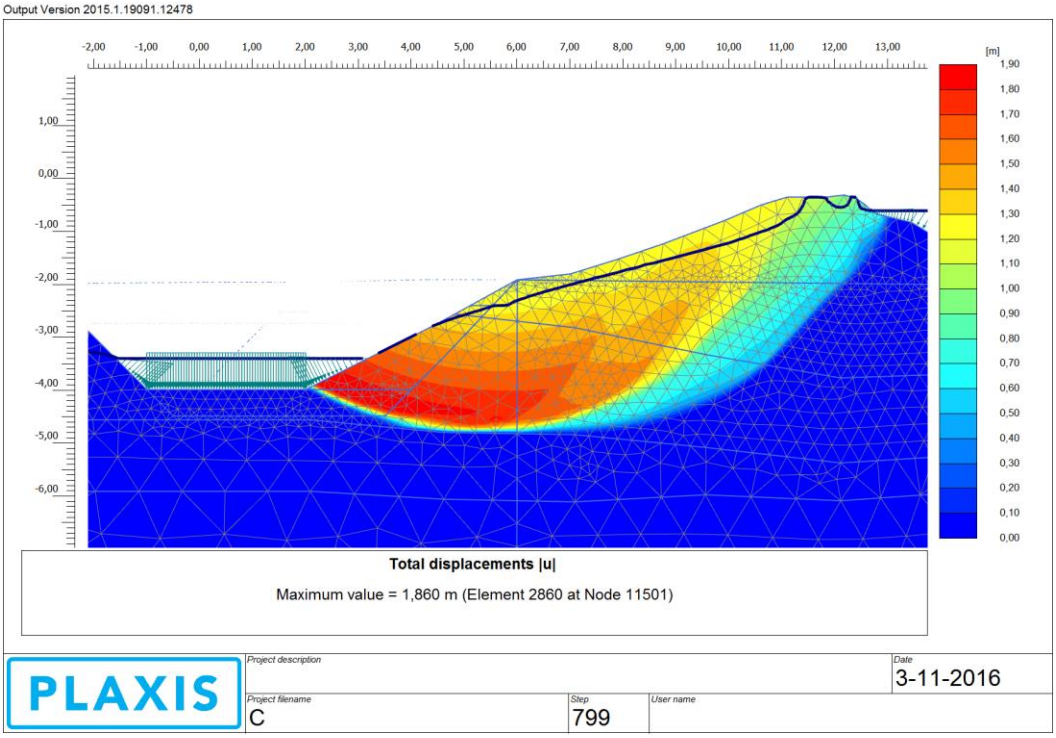

Figure 50: Displacement contour (C, Pumping II)

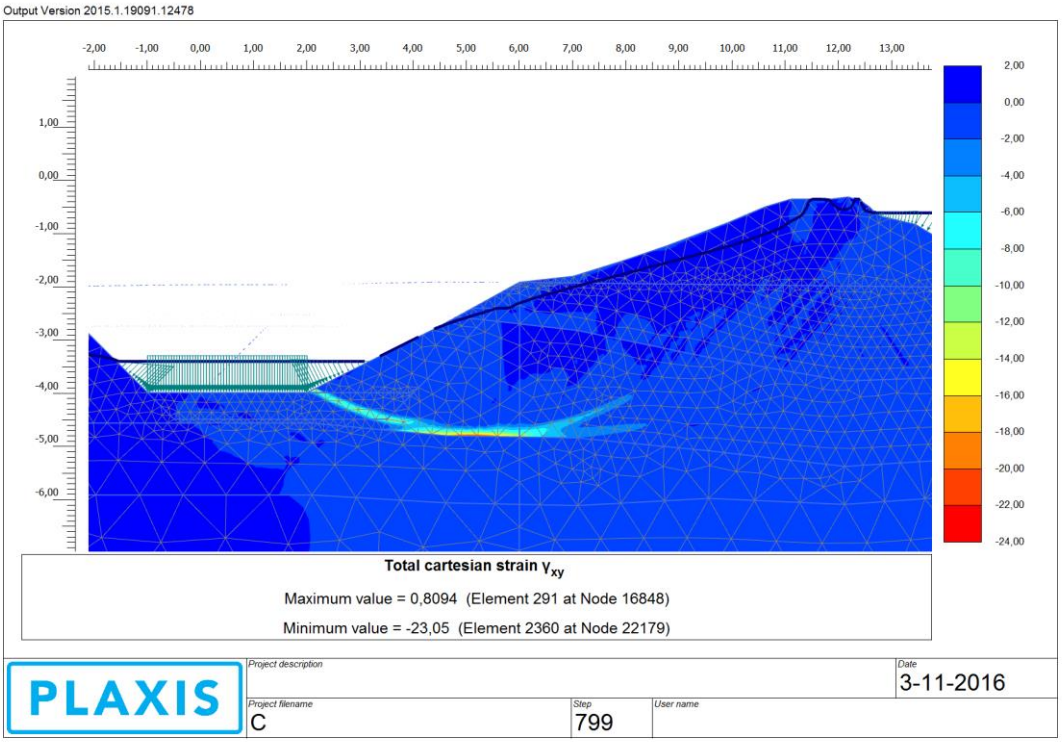

Figure 51: Shear strain contour (C, Pumping II)

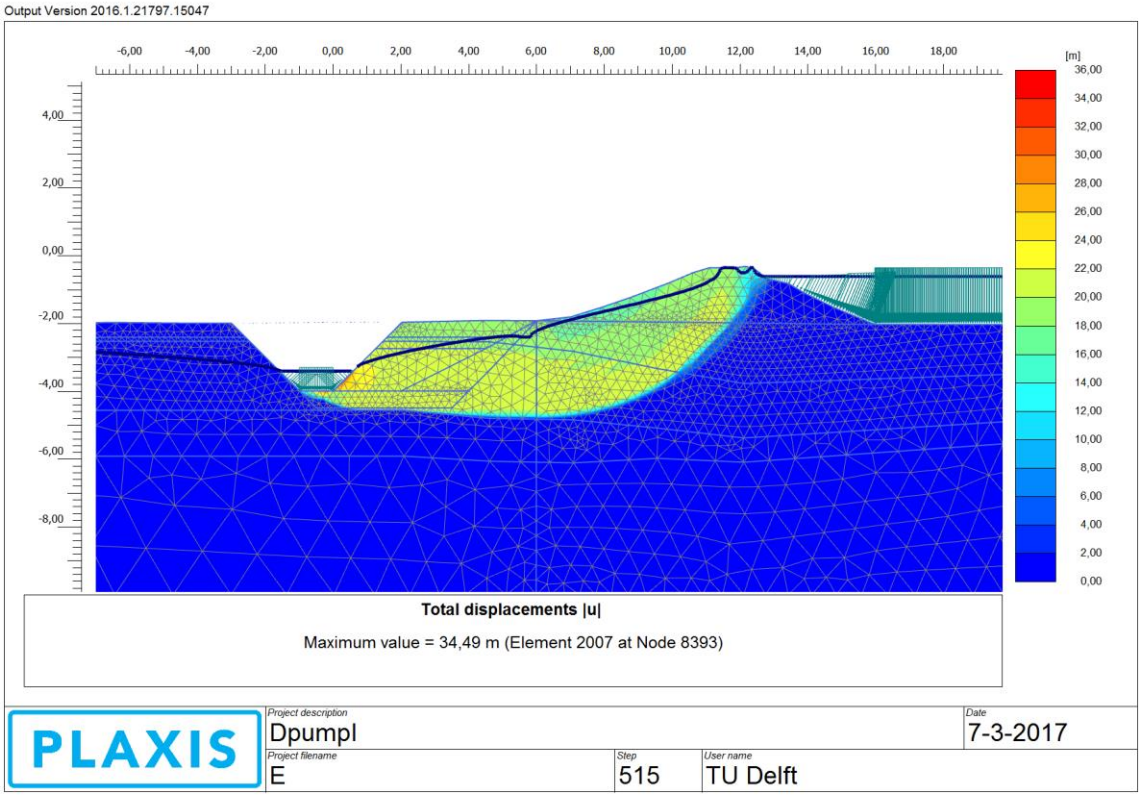

Figure 52: Displacement contour (D, Pumping I)-For comparison with analysis C. Failure seems to happen due to heave on the excavation surface, in contrast to the sliding mechanism of C.

6 COMPRESSIBILITY PARAMETER INVESTIGATION

According to the logic applied in paragraph 4, the safety of each scheme is estimated, in accordance to the characteristic value concept adopted. The effect of the selection of a characteristic stiffness value combination is approached quantitatively and qualitatively. The analyses is applied on Scheme 1b with the Soft Soil model, as selected in the previous paragraph. Analysis C1 is identical to C of the previous chapter (maximum compressibilities) while C2 uses the minimum elastic compressibility. The results are multiplied by 1.25 so that they are equivalent to an overall SRF.

Table 8: SRF results of stiffness sensitivity analysis

Overall Safety Factor of each analysis					
Analysis	Excavation I	Pumping I	Consolidation III	Excavation II	Pumping II
C1	1,52	1,47	1,29	1,26	1,24
C2	1,53	1,48	1,29	1,23	-FAILURE-

The anticipated failure mechanisms of C2 in each phase are presented below.

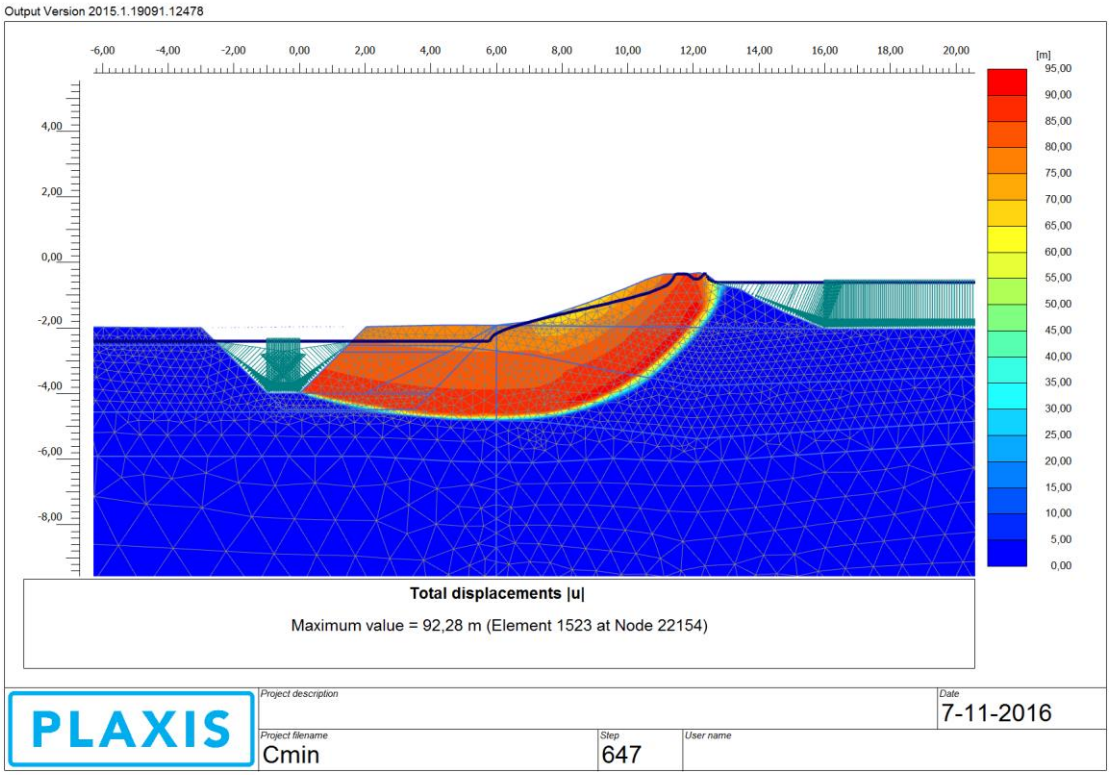

Figure 53: Displacement contour (C2, Excavation I)

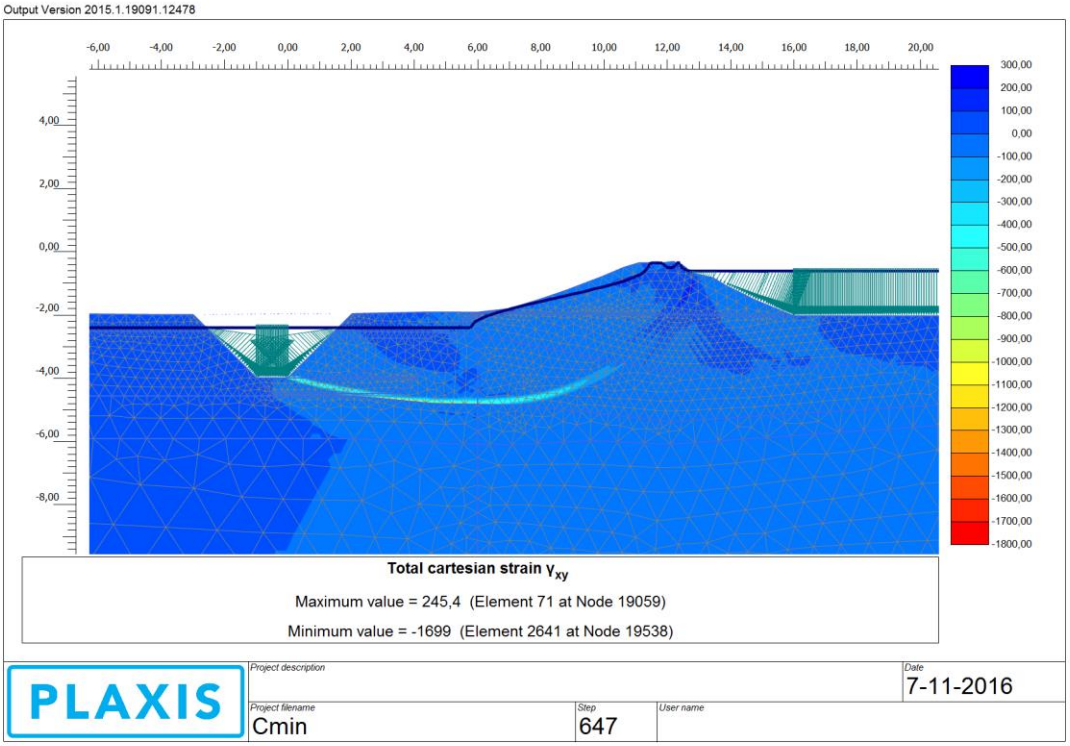

Figure 54: Shear strain contour (C2, Excavation I)

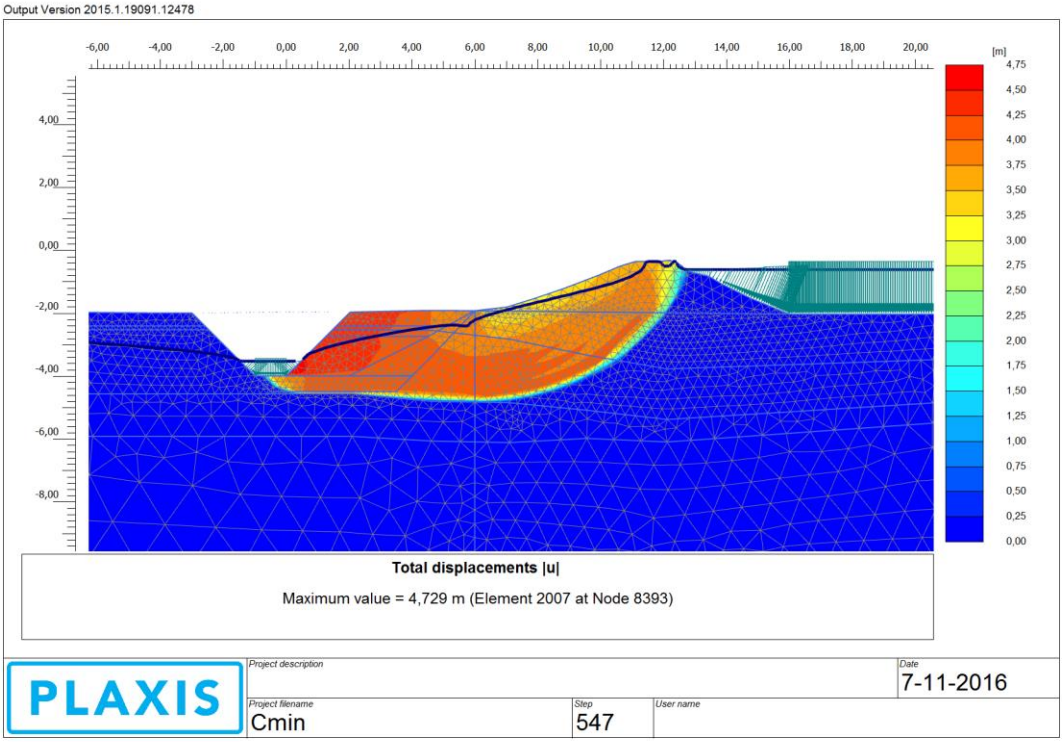

Figure 55: Displacement contour (C2, Pumping I)

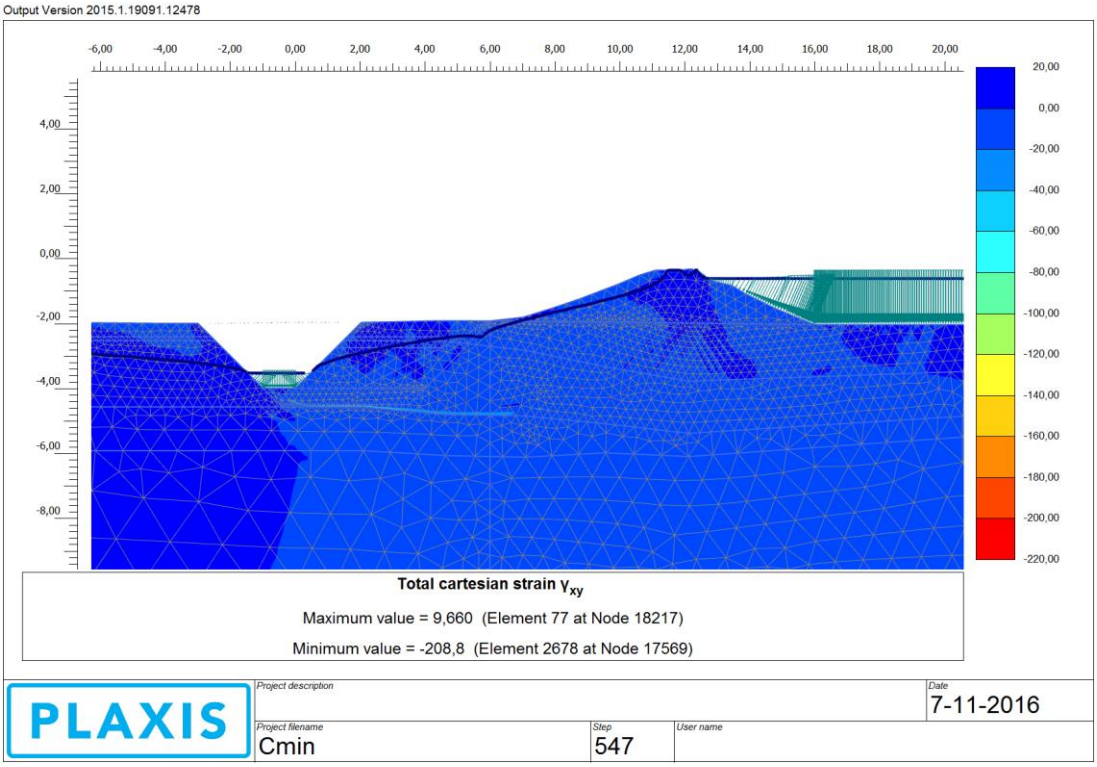

Figure 56: Shear strain contour (C2, Pumping I)

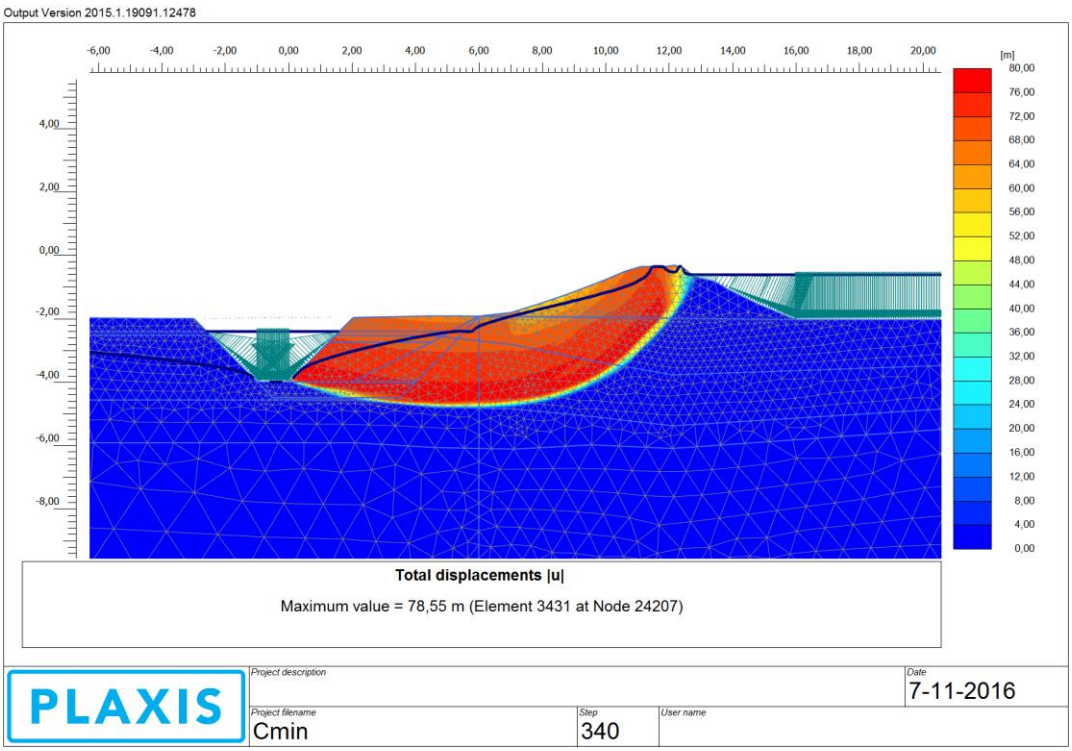

Figure 57: Displacement contour (C2, Consolidation III)

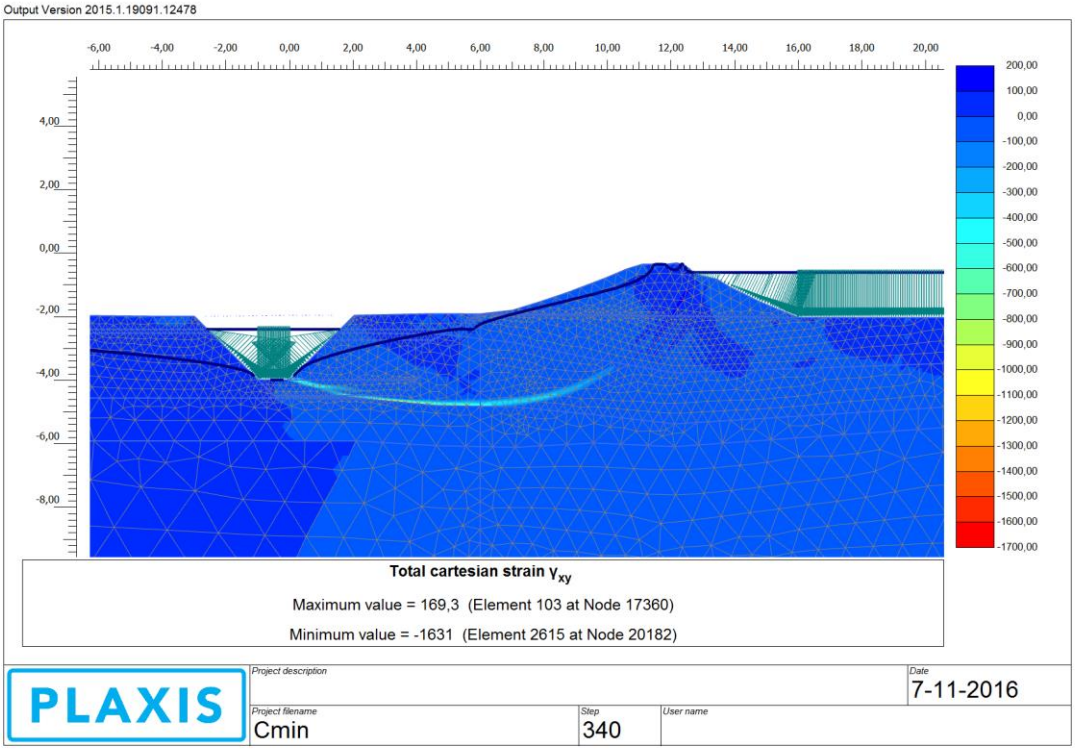

Figure 58: Shear strain contour (C2, Consolidation III)

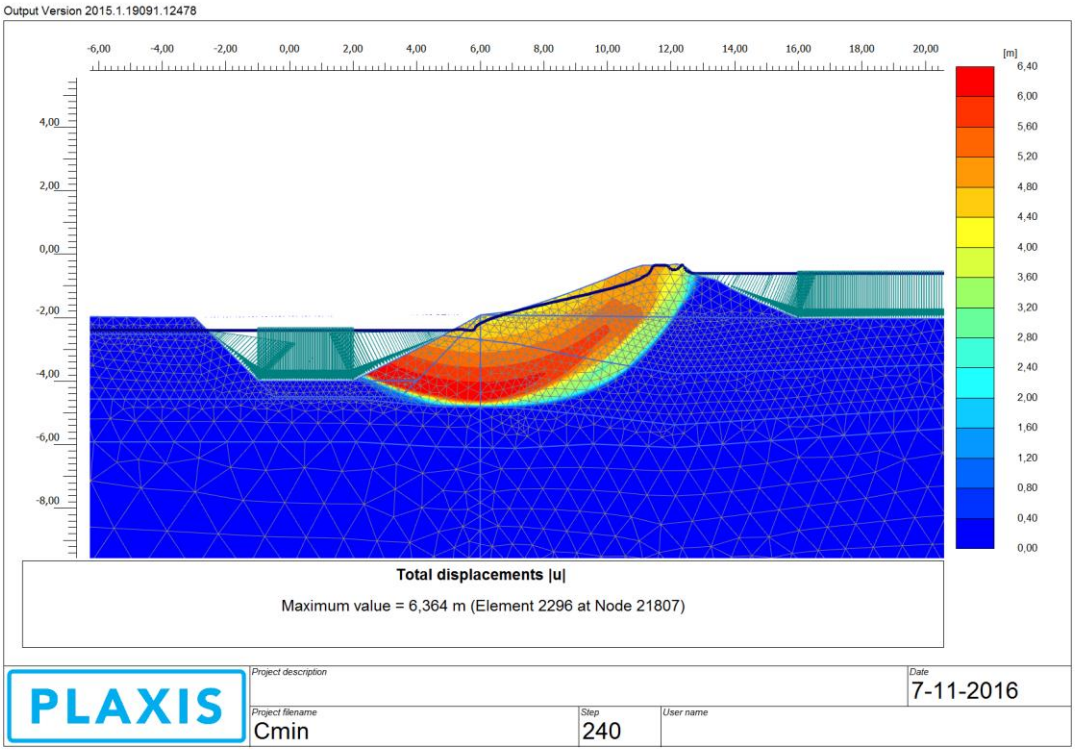

Figure 59: Displacement contour (C2, Excavation II)

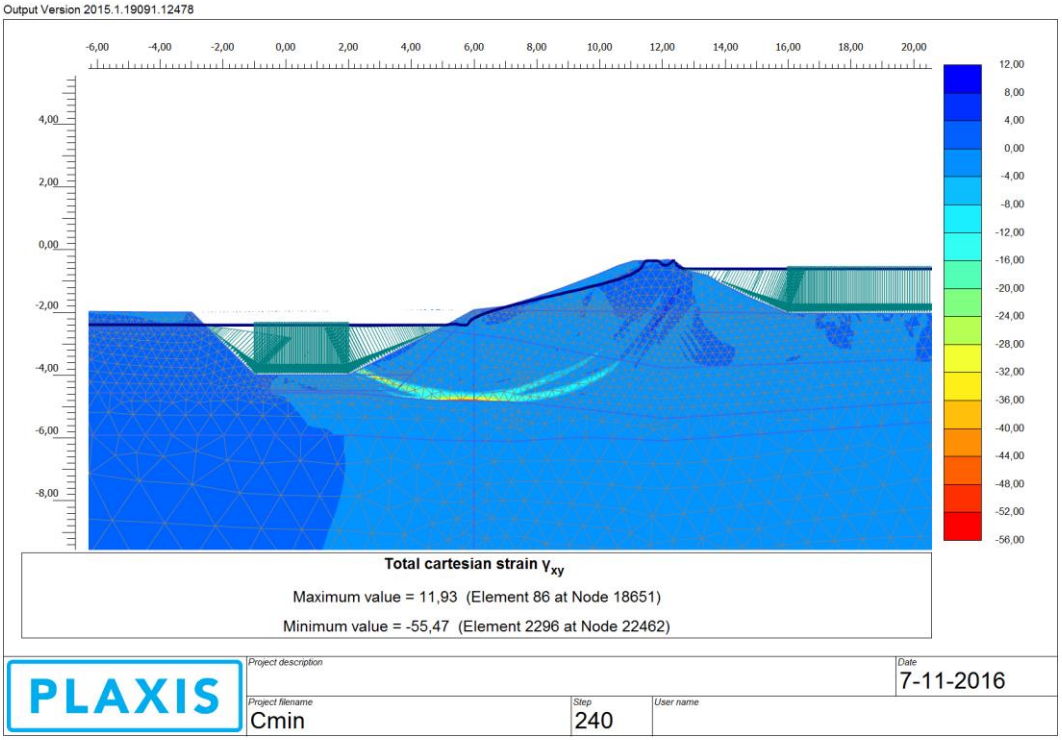

Figure 60: Shear strain contour (C2, Excavation II)

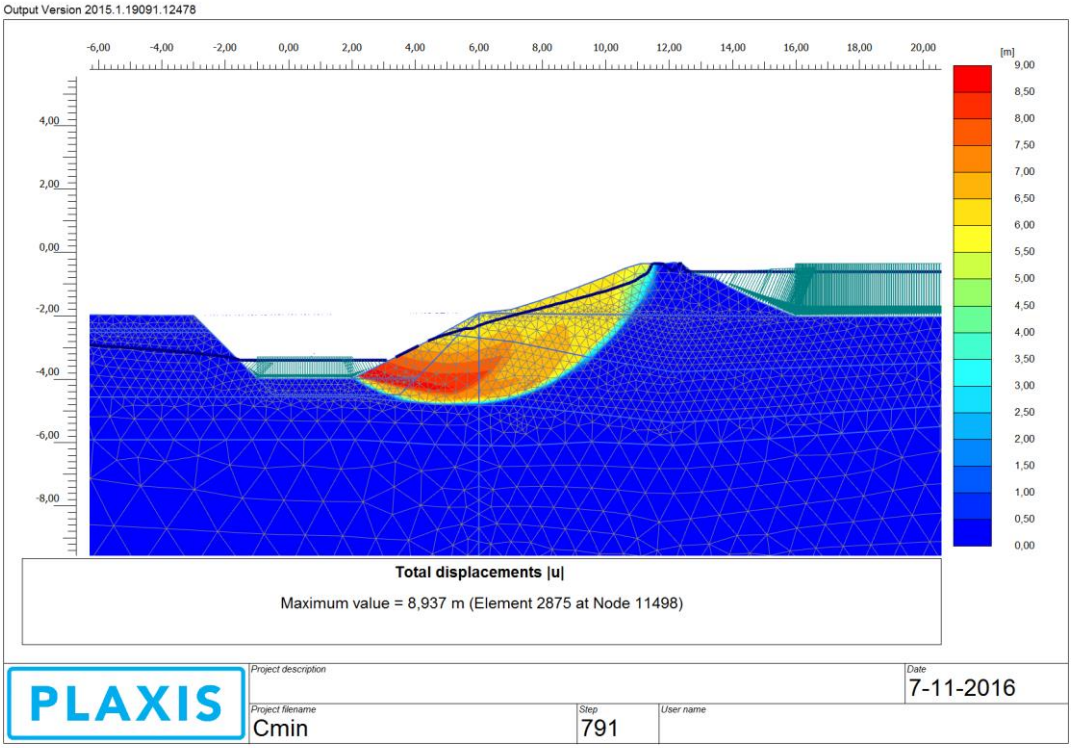

Figure 61: Displacement contour (C2, Pumping II)

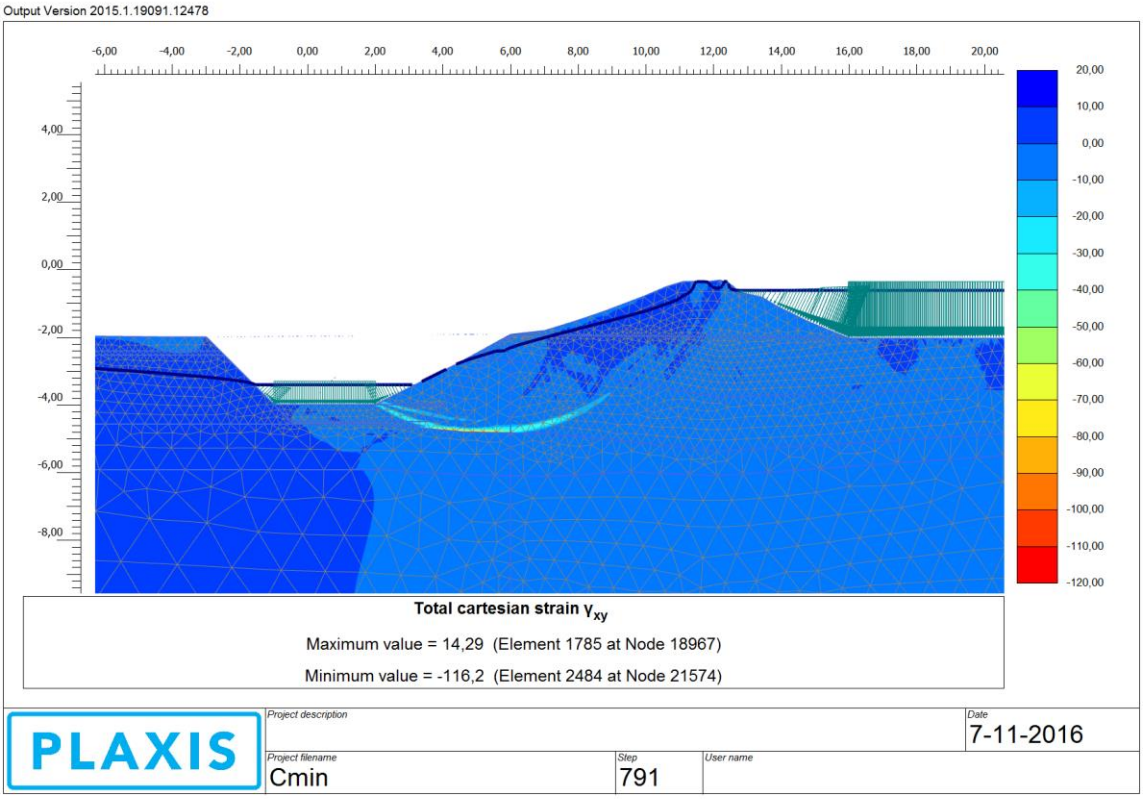

Figure 62: Shear strain contour (C2, Pumping II)

Figure 63: SRF for every construction phase in the compressibility sensitivity analysis

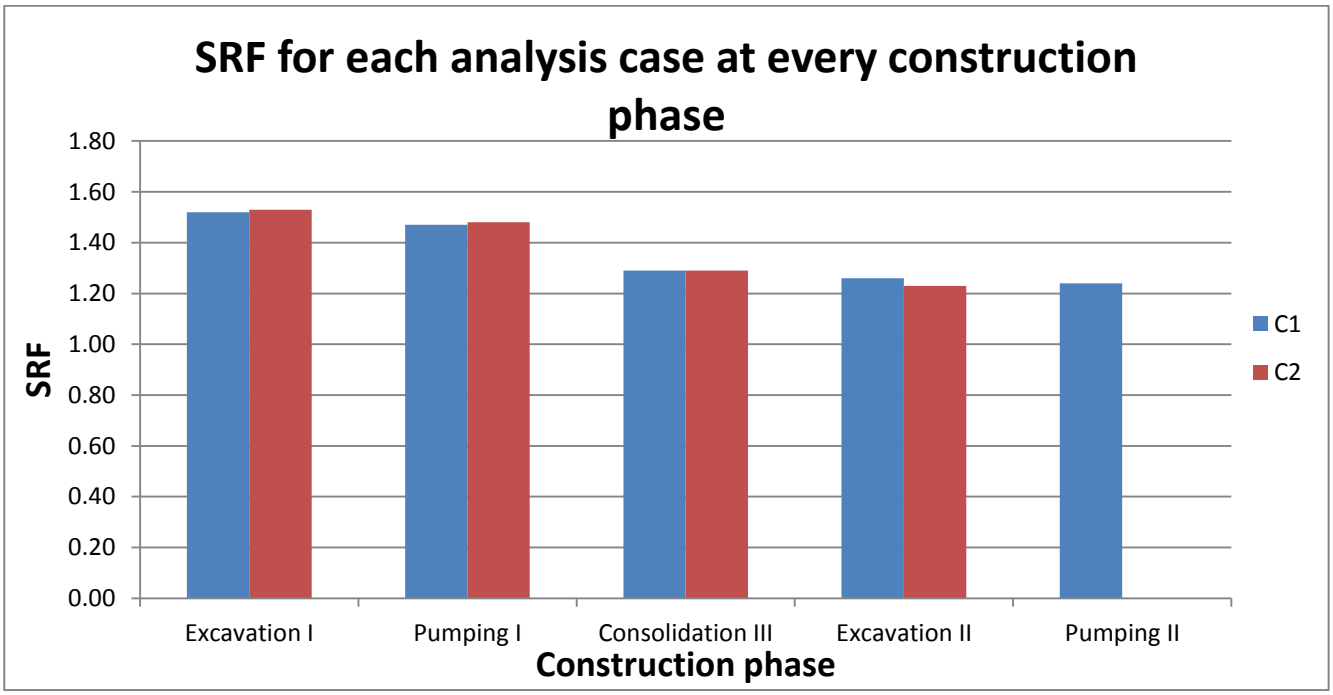

Both analyses exhibit the same performance. Mostly, no notable difference takes place in the SRF in each phase, with minor divergences only being a byproduct of numerical errors. In Pumping II, C1 is at the brink of failure, while C2 has already failed, which is the greatest observable difference in this collation. Furthermore, the failure mechanisms in each construction phase seem to form in the same manner in both cases, showing that the elastic compressibility does not affect the stability analysis of the project.

After all, the elastic component of the compressibility has minor impact on the stress redistribution mechanisms of this slope, meaning that failure happens in a similar way and at the same SRF. However, the elastic compressibility might still be important for stability in other construction types, where loading and unloading happen locally among construction stages (i.e. excavating with a sheet pile wall support).

It is evident that these differences are created in stages where failure approaches. In these cases, shear stress has already increased, and due to elastoplastic loading and lower elastic compressibility, plastic strains are maximized. However, only elastic normal strains increase effective normal stresses, and so, mean stress and confinement. As a result, the mean stress is lower than it used to be in C1, meaning that the Mohr-Coulomb envelope is more easily reached when executing an SRF calculation. However, this effect is not capable of providing a notable difference on the outcomes. In order for this to happen, application of a constitutive model describing soil softening, or an analysis allowing for time passing and creep would have to take place, so that the calculated strain state will have an improved role on the assessment of soil strength.

7 PERMEABILITY PARAMETER INVESTIGATION

Soil permeability is critical in defining the consolidation coefficient of a layer and so affects the staged construction of a project. Especially in peat, permeability can exhibit remarkable uncertainty, as well as a differing anisotropy, because it heavily depends on the void ratio of the soil, which can greatly vary in this case. So, this chapter is dedicated in analyzing and explaining the effect of the permeability on the construction's performance and modes of failure by applying advanced models.

Mainly, 3 orders of magnitude are given ($1.25*10^{-5}$, $1.25*10^{-6}$, $1.25*10^{-7}$), but also the ratio of vertical to horizontal permeability varies (1/1 or 1/100). It should be note that the strength parameters now are assumed to be 1.3 times higher, so that late phase failure is avoided.

Table 9: Analysis chart for permeability parameter investigation applying advanced models

Scheme 2		
Analysis	Parameters	
K1	k_v (m/s)	1,25E-05
	k_h (m/s)	1,25E-05
K2	k_v (m/s)	1,25E-06
	k_h (m/s)	1,25E-06
K3	k_v (m/s)	1,25E-07
	k_h (m/s)	1,25E-07
K4	k_v (m/s)	1,25E-07
	k_h (m/s)	1,25E-05

Scheme 1b		
Analysis	Parameters	
K5	k_v (m/s)	1,25E-05
	k_h (m/s)	1,25E-05
K6	k_v (m/s)	1,25E-06
	k_h (m/s)	1,25E-06
K7	k_v (m/s)	1,25E-07
	k_h (m/s)	1,25E-07
K8	k_v (m/s)	1,25E-07
	k_h (m/s)	1,25E-05

The model was tested firstly for Scheme 2 and then for 1b. Contrarily to the previous case, the resulting SRF is plainly what PLAXIS produced, not multiplied by 1.25, as there is no need to be compared to an overall factor system. Hence, this SRF is the overall stability of the weakened soil (according to DA3 for ULS).

The results of the parametric analysis are summarized in the following table.

Table 10: Results of the parametric investigation on the permeability

Analysis/Phase	Excavation I	Pumping I	Consolidation III	Excavation II	Pumping II
K1	1,64	1,37	1,41	1,29	1,12
K2	1,47	1,18	1,30	1,14	0,97
K3	1,29	1,13	1,22	1,08	1,01
K4	1,48	1,21	1,33	1,11	0,99
K5	1,64	1,38	1,42	1,30	1,16
K6	1,48	1,22	1,29	1,13	1,00
K7	1,30	1,19	1,22	1,10	0,96
K8	1,49	1,25	1,33	1,13	1,02

It should be mentioned that the analyses K3 and K7, in which the peat is assigned lower permeability than that of the clay might be unrealistic for the specific case examined. However, the permeability of the peat is investigated over two orders of magnitude, which is less than what the lab reports suggest. The effect was only checked for this layer, inconsistently to others.

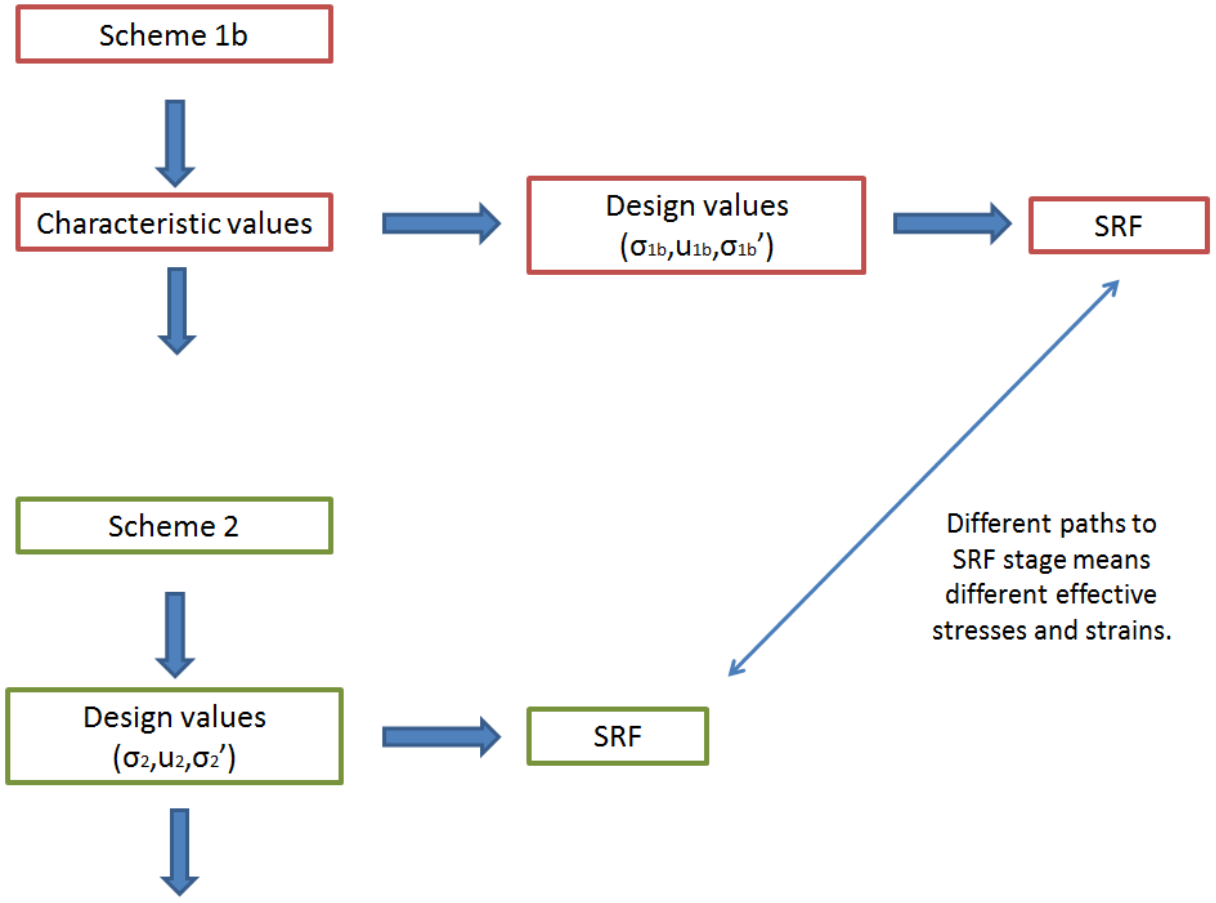

Figure 64: Comparison between schemes regarding the approach of the SRF stage

7.1 Comparison between analysis cases

Firstly, the results of analysis organized by construction phase are elaborated.

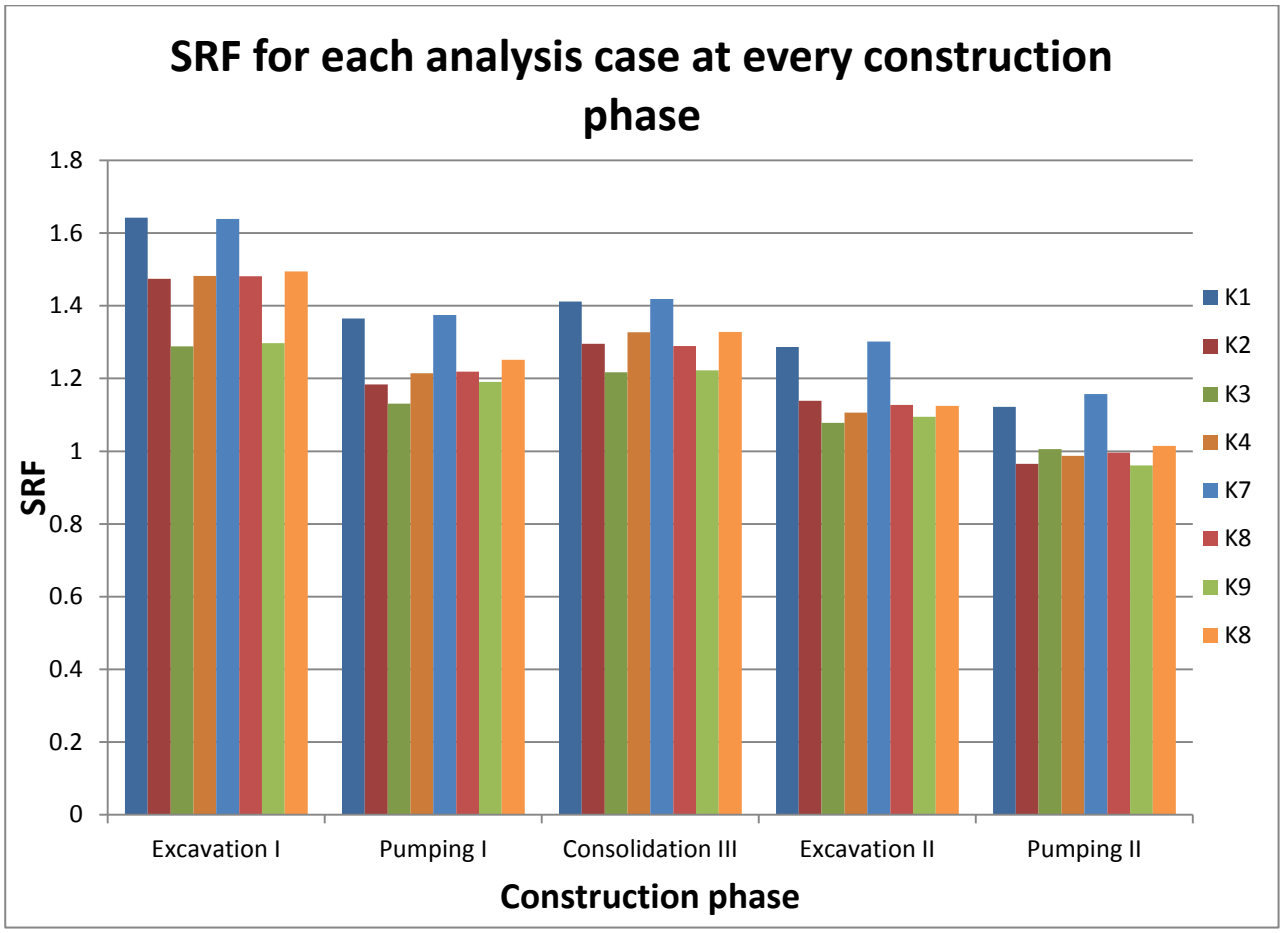

Chart 1: SRF comparison between analysis cases at each phase

Comparing the two schemes, most values are taken as equal, especially in the starting phases. Approaching failure, the difference begins to become noticeable, as minor differences in propagating failure mechanisms take place. However, in an engineering aspect, the results of both schemes are the same. This means that the stress paths in both cases do not have differences potent to make a noteworthy impact. Scheme 2 employs design values along the entire analysis and should have different stress paths and redistribution mechanisms than Scheme 1b. However, at the latter case, a ULS stage is used before the SRF calculation, and so the model goes through a “preparation” phase, mimicking the conditions of Scheme 2. In this circumstance, this internal phase is enough to smoothen any differences.

The pattern detected is that the higher the permeability, the greatest the safety factor. This observation implies the impact of pore water pressures and dissipation for the stability of the dyke in this case. As a coupled calculation is executed, pressures increase due to rising head, soil compression due to loading or normal stress redistribution, as well as elastoplastic shearing. Then, these pressures affect the groundwater state, and a consolidation process initiates. Setting a relatively finite construction duration among phases,

the magnitude of permeability takes a controlling role in dealing with overpressures. As every parameter other than the permeability is constant in the consolidation model (not including the overpressure values), then a higher permeability can be translated to a lower consolidation time. Thus, the duration of each phase equals a larger portion of the said time and means that a higher reduction is inflicted on the overpressures. The effective stresses increase, and in this way, the shear strength of the soil, offering a higher safety factor.

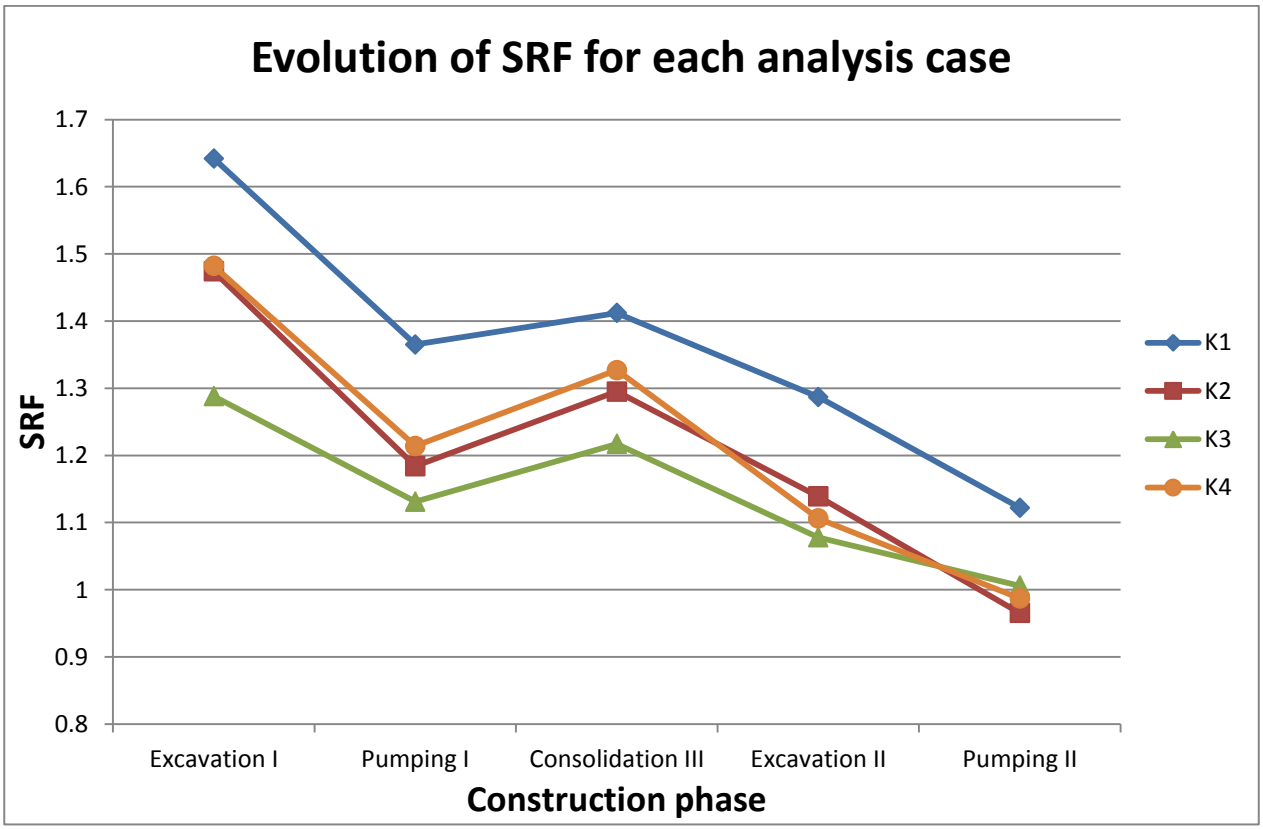

Chart 2: Evolution of SRF for each analysis case for Scheme 2

Analyses K4/K8 contain three parameter elements that attribute a remarkable behavior. Their vertical permeability is equal to the minimum value used (K3/K7), the horizontal one equal to the maximum (K1/K5) and their average is equal to the middle value (K2/K6). Waterflow through multiple porous media is strongly affected by the minimum and maximum values of the permeabilities of consecutive materials. Flow velocity is controlled by the lowest value, while flow gradient is maximum at a low permeability and minimum at a higher one. On the other hand, the measure of water inflow and out flow of each element is connected to the measure of the mean permeability, and so is the pressure dissipation process.

Considering the above, the evolution of K4 is explained (and similarly K8). At the first stage, K4 is equal to K2, as they possess the same average permeability. In Excavation I, the pore pressures are created form the shearing induced due to unloading and the construction of the slope. Thus, dissipation of the pore pressures is the key factor of difference between analyses. It should be noted that the same should apply in Excavation II, but the stress history and stress paths so far alter the effect mentioned beforehand.

Between both cases, the pore water pressures and excess pore water pressures have similar distribution and magnitude over the mesh.

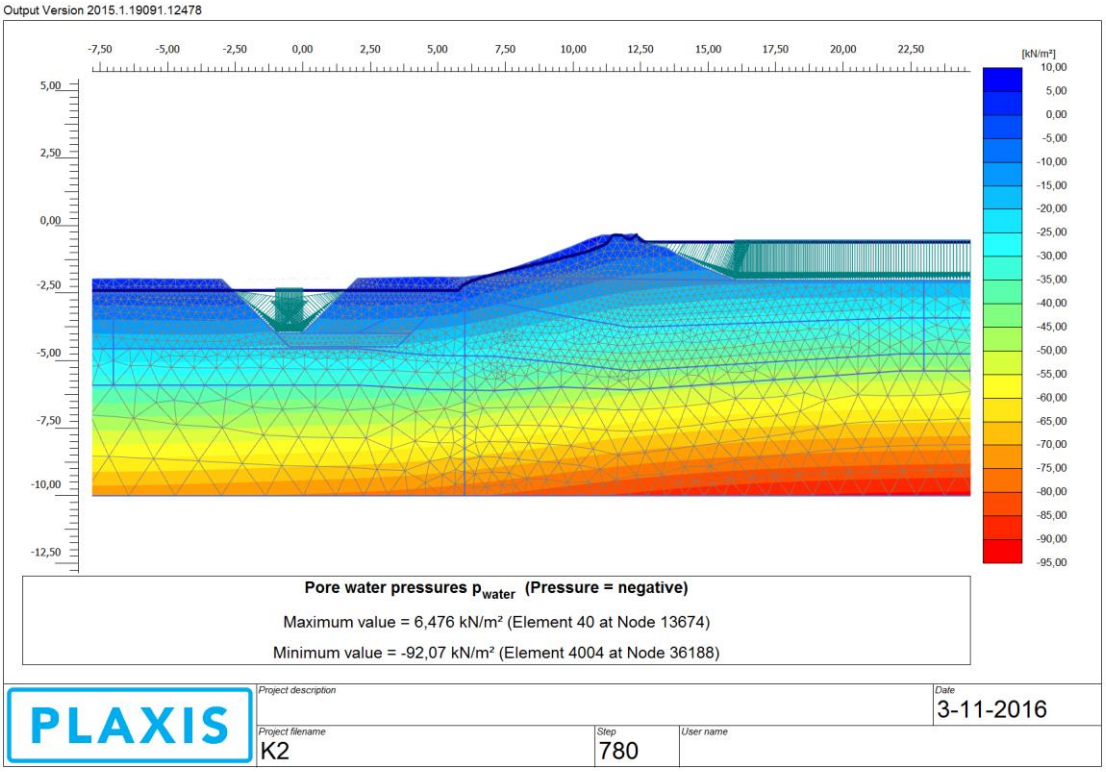

Figure 65: Pore water pressures in Excavation I for K2

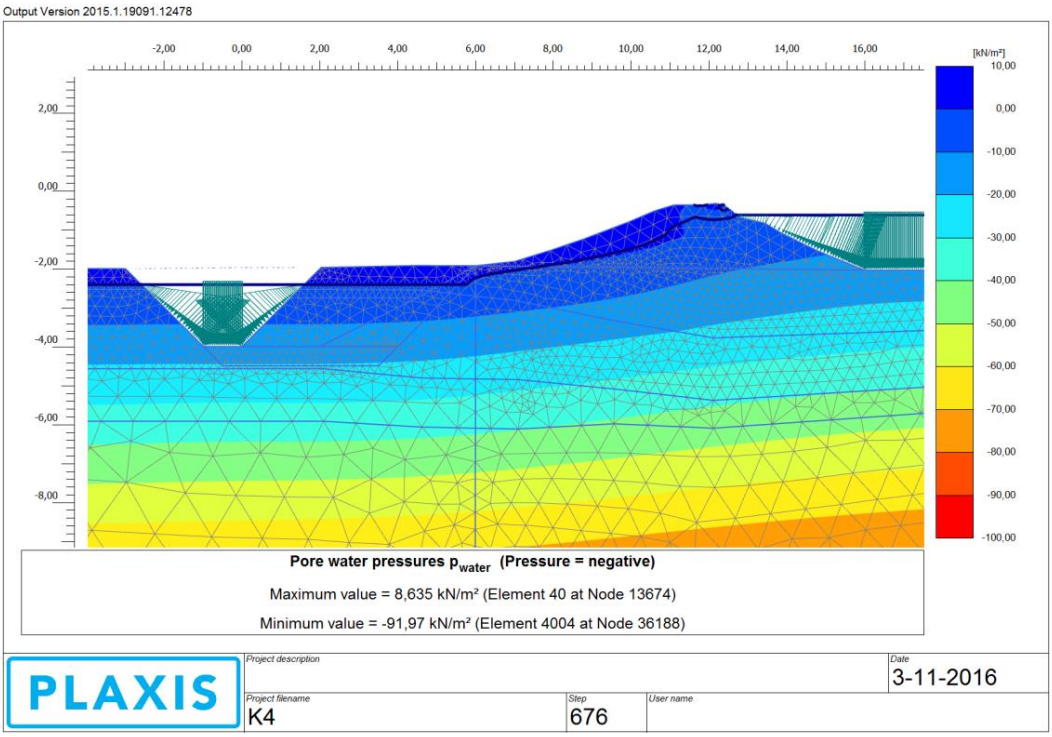

Figure 66: Pore water pressures in Excavation I for K4

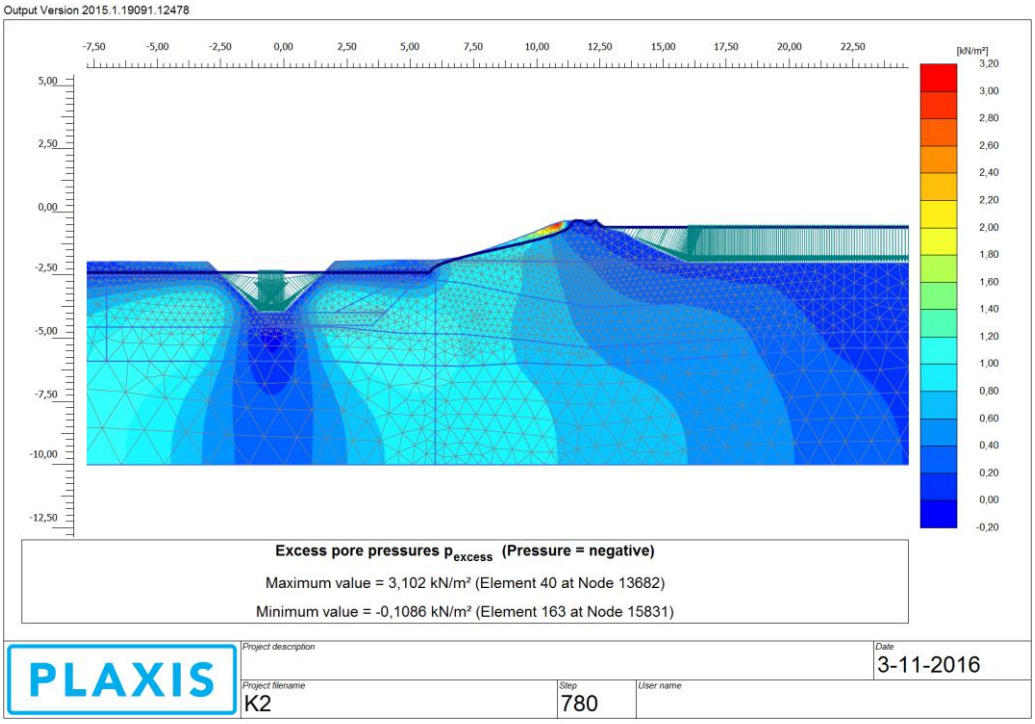

Figure 67:Excess pore water pressures in Excavation I for K2

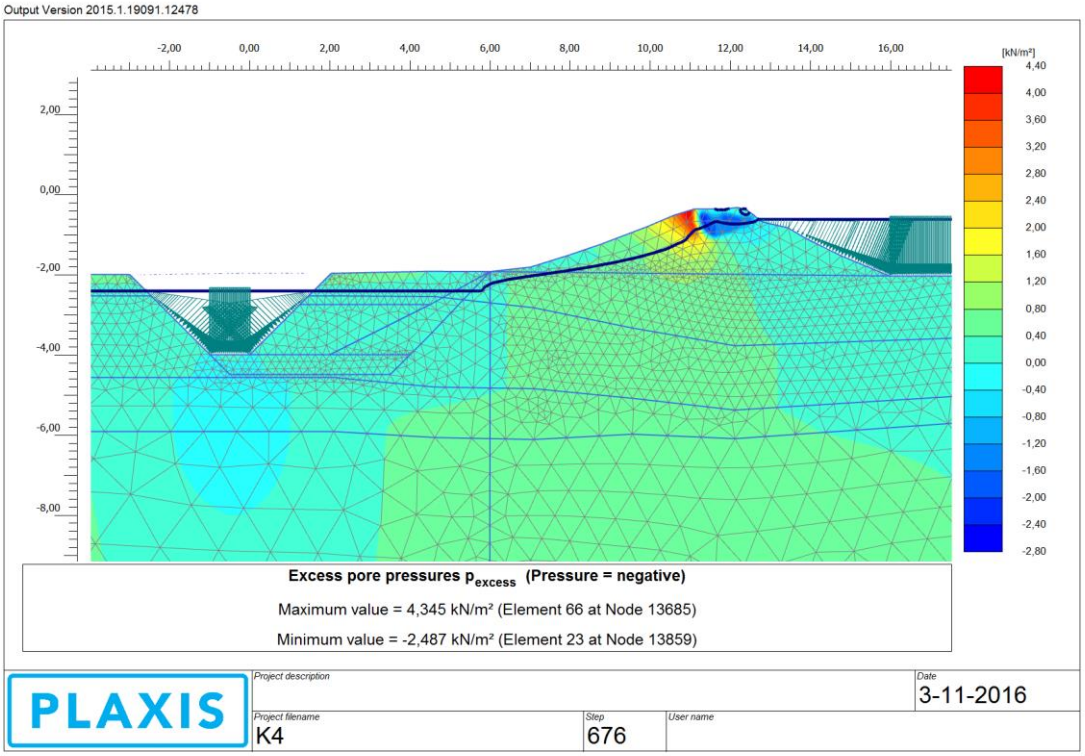

Figure 68:Excess pore water pressures in Excavation I for K4

For the pumping and consolidation phases, the same phenomenon applies, but a major contribution is also accredited to large scale waterflow. The drawdown of the GWL increases the head gradient and amplifies the intensity of waterflow beneath the dyke. This process is widely influenced by the ratio of vertical permeabilities of material encountered, but also the magnitude of the horizontal permeability, for the lateral flow component. It should be noted that even small pressures deviations make a difference, considering the extremely low volumetric weight of the peat. Offering a higher ratio of excess pore water dissipation, K4 has a larger SRF in these phases. However, it is clear that larger pressures build up at the bottom of the excavation. At this area, consolidation is controlled by the vertical flow, as the horizontal is nullified due to symmetry. Then, K4 appears to be unstable near the toe of the slope (see paragraph 7.2: Modes of failure).

Summing up, K4 is always between the two marginal analyses (K1,K3) and always close to each “by average” equivalent K2.

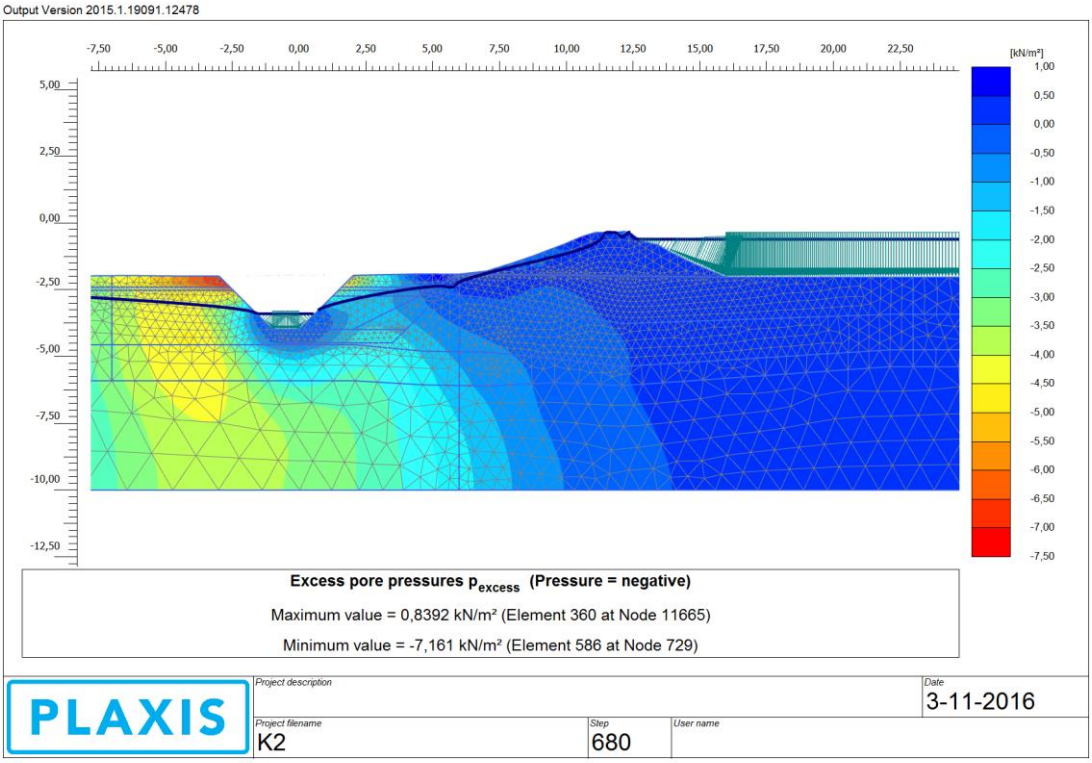

Figure 69: Excess pore water pressures in Pumping I for K2

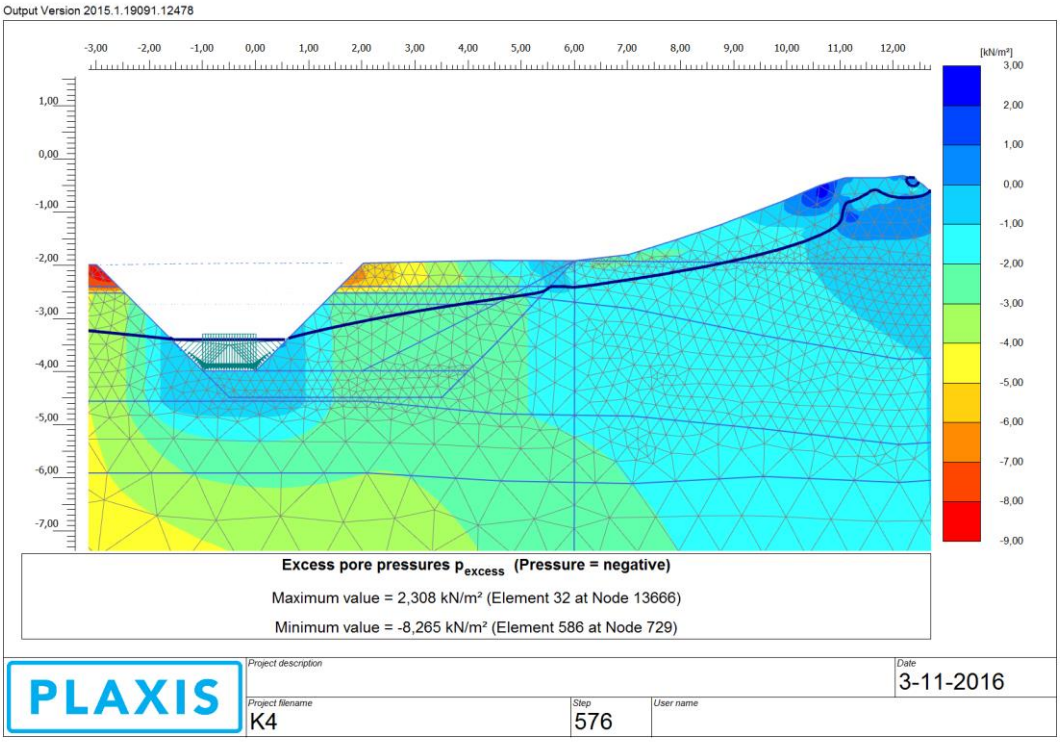

Figure 70:Excess pore water pressures in Pumping I for K4

The SRF change for every analysis varies between phases. The two analyses that have the same average permeability (K2,K4) exhibit the greatest fluctuation. On the other hand, K1 and K3 have the lowest variation. An explanation for this behavior is that the greatest permeability attributes a “drained” response to the model, while with the lowest one, it tends to act in an “undrained” manner. Thus, the behavior between each phase follows a more steady evolution. In K2 and K4 however, the permeability is set in the borderline between two conditions, and so, the response is heavily depended on the loading type and stress path. For example, shear induced pore pressures are going to quickly dissipate in K1, stay almost the same in K3, but it is harder to foretell in K2, K4.

Table 11: Percentage of SRF change along construction phases

Analysis	Pumping I	Consolidation III	Excavation II	Pumping II
K1	-16,9%	3,4%	-8,9%	-12,8%
K2	-19,7%	9,4%	-12,0%	-15,2%
K3	-12,2%	7,6%	-11,4%	-6,7%
K4	-18,1%	9,3%	-16,7%	-10,7%
K5	-16,1%	3,2%	-8,2%	-11,1%
K6	-17,7%	5,7%	-12,6%	-11,6%
K7	-8,2%	2,6%	-10,4%	-12,3%
K8	-16,3%	6,2%	-15,3%	-9,8%

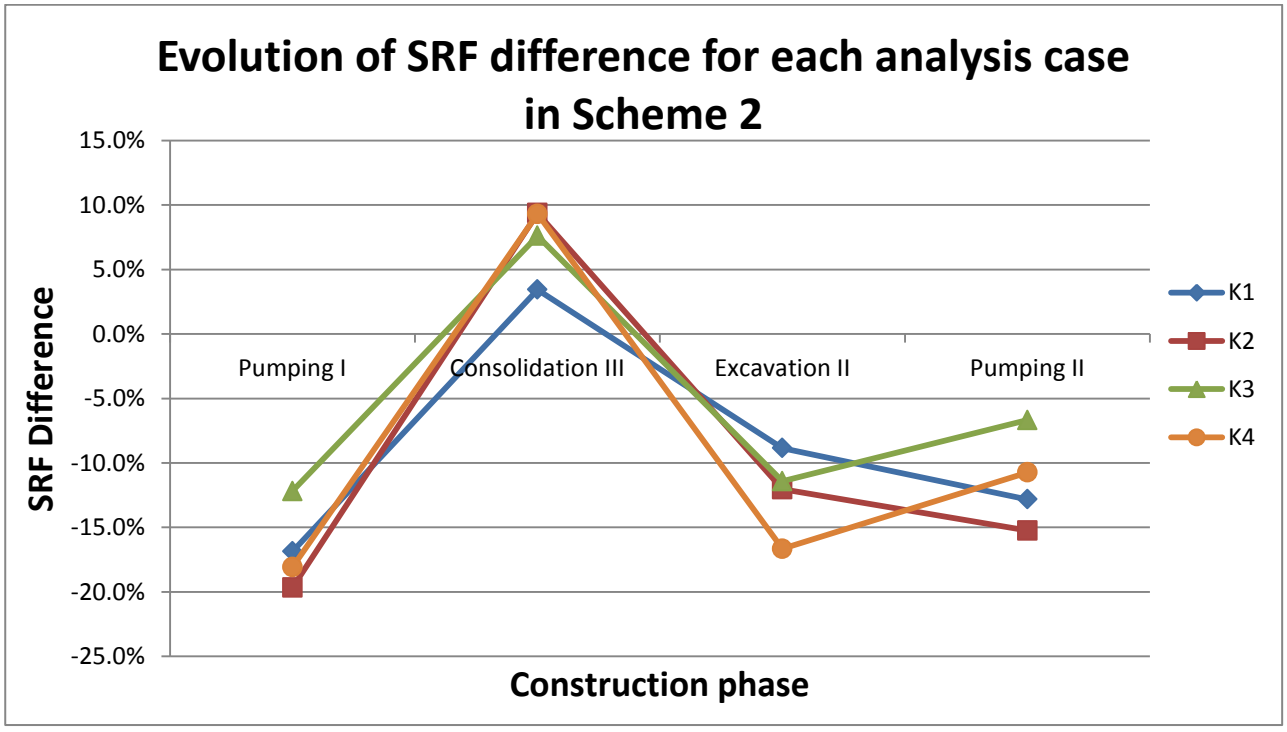

Chart 3: SRF difference among phases for each analysis case in Scheme 2

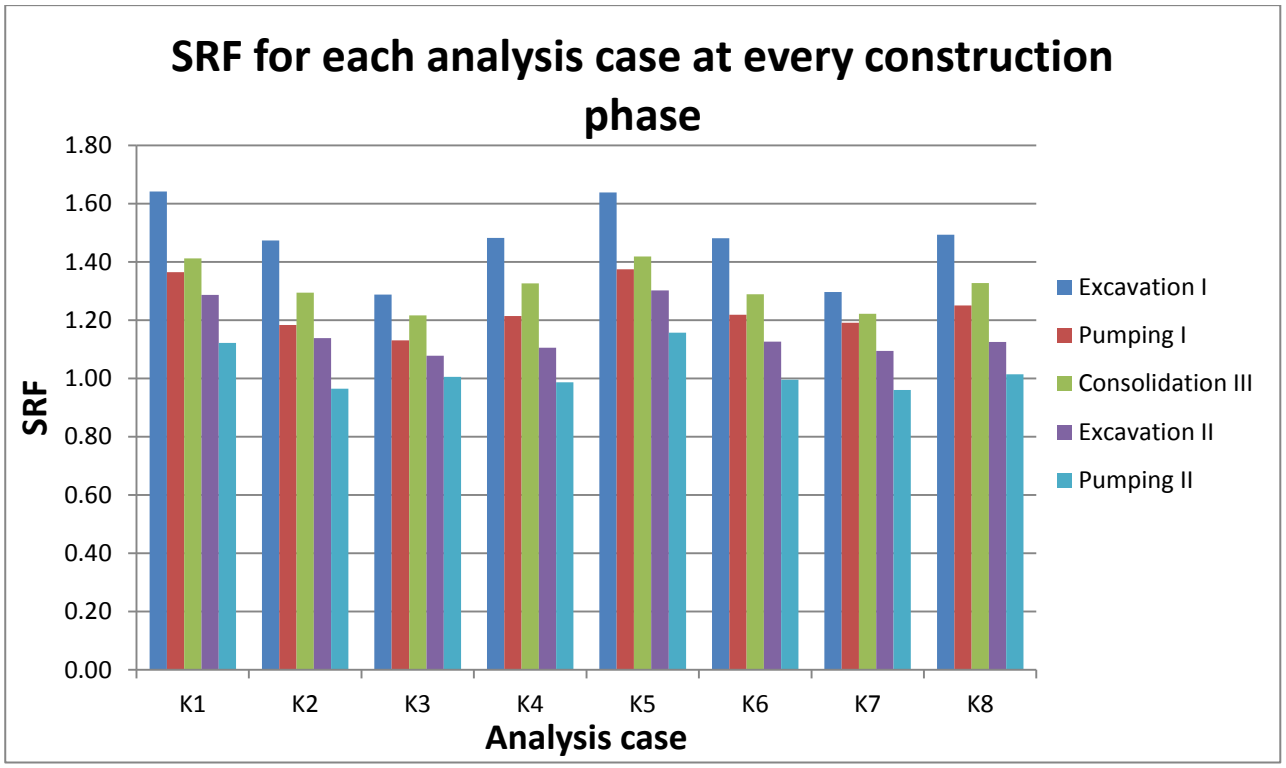

Chart 4: SRF for each analysis at every construction phase

Finally, in every analysis, the SRF follows the exact same trend. Along the construction it decreases, with the exception of Consolidation III, where the water level has risen after Infill I, but the new pressures are not yet fully consolidated. The differences between phases, as well as between analyses, follow the elaboration provided previously in this paragraph.

7.2 Modes of failure

Interfering on the values and ratios of the permeability widely affects the problem. Multiple failure responses are possible and a variety of failure mechanisms are likely to occur. Generally, the failure mechanism takes the form of a large shear zone starting slightly behind the dyke and reaching the toe of the excavation slope. The shear strains contours point out that the shear zone is generally thin, and passes through the Peat-Soft Clay interface. However, this “norm” contains exceptions, the most notable of which are presented later on.

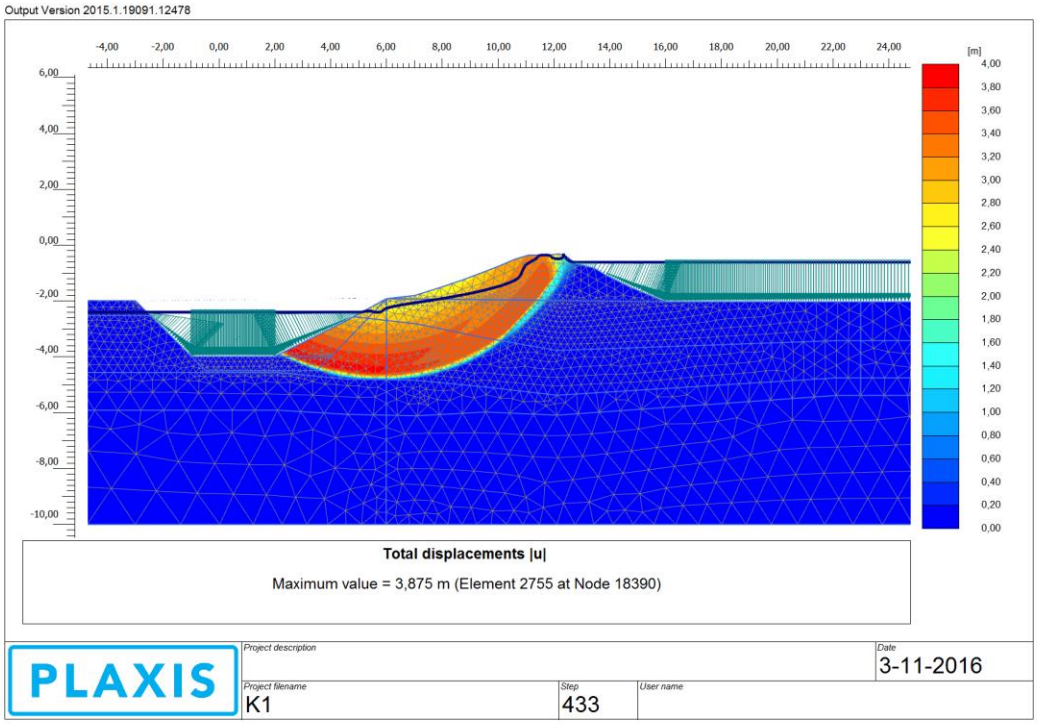

Figure 71: General failure mechanism (Excavation II, K1)

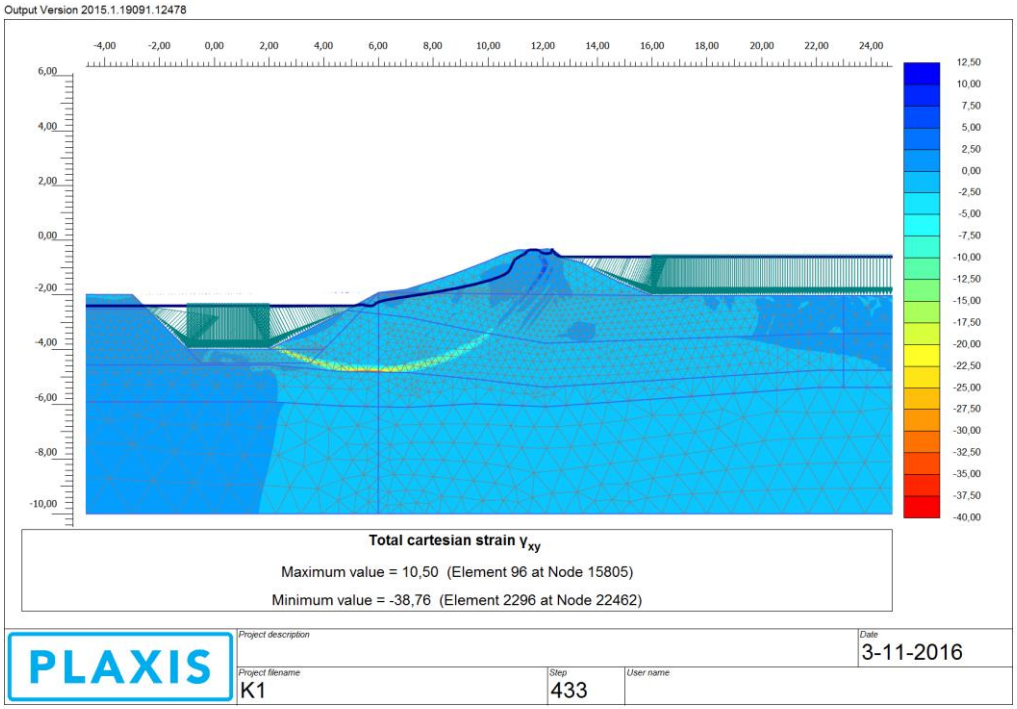

Figure 72: Shear strains of a general failure mechanism (Excavation II, K1)

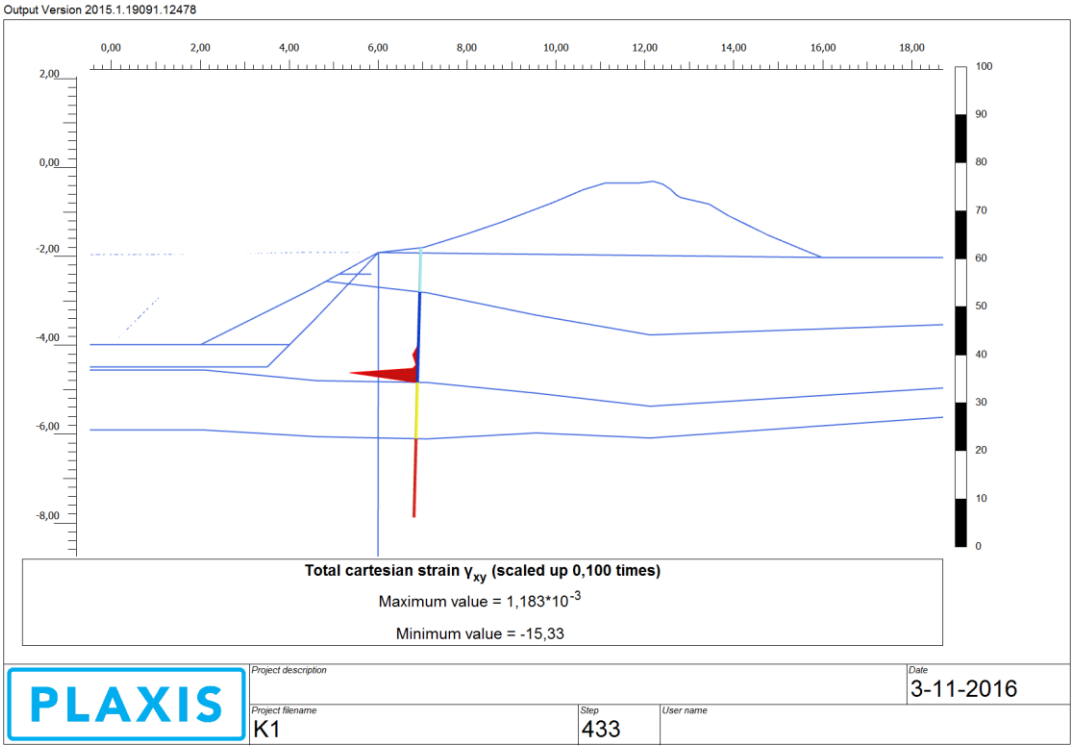

Figure 73: Vertical distribution of shear strains of a general failure mechanism (Excavation II, K1)

Firstly, at excavation I in cases K1 and K4, where the horizontal permeability is maximum, a great lateral waterflow is present through the peat layer. It drops the effective stresses and so, the shear strength of the soil, causing a massive, overall landslide. In both analyses, the deformations, shear strains, waterflow vectors and pore pressures look identical. This implies that in the early stages the horizontal flow (and so, permeability) affect the most the failure mechanism. Furthermore, it is should be mentioned that the failure propagates with a component on the interface between the Peat and Soft Clay layers, which is a weak discontinuity, enhancing failure development. This complies with reality, as failure happened through this interface.

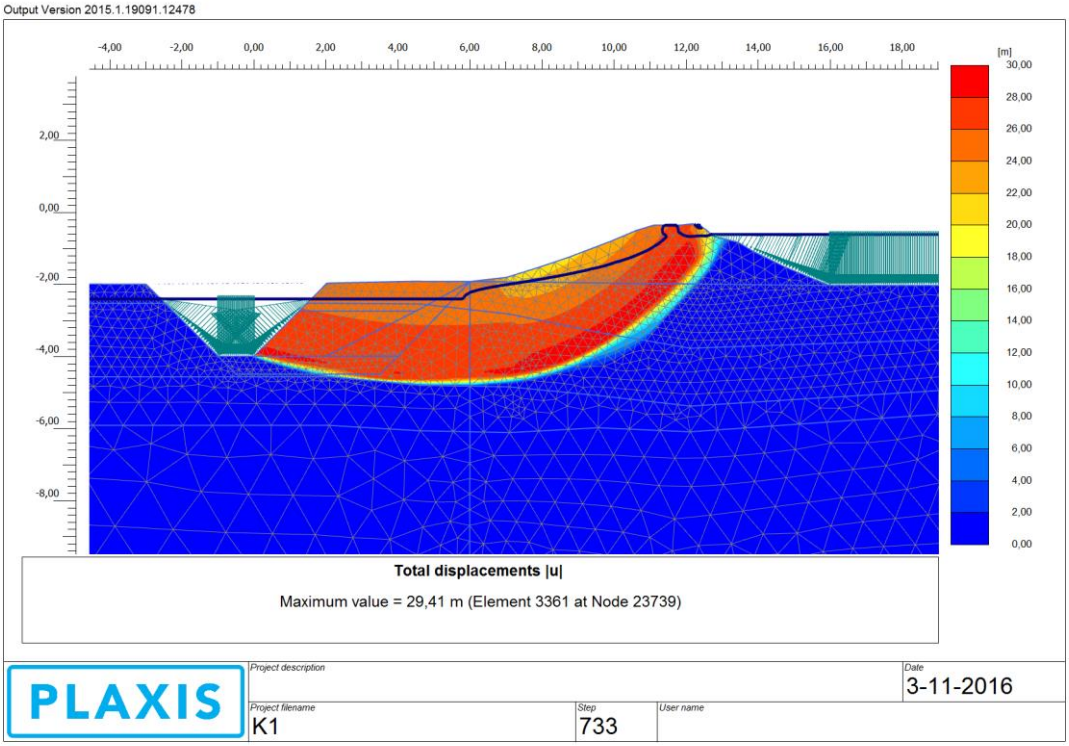

Figure 74: Displacement contour (K1, Excavation I)

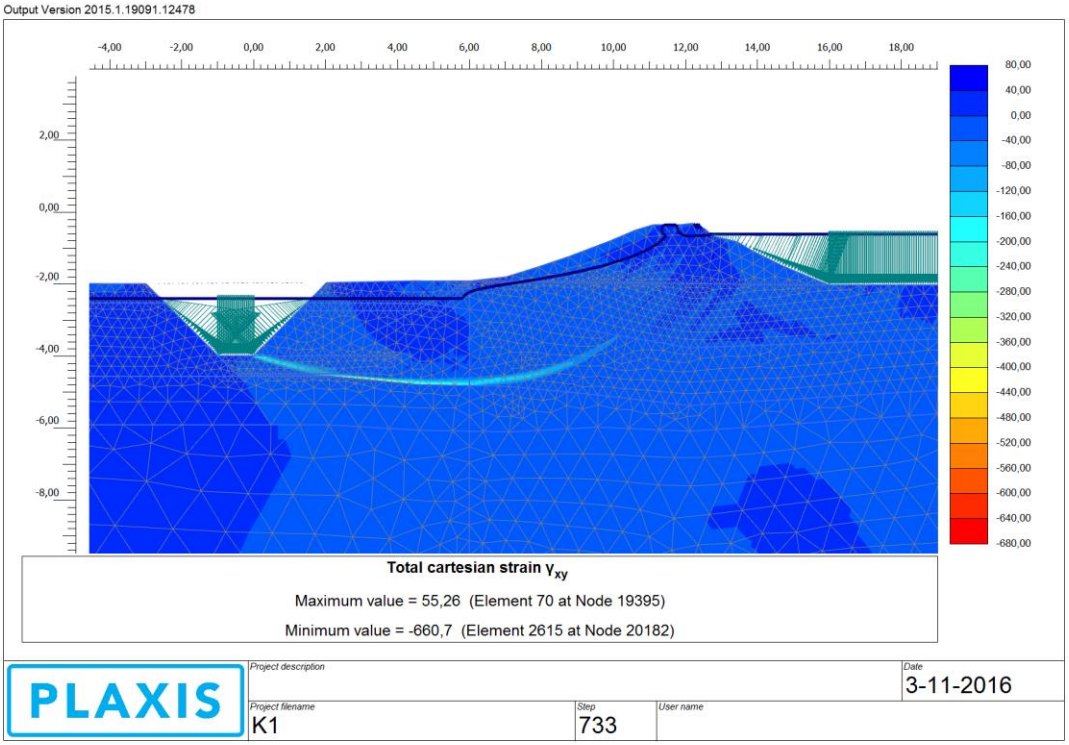

Figure 75: Shear strain contour (K1, Excavation I)

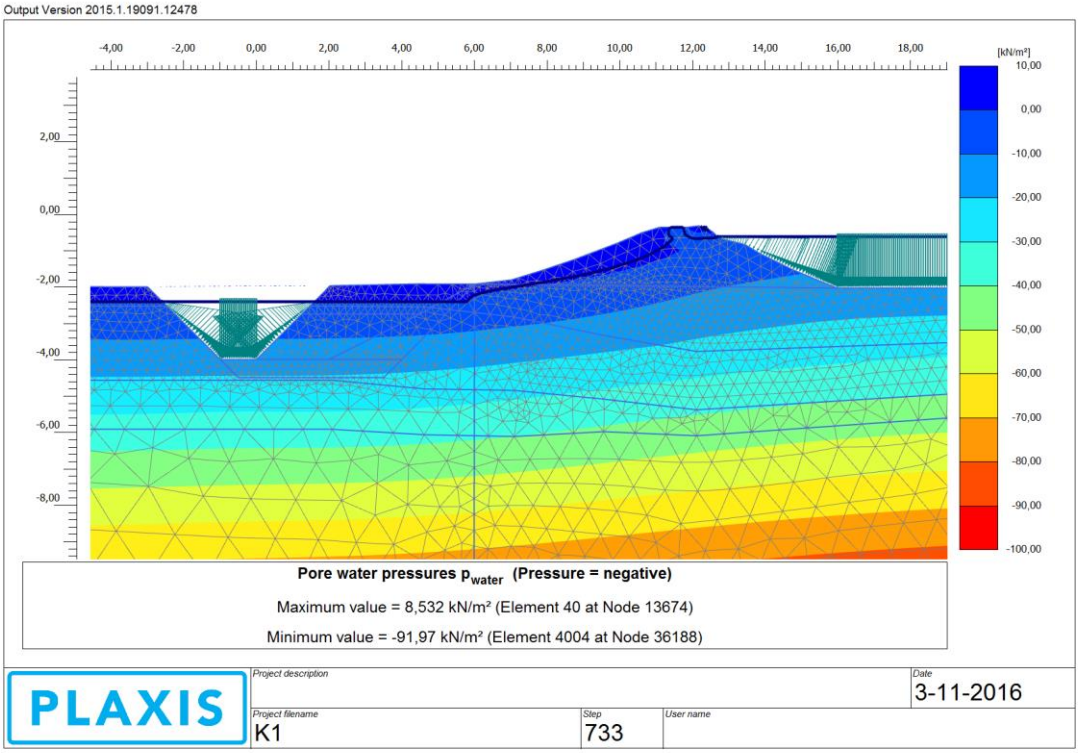

Figure 76: Pore water pressure contour (K1,Excavation I)

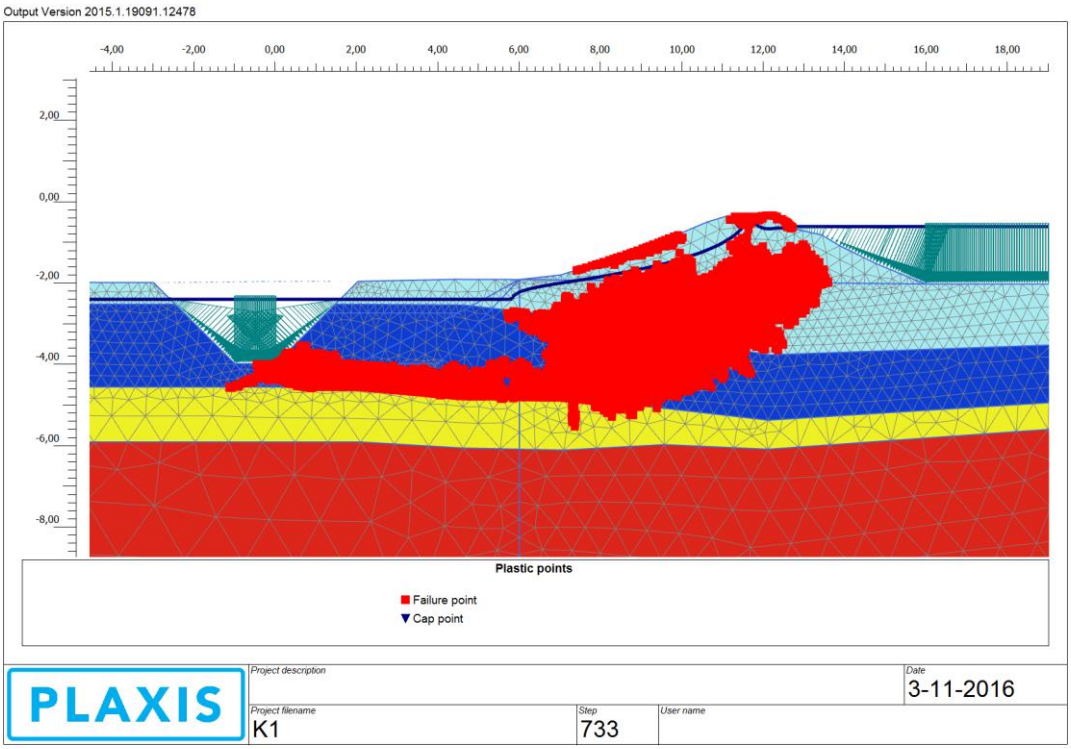

Figure 77: Plastic failure points (K1, Excavation I)

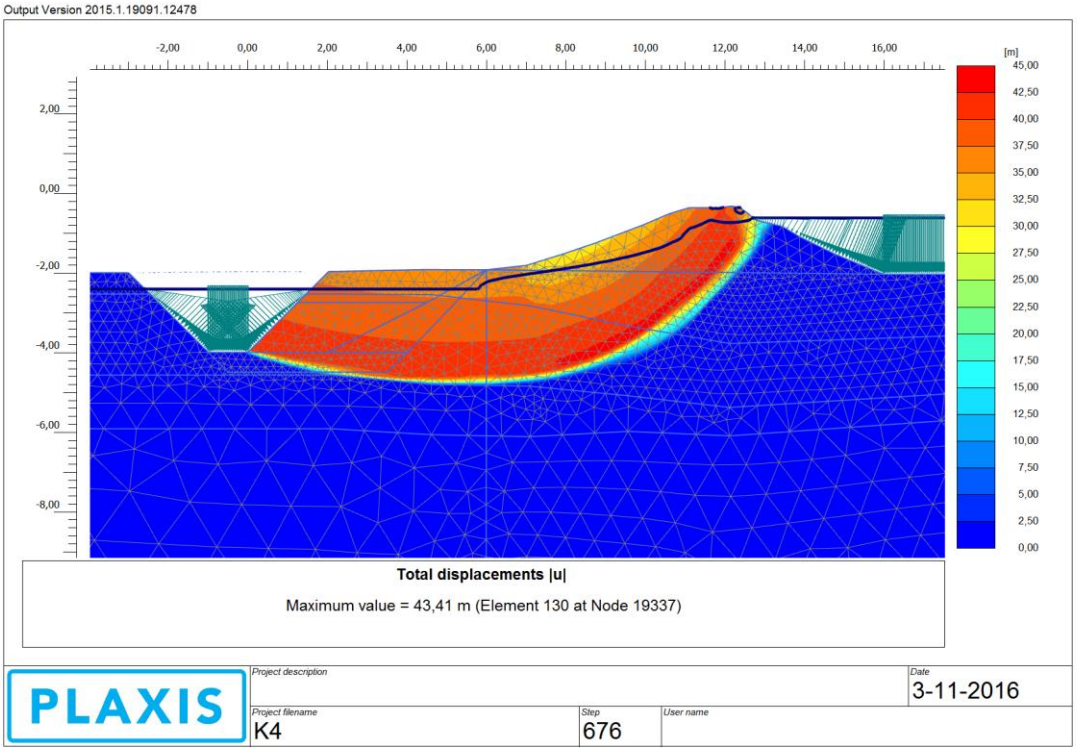

Figure 78: Displacement contour (K4, Excavation I)

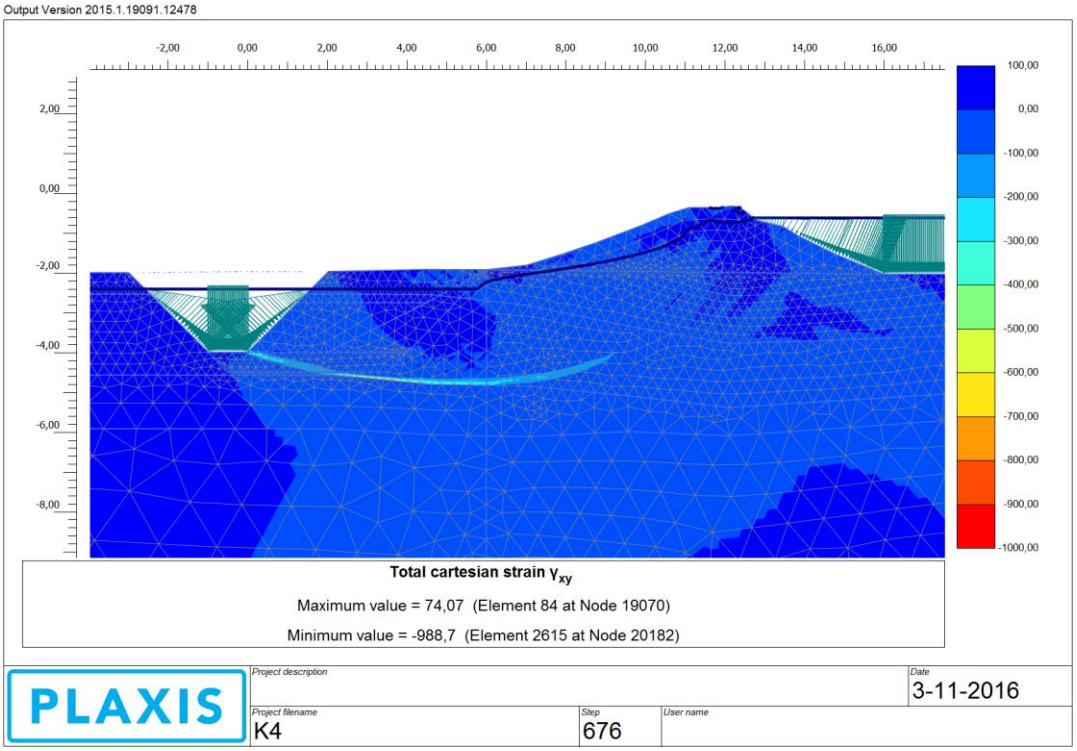

Figure 79: Shear strain contour (K4, excavation I)

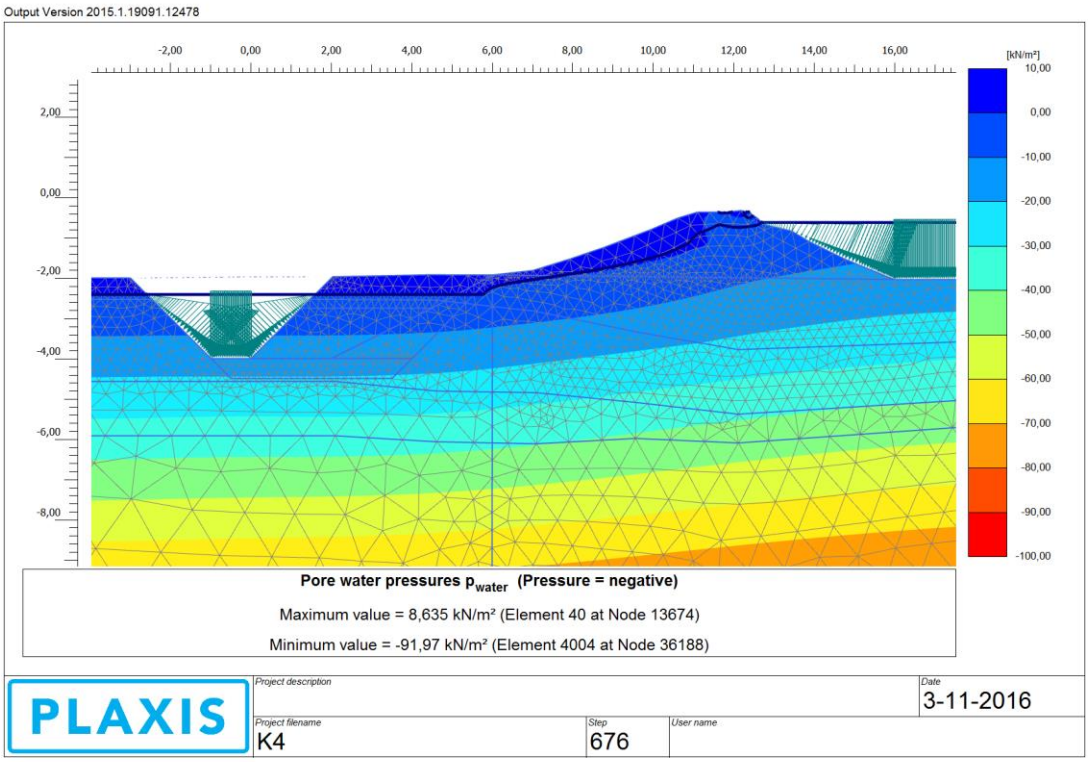

Figure 80: Pore water pressure contour (K4,Excavation I)

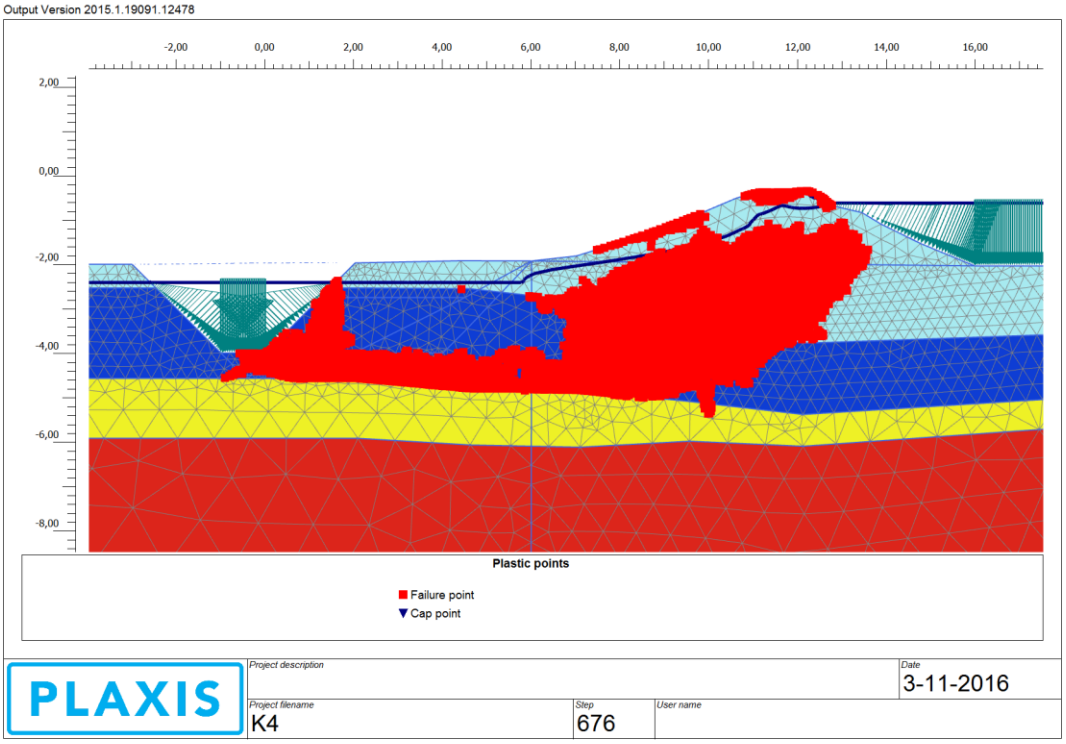

Figure 81: Plastic failure points (K4, Excavation I)

Another common point between analyses K1 and K4 is the mode of failure for stage pumping I. In this situation, the failure seems to be formed as a local slide at the excavation slope. The waterflow of increased intensity due to the pumping affects mostly the uppermost part of the slope, which is the first one to lose stability. Besides, another point of awareness is raised now; just because the slide happens at the excavation slope, the failure is not meant to be localized. Observing the shear strains, it is evident that an overall mechanism is being formed, one that includes the small failure. This hints that the failure takes the form of a retroactive slide mechanism. When the excavation slope mechanism is activated, stress redistribution is impossible for the larger ones. This leads to a domino effect of successive slides, leading up to the general one before mentioned. A minor difference is that the mechanism in K4 seems to form sooner, as there is already some displacement in the along the dyke. This fact aids in the design of the construction (according to Eurocode) as it produces a “ductile” failure, offering warning before the slide. However, it should be kept in mind that in general, a domino-like failure mechanism is brittle, as a much larger soil volume slides, rather than what the localized displacements indicate. Moreover, the shear mechanism in K4 seems to develop largely in parallel to the interface of Peat and Soft Clay layers, because the low vertical permeability enhances the vertical flow component, and so affects the shear strength of the interface.

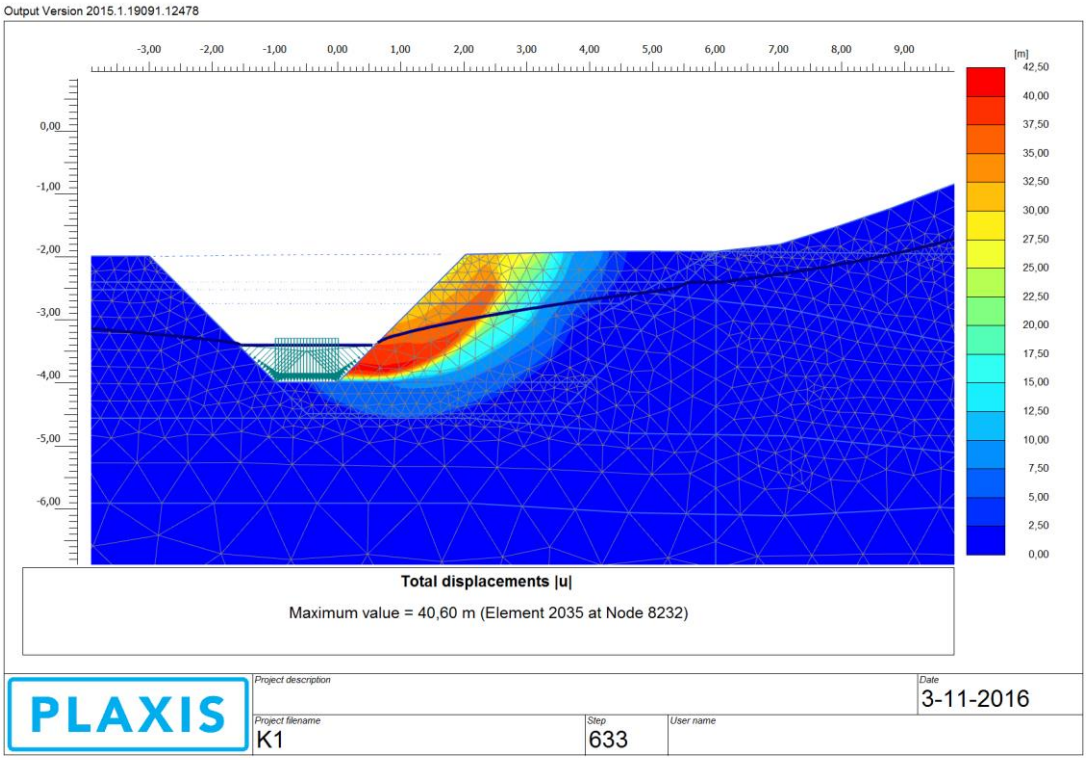

Figure 82: Displacement contour (K1, Pumping I)- First part of retroactive failure mechanism

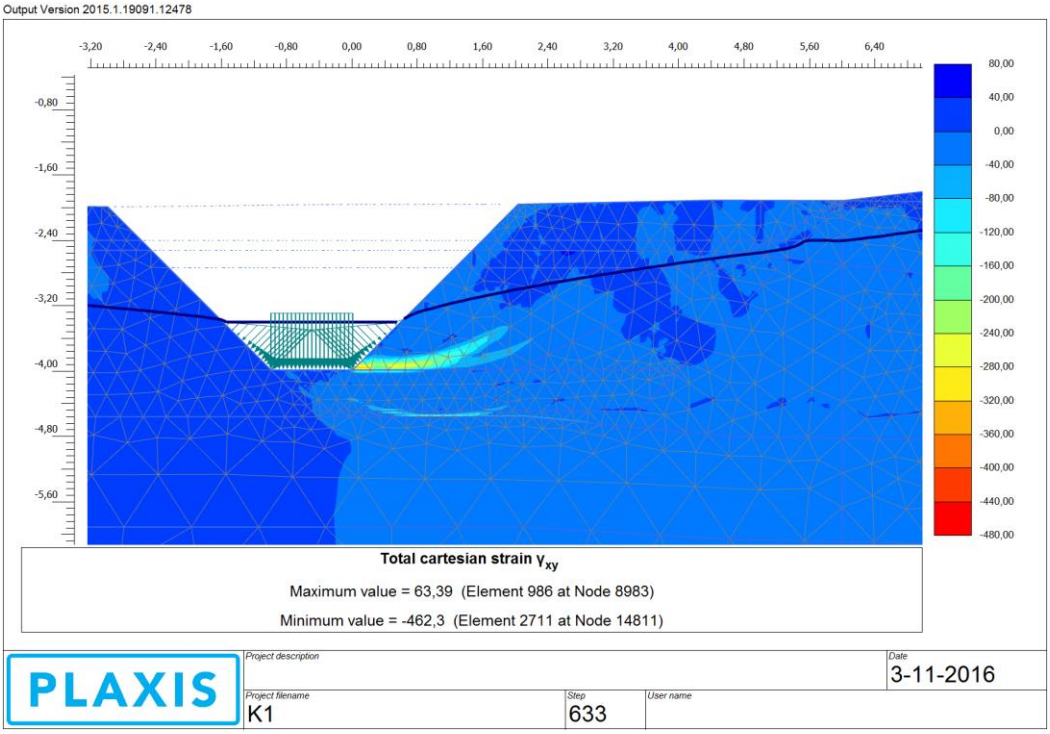

Figure 83: Shear strain contour (K1, Pumping I)- Formation of retroactive failure mechanism

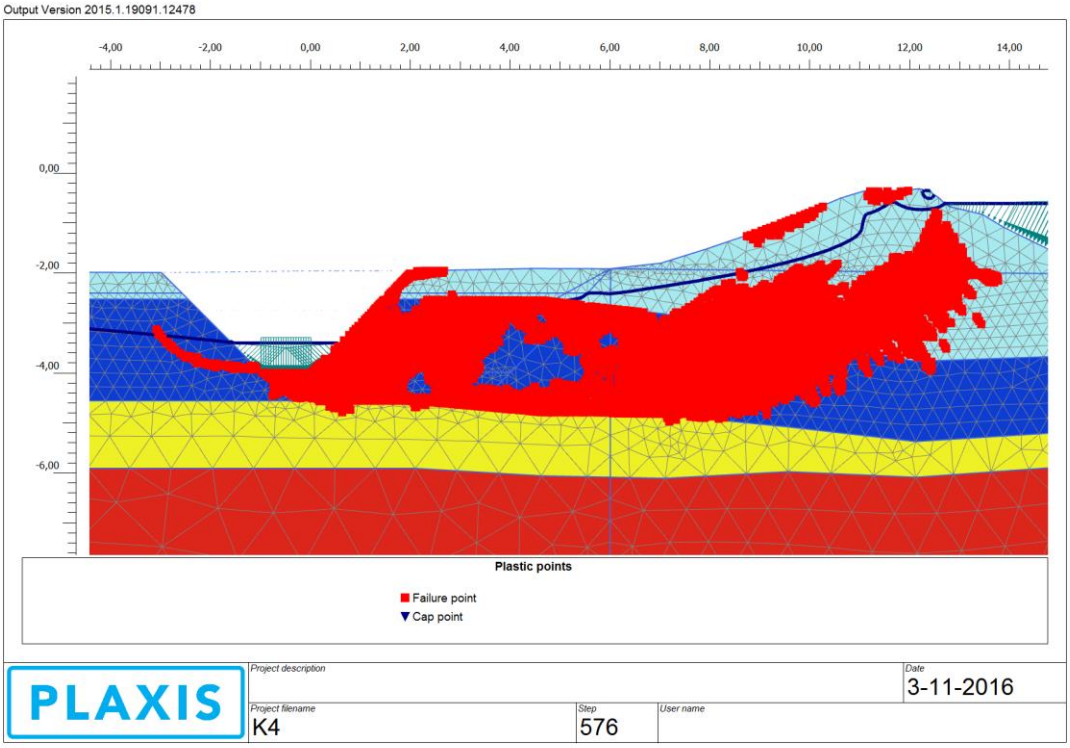

Figure 84: Plastic failure points (K1, Pumping I)- Formation of retroactive failure mechanism

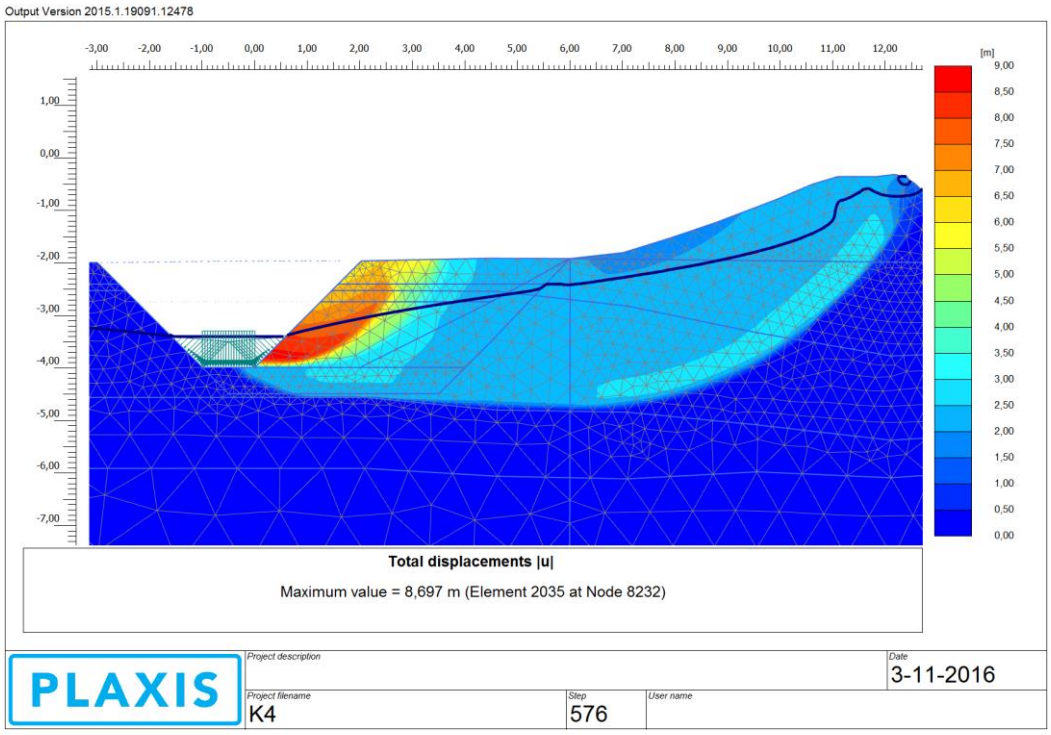

Figure 85Displacement contour (K4, Pumping I)- First part of retroactive failure mechanism

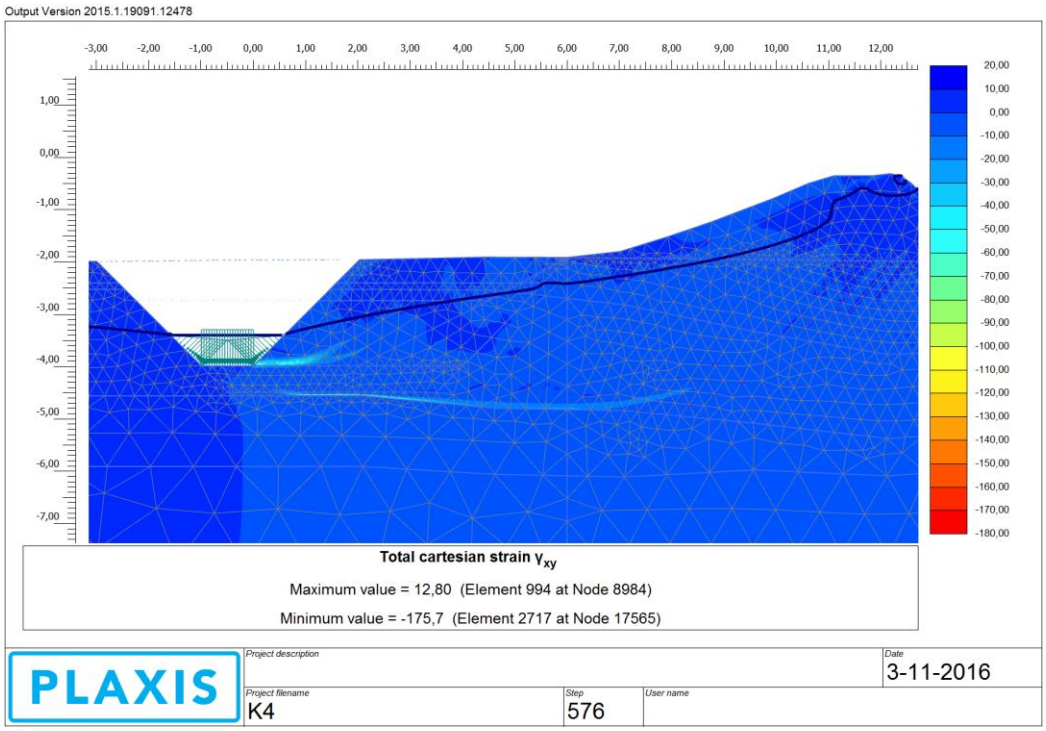

Figure 86Shear strain contour (K4, Pumping I)- Formation of retroactive failure mechanism

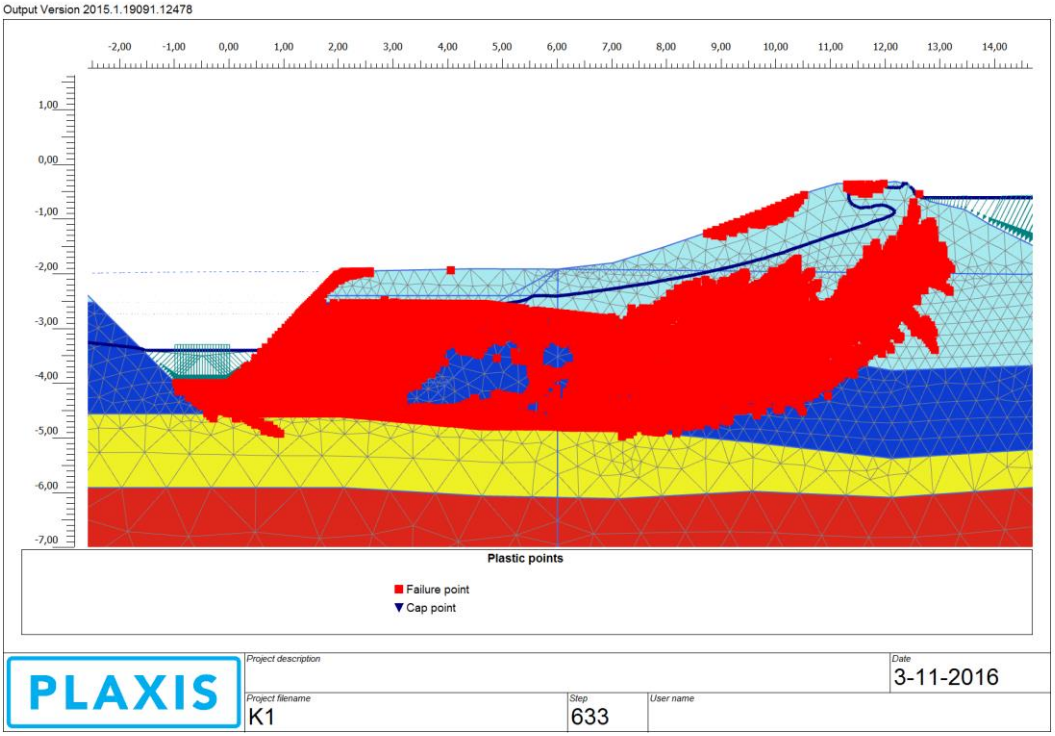

Figure 87: Plastic failure points (K4, Pumping I)- Formation of retroactive failure mechanism

A high horizontal permeability is connected with modes of slope failure, while a low vertical one affects the response of the excavation bottom. In analysis K3, the upwards flow gradient from Soft Clay to Peat is intensified (see 7.1: Comparison between analysis cases, the multiple material flow analogue), and so effective stresses drop. Bearing in mind the low volumetric weight of Peat, even small pressure deviations have a considerable impact. In K3 at phases Excavation I and Pumping I, the overall slide failure mechanism contains the bottom of the excavation, below which it is located on the Peat-Soft Clay interface.

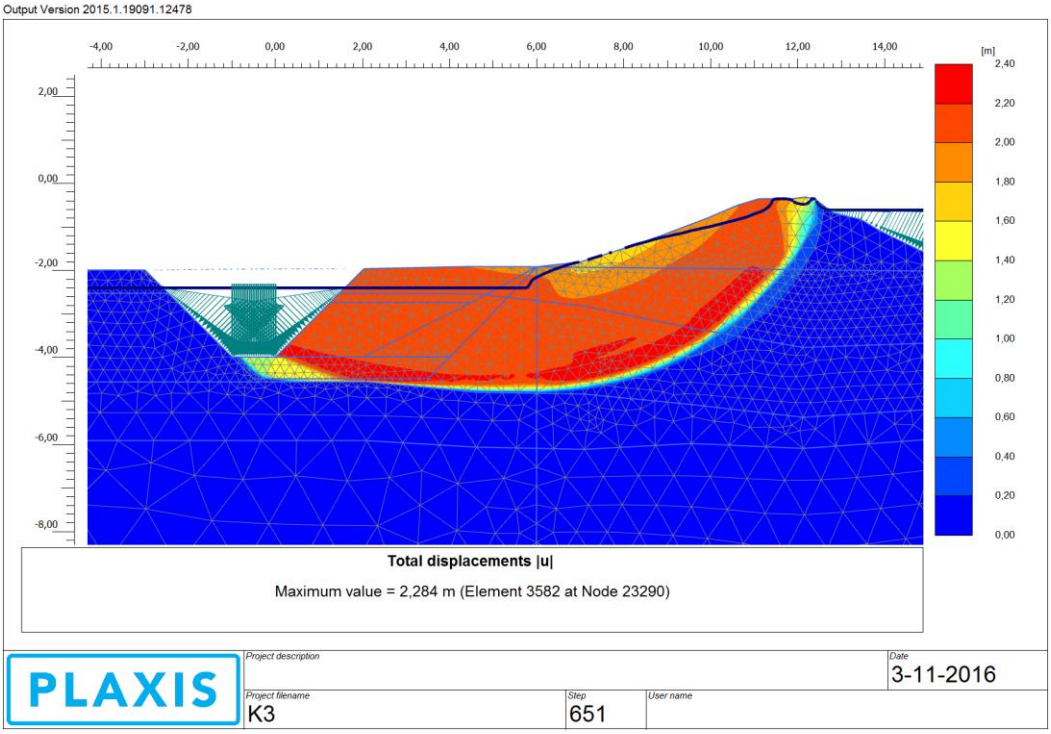

Figure 88: Displacement contour (K3, Excavation I)- Slope slide includes excavation bottom

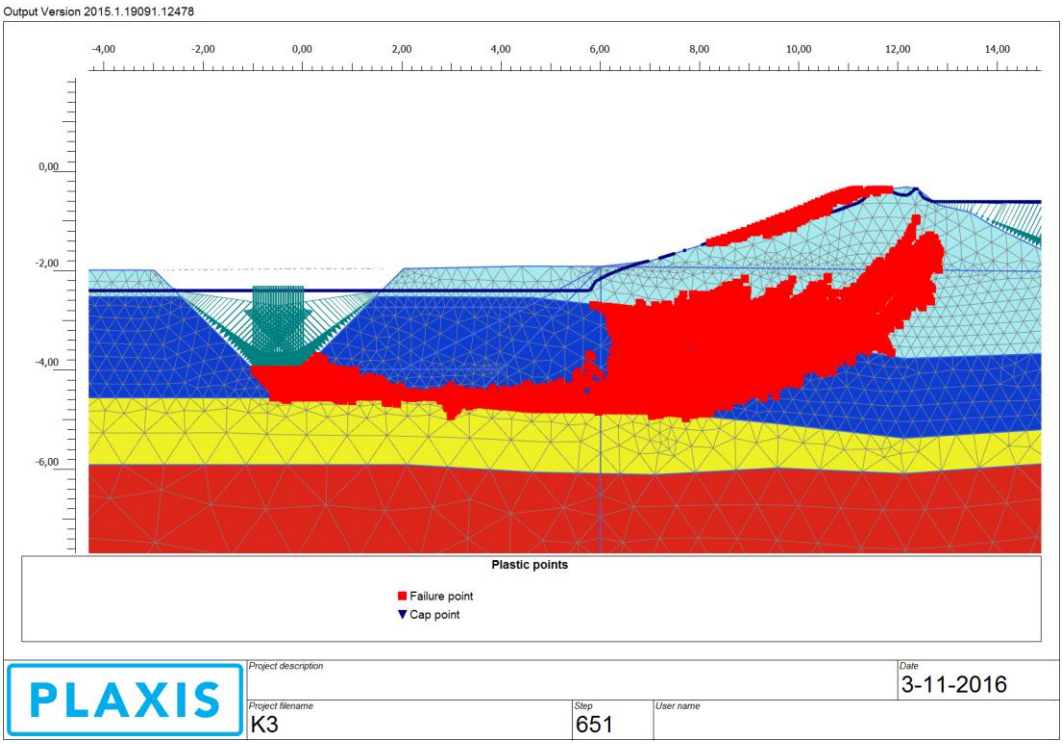

Figure 89: Plastic failure points (K3, Excavation I)- Slope slide includes excavation bottom

The most prominent effect of the upward flow is in phase Pumping II, where a separate bottom uplift mechanism is formed, along with the overall slope failure. It is noted that in all cases where the bottom is at failure, the mechanism starts at the Peat interface. This points out that for a given low volumetric weight, it is the Peat upward flow, and so the vertical permeability, that dictates the bottom response. However, the lateral permeability is major factor of this phenomenon, and this is justified by the following argument; bottom uplift does not occur in analysis K4, where the permeability ratio is 1/100. When the lateral permeability is high, water inflowing into the Peat layer can exit to the horizontal, or in other words, the horizontal component of flow dominates the groundwater calculation. In the opposite conditions, the gradient increases in the Peat layer, and so water pressures build up and lead to soil heave.

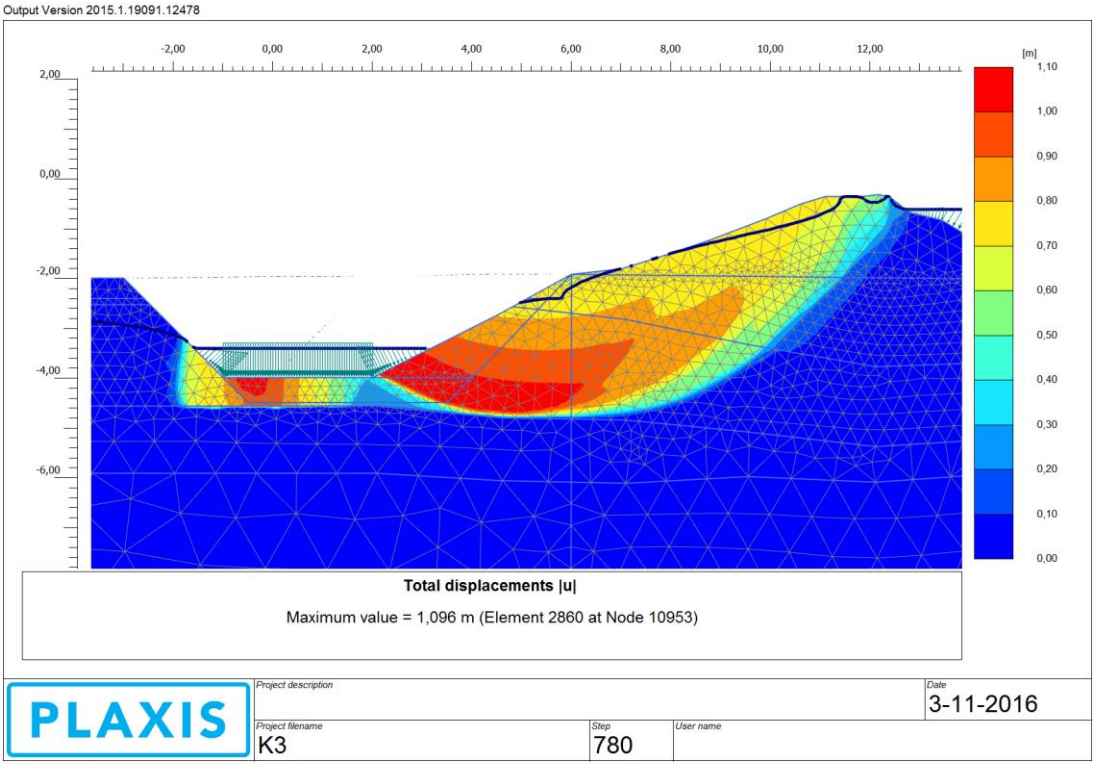

Figure 90: Displacement contour (K3, Pumping II)- Slope slide and bottom uplift develop independently

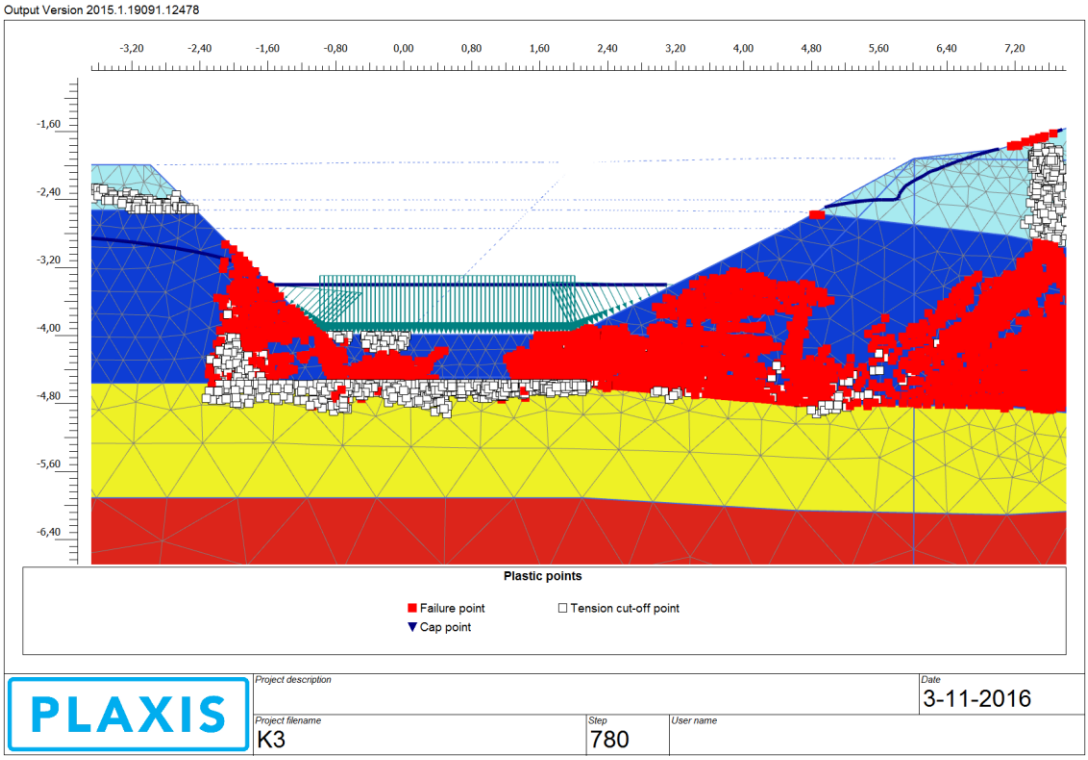

Figure 91: Plastic failure points (K3, Pumping II)- Slope slide and bottom uplift develop independently

It is seen that in Pumping II the flow is less intense than in Pumping I, as also justified by the smoother transition of the groundwater head. However, bottom uplift is easier is Pumping II, as after the second excavation phase, there is less soil volume to redistribute the stresses. If that soil was present, the confinement offered could have been able to hold back the heave.

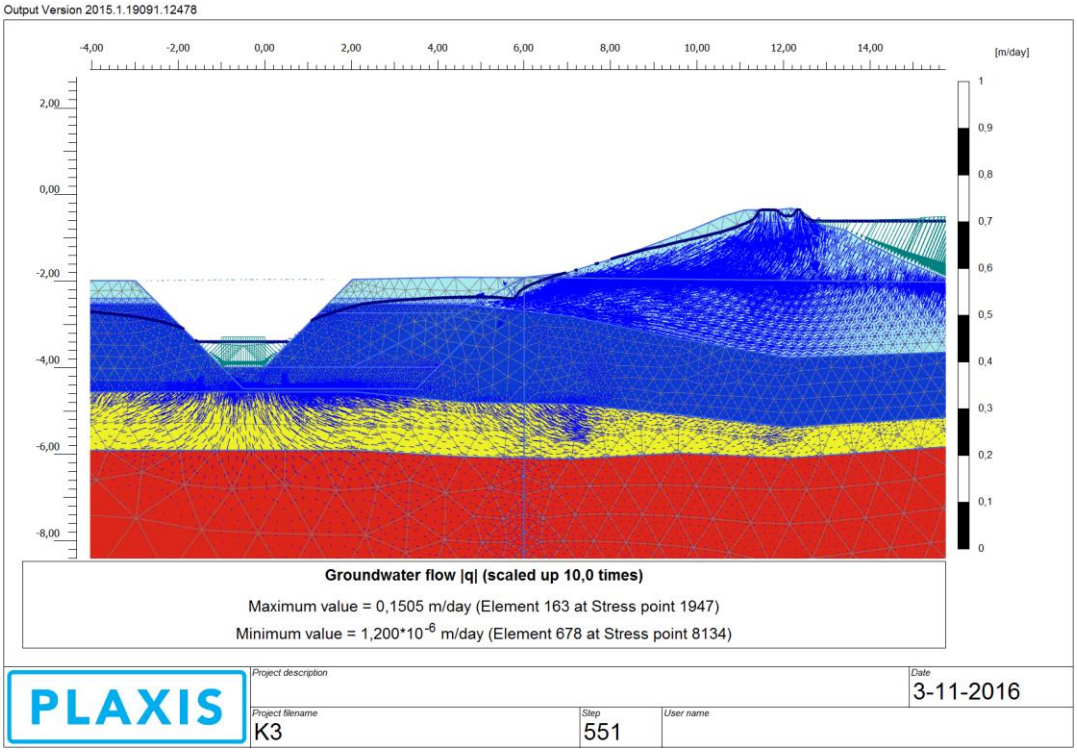

Figure 92: Groundwater flow (K3, Pumping I)- Intense upward flow below the excavation bottom

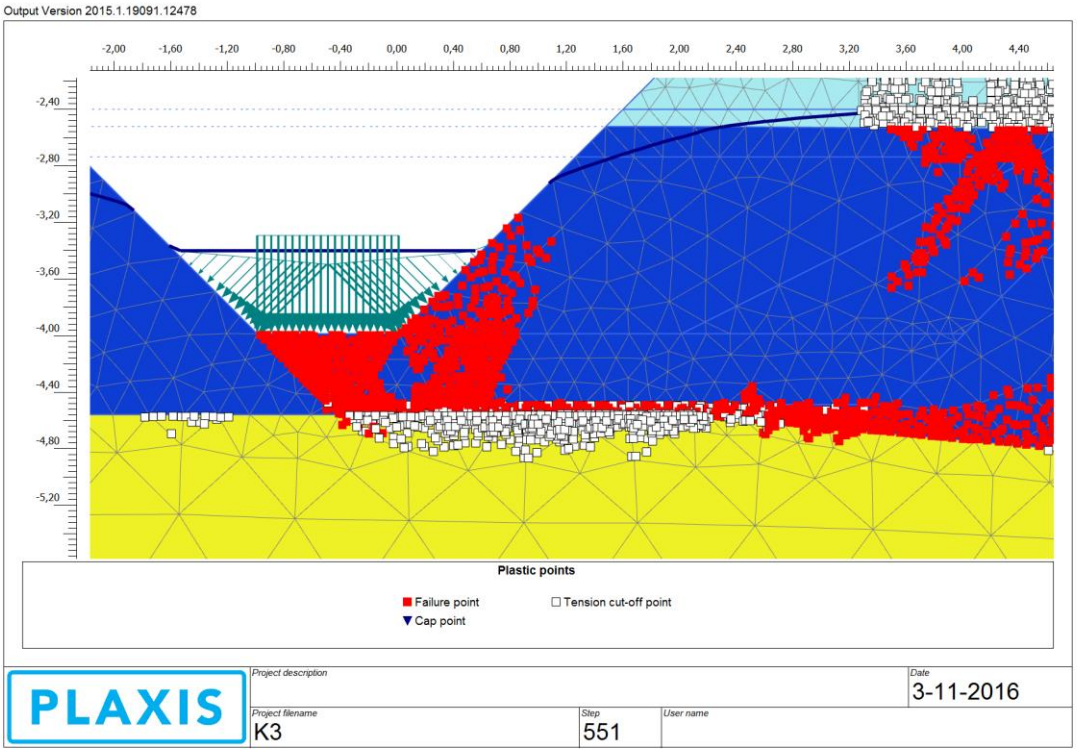

Figure 93: Plastic failure points (K3, Pumping II)- Intense plastification below excavation bottom

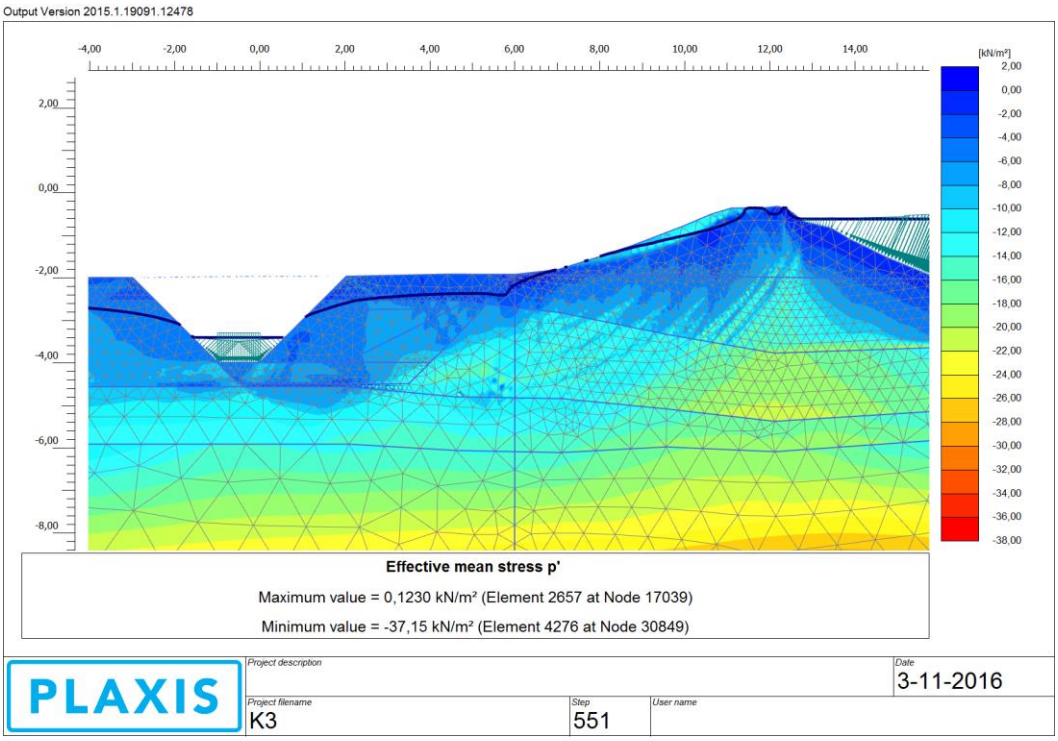

Figure 94: Effective mean stress (K3, Pumping II)

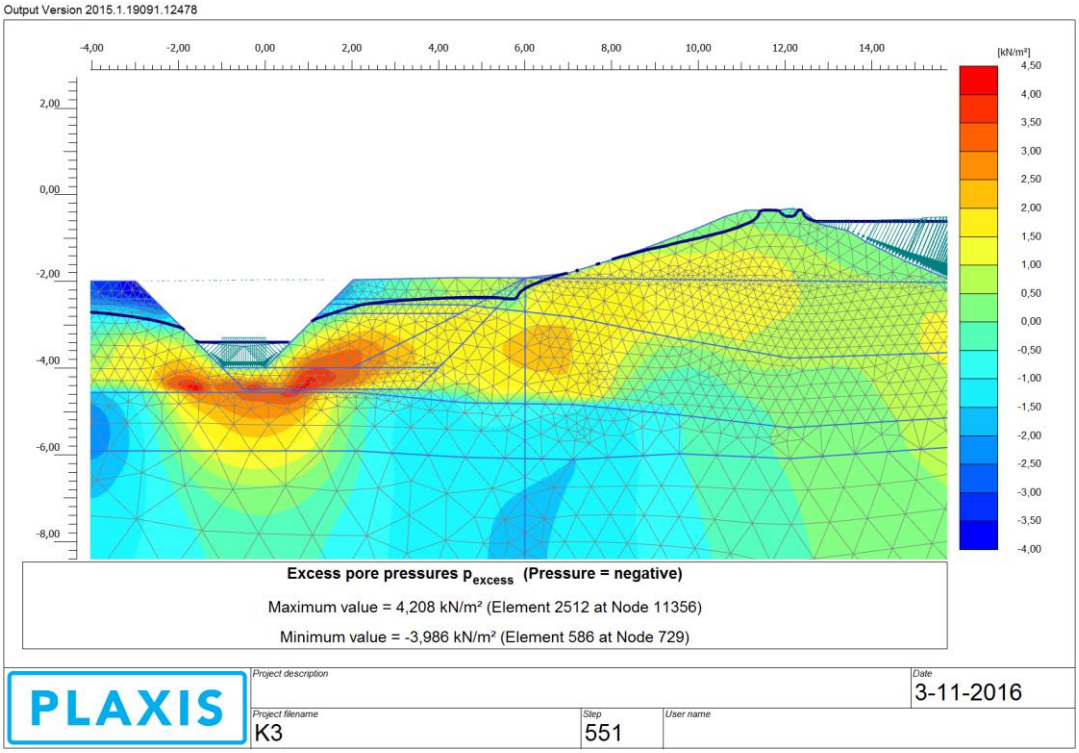

Figure 95: Excess pore pressures (K3, Pumping I)

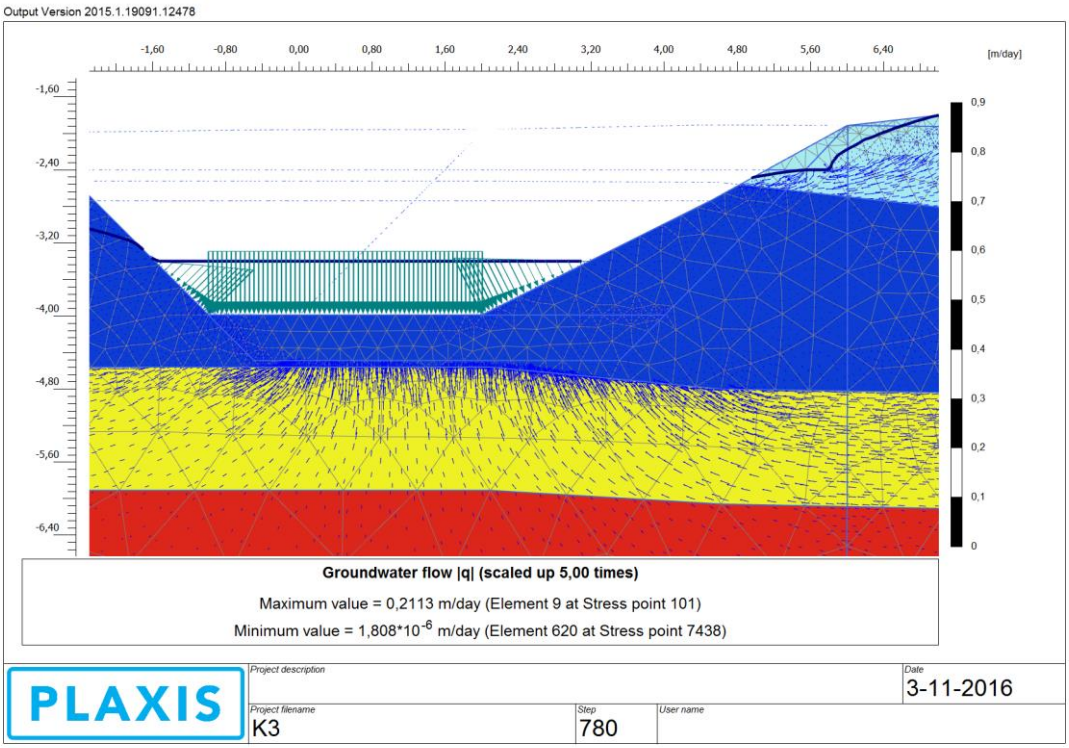

Figure 96: Groundwater flow (K3, Pumping II)- Intense upward flow below the excavation bottom

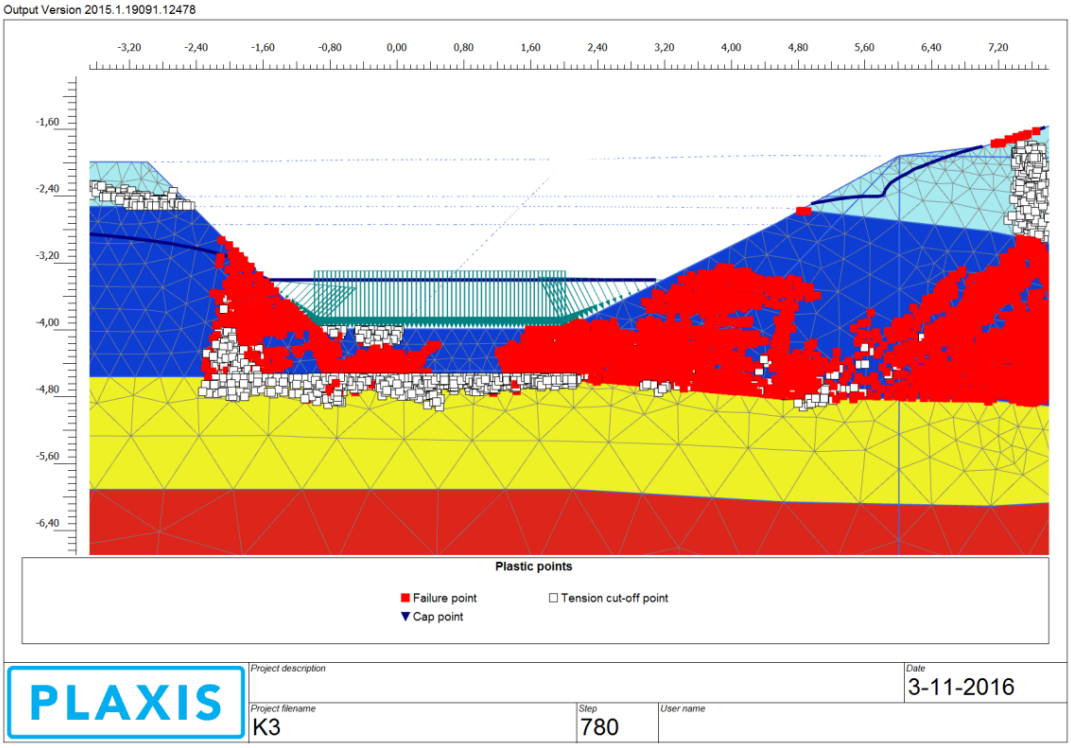

Figure 97: Plastic failure points (K3, Pumping II)- Intense plastification at sides of excavation bottom

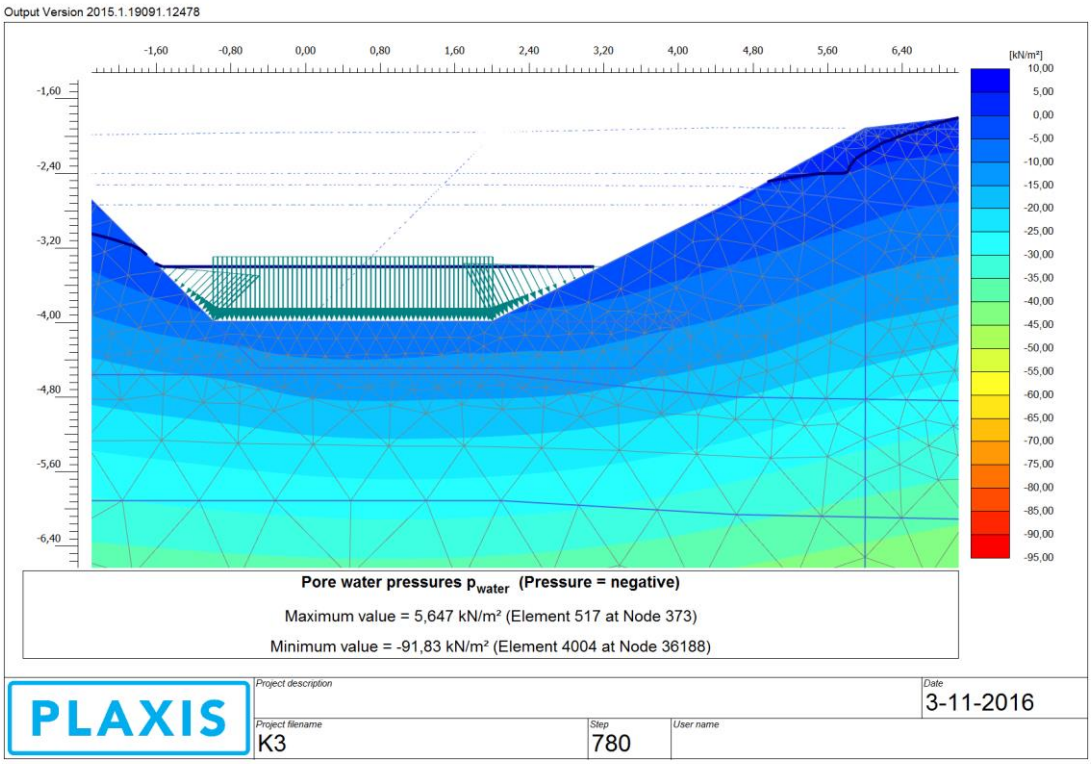

Figure 98: Pore water pressure contour (K3, Pumping II)

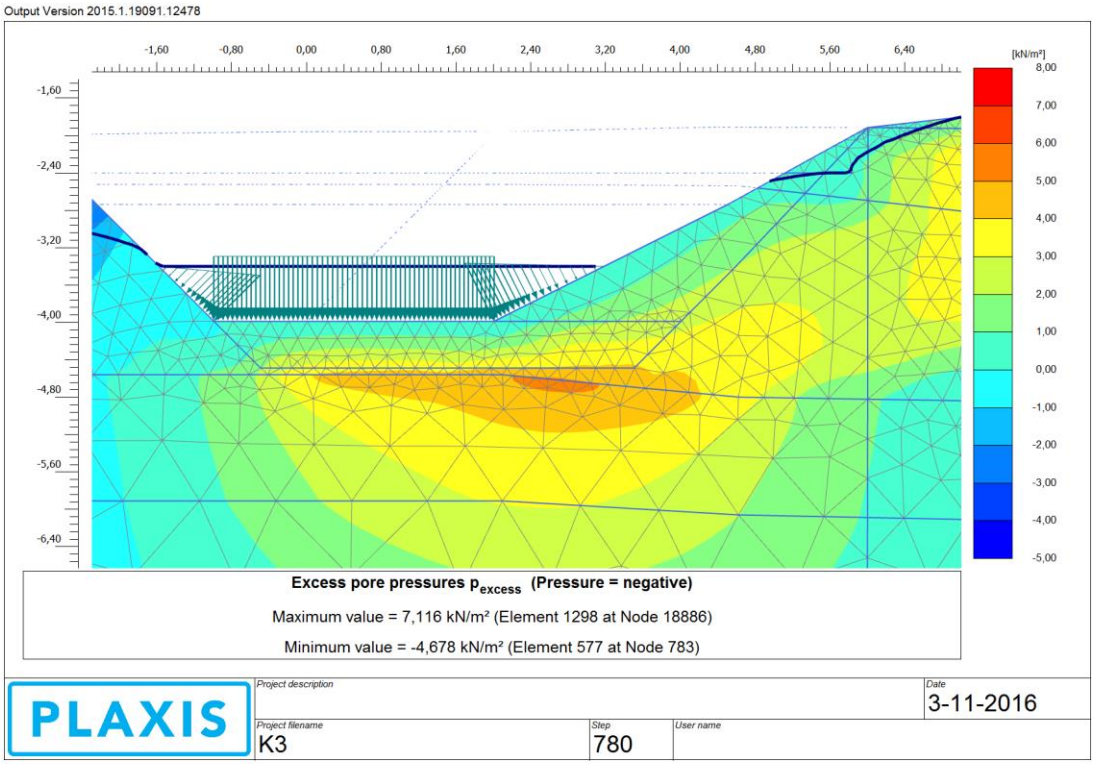

Figure 99: excess pore pressures (K3, Pumping II)

Finally, another mechanism that wasn't mentioned but should be kept in mind is heave on the excavation slope. There are multiple hints of this failure mode, especially in phase Consolidation III.

8 CONCLUSION

Concluding, this report has addressed several issues. Firstly, a comparison between the application of the Mohr-Coulomb linearly elastic-perfectly plastic model and the elastoplastic Soft-Soil advanced model has been made. While at first glance their safety was predicted to be almost equal, the Soft Soil model provides a higher safety factor, while being dependable, as it is expected to capture soil behavior more efficiently. Moreover, of all the safety schemes of Eurocode 7, but also the traditional overall safety factor approach, Scheme 1b is judged to be the fittest for this type of project, mainly because of its cautionary nature, as well as its concept of reality.

Furthermore, a question is raised upon the definition of the characteristic value of the elastic compressibility; although following a "rule of thumb" it should be the upper value given by the statistical treating of the test data as suggested by Eurocode 7, the lower one would lead to the largest plastic strains. Comparing the analyses, no actual difference is present, not even in the unloading phases where the elastic component fluctuation is expected to have an impact. This result signifies the dominance of the elastoplastic compressibility on the phenomenon, which however is model and project sensitive.

On the other hand, the sensitivity analysis on compressibility characteristic values provides significant insight on the application of the characteristic value concept. Upon using the lower characteristic value for the elastic compressibility, the safety factor decreases in cases when failure is about to happen. This means that stress distribution is considerably affected by this value, even though this is not that evident in the displacements. Hence, the importance of proper selection of the compressibility characteristic value is highlighted, along with its effects. However, further investigation is needed on this part, extrapolating the conclusion on similar slope stability projects and furthermore, to general geo-engineering problems.

Finally, the sensitivity analysis on the permeability was conducted. The results were as expected; higher permeability values offer a safer construction. However, the failure mechanisms of each case take a wide variety of forms. The project verified these engineering predictions, identified the patterns of failure mechanisms, connected them to soil permeability, and finally, offered an elaboration on the phenomenon. These analysis gives emphasis on the significance of accurately estimating the permeability, and points out the effects of its variation.

Summing up, the project focused on dealing with engineering misconceptions, or certifying routines that are usually followed when applying Eurocode 7. Hence, it empowers engineering oriented towards critical thinking, which is a cornerstone of both engineering practice as well as the philosophy of the Eurocode, over a simple fulfillment of regulation.

9 REFERENCES

1. *Brinkgreve, R.B.J. and Vermeer, P.A., 1998. Plaxis manual. Version, 7, pp.5-1.*
2. *H. Zhao, E. Poutoni, (2016), TU Delft internal report*
3. *Determination of characteristic soil values by statistical methods, C. Pohl, ELE- Consulting Engineers Ltd., Essen, Germany, ISGSR 2011*
4. *European Committee of Standardization, 2004, Eurocode 7: Geotechnical Design-Part 1: General rules, EN 1997-1*
5. *Bond, A. and Harris, A. (2008),Decoding Eurocode 7. London: Taylor & Francis.*
6. *Brinkgreve, R.B.J. and Bakker, H.L., 1991, May. Non-linear finite element analysis of safety factors. InProc. 7th Int. Conf. on Comp. Methods and Advances in Geomechanics, Cairns, Australia(pp. 1117-1122).*
7. *H.R. Schneider, P. Fitze. (2013). Characteristic shear strength values for EC7: Guidelines based on a statistical framework. Proceedings of the 15th European Conference on Soil Mechanics and Geotechnical Engineering : geotechnics of hard soils, weak rocks.(4), 318-325.*
8. *M. Kavvadas (2008), Application of Eurocode 7 on the design of geotechnical projects, Proceedings of "Greek Civil Engineering Association" conference, Heraklion, 2008*
9. *Brinkgreve, R.B.J., Post, M., (2015), Geotechnical Ultimate Limit State Design Using Finite Elements, In Geotechnical Risk and Safety V; 5th International Symposium on Geotechnical Safety and Risk, Rotterdam (The Netherlands), 13-16 Oct. 2015, Delft (The Netherlands): IOS Press. 464 - 469.*
10. *Brinkgreve, R. B. J., Post, M., (2013), On the use of finite element models for geotechnical design, In Bemessen mit numerischen methoden Workshop, Hamburg (Deutschland), 24 - 25 Sept., 2013, Hamburg: Elbe - Werkstatten GmbH, 111 - 122.*
11. *D.MPotts,L. Zdravkovic. (2012). Accounting for Partial Material Factors in Numerical Analysis. Geotechnique, 62(12), pp.1053–1065.*
12. *A. Bond, B. Schuppener, G. Scarpelli, T. Orr, (2013), Eurocode 7: Geotechnical design -Worked examples, "Eurocode 7: Worked examples" Workshop, Dublin (Ireland), 13 - 14 June, 2013, Luxemburg: Publications Office of the European Union, 2013*

10 BIBLIOGRAPHY

1. *Hicks, MA &S amy, K 2002, 'Reliability-based characteristic values: A stochastic approach to Eurocode 7'*Ground Engineering*, vol 35, no. 12, pp. 30-34.*
2. *Hicks, M. A., & Nuttall, J. D. (2012). Influence of soil heterogeneity on geotechnical performance and uncertainty: a stochastic view on EC7. In Proceedings 10th International Probabilistic Workshop, Universität Stuttgart, Stuttgart (pp. 215-227).*
3. *Hicks, M.A. and Samy, K., 2002c. Reliability-based Characteristic Values: a Stochastic Approach to Eurocode 7. Ground Engineering, 35(12):30–34*
4. *Dealing with uncertainties in EC7 with emphasis on characteristic values and implementation of EC7 in Switzerland, H.R. Schneider, HSR University of Applied Sciences, Switzerland*
5. *Reliability of Earth Slopes : Vanmarcke, Journal of the Geotechnical Engineering Division, , V103, Ngt11, 1977, P1247-1265. (1978). International Journal of Rock Mechanics and Mining Sciences and Geomechanics Abstracts, 15(3), pp.62–62.*
6. *Frank, R. (2004).Designers' guide to EN 1997-1 Eurocode 7 : geotechnical design : general rules. Designe rs' guides to the Eurocodes. London: Thomas Telford.*
7. *Institution of Structural Engineers (Great Britain) (2013). Manual for the geotechnical design of structures to Eurocode 7 : May 2013. London: Institution of Structural Engineers.*
8. *Simpson, B. (2011). Concise Eurocodes : geotechnical design, BSEN 1997-1: Eurocode 7, part 1. London: British Standards Institution.*
9. *Orr, T.L.L. and Farrell, E.R. (2000). Geotechnical design to Eurocode 7. London: Springer.*
10. *Tietje, O., Fitze, P. and Schneider, H.R. (2014). Slope Stability Analysis Based on Autocorrelated Shear Strength Parameters. Geotechnical and Geological Engineering : An International Journal, 32(6), pp.1477–1483.*